A UNIFIED TREATMENT

SCALE, SYMMETRY, AND THE RENORMALIZATION GROUP

FROM DYNAMICAL SYSTEMS TO QUANTUM FIELD THEORY

github.com/muhammadhasyim/rg_ideas

First printing, December 7, 2025

Contents

List of Figures

List of Tables

Preface

This book is the culmination of years spent exploring the surprising connections between renormalization group ideas across seemingly disparate fields. My fascination began while studying Goldenfeld's *Lectures on Phase Transitions and the Renormalization Group*, a text remarkable not only for its treatment of Wilsonian renormalization in statistical mechanics and field theory, but also for its exposition of Barenblatt's work on self-similar solutions in nonlinear porous media flow. That a single mathematical framework could describe both critical phenomena in magnets and the spreading of groundwater through rock struck me as deeply significant.

Goldenfeld's book remains an essential reference for anyone seeking to understand RG beyond the confines of a single discipline.

This discovery became the impetus for a broader investigation. I began tracing the renormalization group through fluid turbulence, chaotic dynamics, and quantum field theory, finding in each case the same essential structure: a flow on a space of theories driven by changes in scale. What eventually emerged from these readings was an appreciation for the group-theoretic and geometric character of renormalization—the recognition that "the renormalization group" is quite literally a group (or more precisely, a semigroup) acting on a manifold of models, with the beta function as its infinitesimal generator.

Why, then, write another book on this subject when Goldenfeld's treatment already exists? The answer is that Goldenfeld's presentation, excellent as it is, was deliberately simplified for pedagogical purposes and does not develop the broader abstract framework that underlies the wide applicability of renormalization group methods. Much has happened in the decades since. Kunihiro and his students took the program to its fullest potential, applying RG techniques systematically to dynamical systems and unifying virtually all singular perturbation theories—work that proceeded in parallel to Goldenfeld's own contributions. Barenblatt laid the mathematical foundations for applications to partial differential equations through his theory of intermediate asymptotics. Fluid mechanicians developed RG approaches to turbulence. And a community of mathematical physicists has explored the Lie group structure and differential geometric foundations of the renormalization group with increasing rigor. The time has come to synthesize these developments into a single cohesive treatment.

The renormalization group stands as one of the most profound conceptual advances in twentieth-century physics. What began as a technical device for handling infinities in quantum electrodynamics has grown into a universal framework for understanding how physical systems behave across different scales. The same mathematical structure appears in statistical mechanics near phase transitions, in fluid turbulence, in chaotic dynamical systems, and throughout quantum field theory.

The unity of these phenomena under a single mathematical umbrella represents a triumph of physical abstraction comparable to the unification of electricity and magnetism.

This book presents the renormalization group as an **exact geometric framework**. The space of all possible theories or models forms a manifold, and the renormalization group generates a flow on this manifold. Fixed points of the flow correspond to scale-invariant theories. The geometry of the manifold encodes deep physical information about how theories relate to one another. This framework exists *independently* of how we compute with it.

Perturbation theory is the primary method for implementing the RG framework—computing beta functions, anomalous dimensions, and fixed point properties order by order in a small parameter. When perturbation theory is insufficient, **transseries methods** extend our computational reach to include non-perturbative physics.

Our pedagogical strategy reflects a clean separation between **structure** and **computation**:

Part I: the exact framework with simple examples. Part II: analytical methods. Part III: applications combining both.

Part I (Algebra and Geometry) develops the exact geometric framework using *simple, exactly solvable examples*. The anharmonic oscillator demonstrates running parameters and the resolution of secular terms. The amplitude equation (Hopf bifurcation normal form) provides a complete illustration of nontrivial fixed points, stability analysis, and universality—without requiring any loop calculations. The porous medium equation exhibits anomalous dimensions and second-kind self-similarity exactly. The ϕ^4 theory introduces the full machinery while emphasizing geometric structure over perturbative details. A distinctive feature of our approach is that geometric structures—metrics, connections, curvature—are *derived* from explicit calculations in these examples rather than postulated abstractly.

Part II (Analysis) develops the analytical methods for computing within the RG framework. Perturbation theory generically produces divergent series, but this divergence *encodes* non-perturbative physics. The Borel transform, resummation, and resurgence theory provide tools for extracting physical predictions from divergent series. Transseries extend perturbation theory to include instanton and renormalon contributions.

Part III (Applications) applies the unified geometric-analytical framework to seven physical systems of increasing complexity: chaotic dynamics in the Lorenz equations, turbulence in fluids, fracture mechanics in solids (following Barenblatt's theory of intermediate asymptotics), phase transitions in the Ising and O(N) models, and quantum field theories including QED and the Hubbard model.

Prerequisites

The reader should be familiar with undergraduate analysis and linear algebra, ordinary and partial differential equations, and elementary quantum mechanics. Some exposure to statistical mechanics and field theory will be helpful but is not strictly required. Each chapter is designed to be self-contained, developing the necessary mathematical background as the physics demands it.

Notation

We adhere to the following notational conventions throughout the book.

Scale and Flow Parameters

ℓ	Scale parameter (logarithm of energy or length scale)
t	Time (when physical time is the flow parameter)
μ	Renormalization scale (energy units)
Λ	UV cutoff (energy or momentum)
ϵ	Small expansion parameter

Parameter Space

g^i	Coupling constants (coordinates on theory space $\mathcal{M}$)
$\beta^i(g)$	Beta function (vector field generating RG flow)
$B^i{}_j$	Stability matrix $\partial\beta^i/\partial g^j\|_{g^*}$ at fixed point
Δ	Scaling dimension (eigenvalue of stability matrix)
γ	Anomalous dimension (interaction correction to scaling)
G_{ij}	Metric on theory space (Fisher/Zamolodchikov)
$\Gamma^i{}_{jk}$	Connection on theory space

Perturbation Theory and Transseries

$\tilde{f}(\epsilon)$	Formal (divergent) power series
$\hat{f}_B(\zeta)$	Borel transform of $\tilde{f}$
$\mathcal{S}[\tilde{f}]$	Borel sum (resummation)
$\mathcal{S}_{\pm}$	Lateral resummations (above/below real axis)
σ^n	Transseries parameters (for non-perturbative sectors)
S_ω	Stokes constant at singularity ω
Δ_ω	Alien derivative probing singularity at ω
$\mathfrak{S}$	Stokes automorphism

Standard Symbols

d	Differential ($\mathrm{d}/\mathrm{d}t$, $\mathrm{d}x$)
∂	Partial derivative ($\partial/\partial x$)
$\mathbb{R}, \mathbb{C}, \mathbb{Z}, \mathbb{N}$	Real, complex, integer, natural numbers
$\mathcal{M}$	Theory space (parameter manifold)
$\langle \cdot \rangle$	Expectation value $\langle \cdot \rangle$
$O(\epsilon^n)$	Terms of order ϵ^n and higher

The Author
December 7, 2025

Prologue: A Preview of the Renormalization Group

The renormalization group is, at its core, an **exact geometric framework** for understanding how physical systems behave across different scales. This framework (flows on parameter space, beta functions as generators, fixed points as destinations) exists independently of any particular computational method. Before we can appreciate this framework, we need to understand what scale means, why it matters, and what happens when our usual tools for exploiting scale symmetry break down.

Scale is the lens through which we view a system. Different scales reveal different physics, and the renormalization group is the systematic framework for moving between them.

This prologue previews the complete RG logic through one concrete example, namely the **damped anharmonic oscillator**. We will see dimensional analysis succeed, then fail. We will see perturbation theory succeed, then fail. Finally, we will see the RG resolve what perturbation theory could not. By the end of this prologue, every element of the RG framework will have appeared in action, and the strange name "renormalization group" will make sense.

What Is Scale?

The concept of scale pervades physics, yet it is rarely examined carefully. What exactly do we mean when we say two phenomena occur at "different scales"? Understanding this question is the first step toward the renormalization group, and answering it requires examining both spatial and temporal examples.

Scales Are Everywhere

Physical systems exhibit characteristic scales of many types, and recognizing these scales is the first step in any analysis. Every physical model implicitly chooses which scales to include and which to ignore. A continuum description ignores atomic scales; a one-body approximation ignores many-body correlations; a mean-field theory ignores fluctuations below a certain wavelength.

Every model implicitly chooses which scales to include. A continuum description ignores atomic scales; a one-body approximation ignores many-body correlations.

Spatial scales range from atomic spacing at roughly 10^{-10} meters to sample size, domain size, and correlation length. Consider a ferromagnet near its Curie temperature, where the correlation length ξ can span many orders of magnitude as criticality is approached. Consider also a coastline, which viewed from space looks smooth, from a boat appears jagged, and at the scale of individual grains of sand becomes smooth again. These examples illustrate how different physical descriptions become appropriate at different length scales.

Temporal scales include oscillation periods, relaxation times, and observation windows. A cup of coffee cools over minutes, but the molecular collisions that transfer heat occur on picosecond timescales. The damped anharmonic oscillator that we will study has a fast scale given by the oscillation period $2\pi/\omega_0$ and a slow scale given by the timescale over which the amplitude and frequency drift, which is approximately $1/\gamma$ for the amplitude decay and $\omega_0/(\epsilon A^2)$ for the frequency shift, where γ is the damping coefficient and ϵ parameterizes the strength of the nonlinearity.

Energy scales include thermal energy $k_B T$, interaction energy, and mass thresholds. In particle physics, the mass m of a particle sets an energy scale mc^2 below which the particle effectively decouples from the dynamics. The electron, the W boson, and the Higgs boson live at vastly different energy scales. Physics looks qualitatively different at each of these scales, with different effective degrees of freedom and different symmetries becoming manifest.

Scale as a Lens

A productive perspective is to think of scale as the lens through which we view a system. Changing the lens brings different features into focus, and what appears simple at one magnification may reveal complex structure at another.

"Zooming in" and "zooming out" are not just metaphors. They correspond to precise mathematical operations that the RG formalizes.

Consider a photograph of a tree. At high resolution (small scale), individual leaves with intricate vein patterns become visible. At larger scales, the leaves blur into a canopy shape. At still larger scales, the tree becomes a green blob among other blobs in a forest. Different physics, or different structure, is visible at each scale, and the appropriate description changes accordingly.

This perspective is not mere metaphor; the RG gives precise mathematical content to the notion of "zooming." What the tree analogy misses is that physical systems often have *no preferred scale*, meaning the structure looks statistically similar at all zoom levels. Coastlines, clouds, and critical phenomena share this property of scale invariance. The RG is the framework for understanding *why* certain systems are scale-invariant and what happens when they are not.

When Scales Do Not Talk to Each Other

The simplest situation occurs when scales are *well-separated* in the sense that the ratio of two characteristic scales is very large. When this happens, we can treat the physics at each scale independently. The fast dynamics "averages out" on slow timescales, and effective descriptions become possible.

Scale separation occurs when $\tau_{\text{fast}} \ll \tau_{\text{slow}}$. The fast dynamics then averages out on slow timescales.

Consider the damped anharmonic oscillator with small perturbation parameter ϵ and weak damping γ. The fast timescale is the oscillation period $\tau_{\text{fast}} \sim 1/\omega_0$. The slow timescale is the amplitude-decay time $\tau_{\text{slow}} \sim 1/\gamma$. Because $\gamma \ll \omega_0$, we have $\tau_{\text{fast}} \ll \tau_{\text{slow}}$, meaning the scales are well-separated. This separation enables an *effective description* where we can average over the fast oscillations to obtain a simpler equation for the slow amplitude dynamics.

When Scales Collide

The interesting and difficult situation occurs when scales are *not* well-separated. This happens in several important contexts, and it is precisely here that the renormalization group becomes essential. The most common example is when a physical scale of the problem tends towards the macroscopic limit.

For instance, near critical points, the correlation length diverges and all scales become coupled. In fact, the divergence of the correlation length approaches the thermodnamic limit of the problem. This means that the physics at all scales is coupled, and no small parameter exists to separate the physics at different scales. Thus, when we push perturbation theory beyond its domain of validity, it attempts to encode physics from all scales simultaneously and fails. Each of these situations requires a framework that can handle the coupling between scales.

Non-commuting limits signal scale collision. The mathematical signature is $\lim_{t\to\infty}\lim_{\epsilon\to 0} \neq \lim_{\epsilon\to 0}\lim_{t\to\infty}$.

The mathematical signature of scale collision is **non-commuting limits**. In our simplest example, which is that of the damped anharmonic oscillator, there's a clash between the timescale of frequency shift/renormalization (occuring at timescales ($\sim 1/\epsilon \to \infty$) and the long-time limit ($T \to \infty$) of the problem.

$$\lim_{t\to\infty}\lim_{\epsilon\to 0} x(t;\epsilon) \neq \lim_{\epsilon\to 0}\lim_{t\to\infty} x(t;\epsilon). \tag{1}$$

If we first set $\epsilon = 0$ and then evolve forever, we get simple harmonic motion. If we first evolve forever at fixed $\epsilon \neq 0$ and then try to take $\epsilon \to 0$, we must account for the accumulated amplitude decay and frequency shift. The renormalization group provides a systematic framework for handling these situations by allowing parameters to "run" with scale.

Dimensional Analysis and the Classical Theory of Scale

Before the renormalization group, physicists had a powerful tool for exploiting scale symmetry, namely **dimensional analysis**. Understanding when it works and when it fails is essential preparation for the RG. The successes of dimensional analysis illuminate why scale symmetry is so powerful, while its failures point toward the need for more sophisticated methods.

Dimensional analysis is representation theory of the dilation group in disguise. It identifies quantities that transform simply under scaling.

Units and Dimensions

Every physical quantity has **dimensions** that specify what kind of thing it is. In mechanics, we typically use three base dimensions, namely length L, time T, and mass M. Derived quantities have dimensions that are products of powers of these base dimensions; velocity has dimensions $[v] = LT^{-1}$, force has dimensions $[F] = MLT^{-2}$, and energy has dimensions $[E] = ML^2T^{-2}$.

The key insight is that **physical laws cannot depend on our choice of units**. If one observer measures length in meters and another measures in feet, both must obtain the same physics. This simple requirement of dimensional consistency has surprisingly powerful consequences that constrain the form of physical relationships.

The Buckingham Pi Theorem

The fundamental result of dimensional analysis is the Buckingham Pi theorem, which tells us how the form of physical relationships is constrained by dimensional consistency. This theorem, established in the early twentieth century, remains one of the most useful tools in applied physics.

Theorem 0.1 (Buckingham Pi Theorem)**.** *If a physical quantity Q depends on n parameters $p_1, \ldots, p_n$ involving k independent base dimensions, then*

$$Q = [p_1]^{\alpha_1} \cdots [p_n]^{\alpha_n} \cdot \Phi(\Pi_1, \ldots, \Pi_{n-k}) \tag{2}$$

where Φ is an arbitrary function of $n - k$ independent dimensionless combinations Π_i.

The Π theorem reduces a problem with n parameters to one with $n - k$ dimensionless parameters.

The power of this theorem becomes manifest when $n = k$, because then there are *no* dimensionless combinations, and the answer is determined up to a pure number. In such cases, dimensional analysis alone fixes the functional form of the answer.

Box 1.1: The Simple Pendulum

Problem: Find the period T of a simple pendulum of length ℓ in gravitational field g.
Step 1: List parameters and dimensions.

Parameter	Symbol	Dimensions
Period	T	T
Length	ℓ	L
Gravity	g	LT^{-2}

Step 2: Count. We have $n = 2$ parameters (ℓ, g) and $k = 2$ dimensions (L, T). So $n - k = 0$ means no dimensionless combinations.
Step 3: Solve. The period must have the form $T = C \cdot \ell^a g^b$ where

$$T: \quad 1 = -2b \implies b = -1/2 \tag{3}$$

$$L: \quad 0 = a + b \implies a = 1/2 \tag{4}$$

Result:

$$T = C\sqrt{\frac{\ell}{g}} \tag{5}$$

The constant $C = 2\pi$ requires solving the ODE. But dimensional analysis determined the *form* completely.
Check: For $\ell = 1$ m and $g = 10$ m/s^2, we obtain $T \approx 2$ s. ✓

Why does dimensional analysis work so well? The answer lies in symmetry. When we change units, we are performing a *scale transformation*. Dimensional analysis succeeds because it captures everything that symmetry alone can tell us. But symmetry has limits, and those limitations motivate the developments that follow.

When Dimensional Analysis Fails

Dimensional analysis is the first tool in a physicist's kit, and it often yields surprisingly complete answers. But there are systematic situations where it fails or is incomplete. Understanding these failures motivates everything that follows, because the renormalization group is precisely the framework that addresses them.

When dimensionless parameters exist, we must actually solve the problem. Dimensional analysis only tells us the form.

The Damped Oscillator and Failure by Dimensionless Parameter

Consider the damped harmonic oscillator governed by $m\ddot{x} + \gamma\dot{x} + kx = 0$, and ask for the oscillation frequency. The parameters are mass m with dimensions $[M]$, damping γ with dimensions $[MT^{-1}]$, and spring constant k with dimensions $[MT^{-2}]$.

We have $n = 3$ parameters and $k_{\text{dim}} = 2$ base dimensions (M and

T), so there is $n - k_{\text{dim}} = 1$ dimensionless combination, namely the **damping ratio**

$$\zeta = \frac{\gamma}{2\sqrt{mk}}. \tag{6}$$

Dimensional analysis tells us the frequency has the form

$$\omega = \sqrt{\frac{k}{m}} \cdot f(\zeta) \tag{7}$$

for some function f. But dimensional analysis cannot determine what the function f is. To find that $f(\zeta) = \sqrt{1 - \zeta^2}$ for underdamping, we must solve the differential equation.

The lesson is that dimensionless parameters are "blind spots" for dimensional analysis. When they exist, the physics depends on their values in ways that symmetry alone cannot predict. We must perform a dynamical calculation.

Barenblatt's Second Kind and Failure by Anomalous Dimensions

"First kind" self-similarity occurs when dimensional analysis determines the scaling exponents. "Second kind" occurs when the exponents are anomalous and must be computed.

A more dramatic failure occurs in certain nonlinear PDEs. Consider the porous medium equation

$$\frac{\partial u}{\partial t} = \nabla \cdot (u^m \nabla u) \tag{8}$$

for $m > 0$, which describes gas flow through porous rock, groundwater seepage, and heat conduction in certain materials. This equation exhibits fundamentally different behavior depending on the value of m.

For $m = 1$ (ordinary diffusion), dimensional analysis works perfectly. If u has dimensions $[U]$ and we have initial data localized at the origin, then

$$u(x,t) = t^{-d/2} F\left(\frac{x}{\sqrt{t}}\right) \tag{9}$$

for some profile function F. The exponent $-d/2$ (where d is spatial dimension) comes directly from dimensional analysis without solving the equation.

For $m \neq 1$, something strange happens. Dimensional analysis suggests a similar scaling form, but the **actual exponents are different**. The spreading of a localized pulse goes like t^α where α is *not* the dimensional-analysis prediction. The "correct" exponent depends on m through a relationship that must be computed and cannot be read off from dimensions.

Barenblatt called these **anomalous dimensions** or "self-similarity of the second kind." The RG provides a systematic framework for computing them by tracking how effective parameters flow under scale transformations.

The Phase Transition Problem

Perhaps the most famous failure of dimensional analysis occurs in statistical mechanics near a phase transition, and this failure was the historical motivation for developing the renormalization group. The story begins with a simple question that dimensional analysis appears to answer but actually does not.

Consider a ferromagnet near its Curie temperature T_c and ask how the magnetization M depends on temperature. Dimensional analysis, combined with thermodynamic reasoning, suggests

$$M \propto (T_c - T)^{1/2} \tag{10}$$

as $T \to T_c^-$. This is the "mean-field" exponent $\beta = 1/2$.

Experiment gives $\beta \approx 0.326$ in three dimensions. The actual exponent is *not* a simple rational number. It depends on spatial dimension, symmetry of the order parameter, and range of interactions, but not in any way that dimensional analysis can predict.

Critical exponents like $\beta \approx 0.326$ are "universal" (the same for all systems in the same universality class) but are not given by dimensional analysis.

These anomalous critical exponents were the historical motivation for developing the renormalization group. Wilson's breakthrough was showing that they arise from the geometry of RG flows near fixed points, where the structure of parameter space determines the observable exponents.

The Pattern of Failure

What do these failures have in common? In each case, dimensional analysis gives us the **form** of the answer but not the full content. The missing information involves **dynamics**, meaning we must solve differential equations rather than just count dimensions. The answer depends on **dimensionless parameters** (coupling constants, nonlinearity exponents) in ways that require computation.

The renormalization group provides this computational framework. But before we can appreciate it, we need to understand how physicists typically *try* to solve equations and how that approach fails in precisely the situations where the RG succeeds.

The Philosophy of Local Solutions

Most equations in physics cannot be solved exactly, and this simple fact shapes everything we do. The standard approach is to build solutions locally and extend outward, and this works remarkably well in many contexts. Understanding when and why it fails prepares us for the RG.

The Power Series as Foundational Tool

Power series are analogous to local maps in cartography, accurate nearby but potentially useless far away.

Suppose we want to solve a differential equation near some point. The most natural approach is to expand in a **power series** by assuming the solution has the form

$$x(t) = \sum_{n=0}^{\infty} c_n t^n \tag{11}$$

and determining the coefficients order by order. This approach is foundational to applied mathematics and forms the basis for most analytical solution methods.

When we are fortunate, the series converges in some region and may even sum to a closed-form expression. The exponential function, for example, is defined by its power series $e^t = \sum t^n/n!$, which converges for all t and provides the complete solution.

When we are less fortunate, the series may converge only in a limited region, or not at all. The geometric series $\sum t^n$ converges only for $|t| < 1$. Still worse, some series diverge for *any* nonzero argument while still being useful for computation.

Asymptotics and Making Peace with Divergence

A series that diverges can still be **asymptotic**, meaning that truncating after N terms gives an approximation whose error decreases as the expansion parameter goes to zero. The classic example is the complementary error function

$$\operatorname{erfc}(x) \sim \frac{e^{-x^2}}{x\sqrt{\pi}} \left(1 - \frac{1}{2x^2} + \frac{3}{4x^4} - \cdots\right) \tag{12}$$

for large x. This series diverges for any finite x, yet truncating at the smallest term gives an excellent approximation that improves as x increases.

Asymptotic series diverge, but their partial sums can be spectacularly accurate. The art is knowing when to stop.

This is **asymptotics**, the systematic study of limits and approximations. An asymptotic expansion tells us how a function behaves as some parameter approaches a limiting value (often zero or infinity), even when no convergent series exists. The theory of asymptotic expansions, developed by mathematicians including Poincaré, Stokes, and Erdélyi, provides the rigorous foundation for much of applied mathematics.

The Small Parameter

Perturbation theory, our main tool for physics problems, is asymptotics organized around a **small parameter** ϵ. We write

$$x(\epsilon) = x_0 + \epsilon x_1 + \epsilon^2 x_2 + \cdots \tag{13}$$

and solve for x_0, x_1, and so on in succession. Each correction is determined by the previous ones through a hierarchy of linear equations.

The small parameter tells us what is "small" and can be treated as a correction to a known solution. In mechanics, ϵ might be a nonlinearity strength. In quantum field theory, it might be a coupling constant. In fluid mechanics, it might be an aspect ratio or Reynolds number.

Physics chooses the small parameter. The art of perturbation theory is identifying what to expand in. A good choice makes the leading term capture most of the physics; a bad choice yields useless results even at low order.

Local versus Global and the Fundamental Tension

Perturbation theory is local. The RG extends it globally by letting parameters "run" with scale.

The key point is that perturbation theory is **local**. It gives approximations valid in a neighborhood of the expansion point, but that neighborhood may be small. The expansion is "centered" at a particular value of the independent variable and becomes less accurate as we move away.

Consider expanding $\cos(\omega t)$ in powers of ωt. The resulting Taylor series

$$\cos(\omega t) = 1 - \frac{(\omega t)^2}{2!} + \frac{(\omega t)^4}{4!} - \cdots \tag{14}$$

converges for all t, but if ωt is large, many terms are needed for accuracy. The expansion is centered at $t = 0$ and becomes increasingly inefficient as we move to large times.

The pathology of **secular terms**, namely terms that grow without bound in time, is an extreme version of this locality problem. When perturbation theory produces $t \sin(\omega_0 t)$ terms, it is signaling that the local expansion cannot be extended globally without modification.

The RG resolution is to let the "constants" in the leading-order solution become *slowly varying functions*. This amounts to continuously re-centering the local expansion as we evolve in time (or scale). The parameters "run" so that the expansion always stays valid in its current neighborhood.

This is the conceptual core of the renormalization group. The technical machinery implements this idea in different contexts.

The Damped Anharmonic Oscillator

We now turn to the problem that will accompany us through much of this book. The **damped anharmonic oscillator** is the simplest system that exhibits the failure of naive perturbation theory and its resolution through renormalization group ideas. By including damping from the outset, we obtain a richer example where both amplitude and phase evolve under the RG flow.

The Setup

Consider a particle of unit mass moving in an anharmonic potential with linear damping. Real oscillators always experience some friction, whether from air resistance, internal material losses, or coupling to other degrees of freedom. The equation of motion is

$$\ddot{x} + 2\gamma\dot{x} + \omega_0^2 x + \epsilon x^3 = 0 \tag{15}$$

where ω_0 sets the frequency of small oscillations, $\gamma > 0$ is the damping coefficient (assumed small for the perturbative analysis), and $\epsilon > 0$ is a small parameter that controls the cubic nonlinearity. We assume weak damping $\gamma \ll \omega_0$ (underdamped regime) so that both damping and nonlinearity produce slow corrections to simple harmonic motion.

The quartic potential x^4 is the simplest nonlinearity that preserves $x \to -x$ symmetry and keeps motion bounded. Linear damping is the leading dissipative effect.

This is a nonlinear, dissipative oscillator. For small amplitudes and weak perturbation ($\epsilon \ll 1$), the system behaves approximately like a simple harmonic oscillator. For larger amplitudes or longer times, both the cubic nonlinearity and the damping become important. The nonlinearity shifts the frequency, while the damping causes the amplitude to decay.

Box 1.2: Dimensional Analysis of the Damped Anharmonic Oscillator

Question: How does the effective frequency ω depend on amplitude A?

Step 1: List parameters and dimensions. The natural frequency ω_0 has dimensions $[T^{-1}]$. The damping γ has dimensions $[T^{-1}]$. The perturbation parameter ϵ is dimensionless (we have absorbed appropriate factors into the definition of γ and the nonlinear term). The amplitude A has dimensions $[L]$. There is also a coupling constant with dimensions $[T^{-2}L^{-2}]$ implicit in the ϵx^3 term.

Step 2: Identify dimensionless combinations. There are two dimensionless combinations, namely γ/ω_0 (ratio of damping to natural frequency) and $\epsilon A^2/\omega_0^2$ (ratio of nonlinear to linear restoring force).

Step 3: Apply dimensional analysis. The effective frequency has the form

$$\omega_{\text{eff}} = \omega_0 f\left(\frac{\gamma}{\omega_0}, \frac{\epsilon A^2}{\omega_0^2}\right) \tag{16}$$

with $f(0,0) = 1$ (harmonic limit).

What dimensional analysis tells us: The frequency depends on amplitude only through $\epsilon A^2/\omega_0^2$ and on damping through γ/ω_0.

What it cannot tell us: The function f. We must solve the dynamics to find it.

Physical Intuition

Before calculating, let us think physically about what we expect. The quartic term provides extra restoring force when x is large, and a larger amplitude means more time spent in the "stiff" part of the potential. We expect that larger amplitude leads to higher effective frequency, meaning the frequency should increase with amplitude.

The damping, on the other hand, causes the oscillation amplitude to decay over time. As energy is dissipated, the amplitude decreases, which in turn affects the frequency shift from the nonlinearity. We therefore expect both the amplitude and the effective frequency to evolve in time.

Physical intuition suggests amplitude decay and frequency shift. The RG calculation will quantify both effects precisely.

This is exactly the kind of question that dimensional analysis leaves open and that dynamics must answer. The coefficient c in $\omega_{\text{eff}} = \omega_0(1 + c\,\epsilon A^2/\omega_0^2 + \cdots)$ encodes the physics that dimensional analysis cannot capture.

Naive Asymptotics and Its Failure

Let us solve the damped anharmonic oscillator using the standard approach of expanding in the small parameter ϵ and observe its failure. The failure has two aspects that are often discussed separately but are actually related.

Setting Up the Expansion

Assume $\epsilon \ll 1$ and expand the solution as

$$x(t) = x_0(t) + \epsilon x_1(t) + \epsilon^2 x_2(t) + \cdots \tag{17}$$

Perturbation theory assumes the answer is close to a known solution and computes corrections order by order.

Substituting into equation (15) and collecting powers of ϵ gives a hierarchy of equations.

At order $O(\epsilon^0)$, we have

$$\ddot{x}_0 + \omega_0^2 x_0 = 0. \tag{18}$$

The solution is $x_0(t) = A\cos(\omega_0 t)$ when we choose initial conditions $x(0) = A$ and $\dot{x}(0) = 0$.

At order $O(\epsilon^1)$, we have

$$\ddot{x}_1 + \omega_0^2 x_1 = -2\gamma\dot{x}_0 - x_0^3 = 2\gamma A\omega_0 \sin(\omega_0 t) - A^3\cos^3(\omega_0 t). \tag{19}$$

Box 1.3: Deriving the Secular Terms

Goal: Solve for x_1 in the presence of both damping and nonlinearity.

Step 1: Expand the forcing terms. Using the identity $\cos^3\theta =$

$\frac{3}{4}\cos\theta + \frac{1}{4}\cos 3\theta$, the equation becomes

$$\ddot{x}_1 + \omega_0^2 x_1 = 2\gamma A\omega_0 \sin(\omega_0 t) - \frac{3A^3}{4}\cos(\omega_0 t) - \frac{A^3}{4}\cos(3\omega_0 t). \tag{20}$$

Step 2: Identify resonant terms. The $\sin(\omega_0 t)$ and $\cos(\omega_0 t)$ terms oscillate at the natural frequency. These are *resonant forcing* terms. The $\cos(3\omega_0 t)$ term is non-resonant.

Step 3: Solve for the non-resonant term. The non-resonant part contributes $x_{1,\text{nr}} = \frac{A^3}{32\omega_0^2}\cos(3\omega_0 t)$, which remains bounded.

Step 4: The resonant terms produce secular growth. For resonant forcing, the particular solution grows linearly in time. The $\sin(\omega_0 t)$ forcing produces a term proportional to $t\cos(\omega_0 t)$, and the $\cos(\omega_0 t)$ forcing produces a term proportional to $t\sin(\omega_0 t)$.

The secular terms:

$$\boxed{x_1(t) \supset \gamma A\, t\cos(\omega_0 t) - \frac{3A^3}{8\omega_0} t\sin(\omega_0 t)} \tag{21}$$

Both terms grow *linearly in time*. At $t \sim 1/\epsilon$, they become $O(A)$, as large as the leading term.

What Went Wrong?

Secular terms grow without bound. At time $t \sim 1/\epsilon$, perturbation theory has failed.

The complete solution to first order contains terms that grow linearly in time. These **secular terms** (from the Latin *saeculum*, "age") signal the breakdown of naive perturbation theory. They grow without bound as $t \to \infty$, eventually becoming larger than the leading-order solution.

The physical origin of the secular terms is clear. The damping causes the amplitude to decay, and the nonlinearity causes the frequency to shift. The *true* solution has time-dependent amplitude $A(t)$ and oscillates at an effective frequency $\omega_{\text{eff}}(t)$ that differs from ω_0. But our expansion assumed fixed amplitude A and fixed frequency ω_0. The accumulated errors from these incorrect assumptions grow linearly in time.

The secular terms are the perturbative expansion "trying" to represent amplitude decay and frequency shift using polynomial corrections in t. But amplitude decay requires exponential functions of t, and frequency shifts require trigonometric functions with modified arguments, not polynomial corrections. The perturbative series is attempting to encode information that it cannot naturally accommodate.

The Second Problem and Factorial Divergence

Even without secular terms, perturbation series diverge. The coefficients grow as $n!$, giving zero radius of convergence.

The secular term is not the only problem. Even if we could somehow avoid secular terms (or work at times short enough that they remain small), the perturbative coefficients grow **factorially** with order, so that

$$|c_n| \sim A^n \cdot n! \tag{22}$$

This means the series diverges for any nonzero coupling. The perturbation series for the anharmonic oscillator has zero radius of convergence.

This sounds like a disaster, but it is actually a meaningful signal rather than a defect. The factorial divergence encodes information about non-perturbative physics, namely effects that are invisible to any finite order of perturbation theory. We will explore this in Part II.

For now, the key insight is that **the RG framework (beta functions, flows, fixed points) is exact**. It exists independently of perturbation theory. What fails is one particular method of computing within the framework, but the framework itself remains intact.

The RG Resolution

We now solve the secular term problem using the **method of multiple scales**, a well-established technique in applied mathematics that reveals the essential logic of the renormalization group.

The method of multiple scales was developed by applied mathematicians (Kevorkian, Cole, Nayfeh) for singular perturbation problems. Its connection to the RG was recognized later.

The method of multiple scales predates the renormalization group and was systematically developed by applied mathematicians including Kevorkian, Cole, and Nayfeh for singular perturbation problems in mechanics and fluid dynamics. The deep connection between this classical technique and the physics of renormalization was recognized later. The solvability conditions that eliminate secular terms in multiple-scales analysis turn out to be precisely the RG equations. This correspondence reveals that the RG is not just a physics technique but has roots in the broader theory of asymptotic analysis.

The key idea is to let the parameters that naive perturbation theory holds fixed become slowly varying functions. This allows the expansion to accommodate physics (like amplitude decay and frequency shifts) that would otherwise appear as pathologies.

The Multiple-Scales Ansatz

In naive perturbation theory, we wrote $x(t) = A\cos(\omega_0 t + \phi)$ with *fixed* A and ϕ. The multiple-scales approach promotes these to *slow variables* that depend on a "slow time" $\tau = \epsilon t$. We seek a solution of the form

$$x(t) = A(\tau)\cos\big(\omega_0 t + \phi(\tau)\big) + O(\epsilon) \tag{23}$$

where the requirement that secular terms cancel determines how $A(\tau)$ and $\phi(\tau)$ must evolve.

Box 1.4: The RG Solution of the Damped Anharmonic Oscillator

Goal: Find how amplitude A and phase ϕ must evolve to eliminate secular terms.

Step 1: Multiple-scales expansion. Introduce slow time $\tau = \epsilon t$ and seek

$$x(t) = x_0(t,\tau) + \epsilon x_1(t,\tau) + O(\epsilon^2). \tag{24}$$

The time derivative becomes $\mathrm{d}/\mathrm{d}t = \partial/\partial t + \epsilon\,\partial/\partial\tau$.

Step 2: Zeroth order. $\partial^2 x_0/\partial t^2 + \omega_0^2 x_0 = 0$ gives

$$x_0 = A(\tau)\cos\big(\omega_0 t + \phi(\tau)\big). \tag{25}$$

Step 3: First order. The $O(\epsilon)$ equation is

$$\frac{\partial^2 x_1}{\partial t^2} + \omega_0^2 x_1 = -2\frac{\partial^2 x_0}{\partial t \partial \tau} - 2\gamma\frac{\partial x_0}{\partial t} - x_0^3. \tag{26}$$

Writing $\Theta = \omega_0 t + \phi$ and collecting terms, the right-hand side contains resonant forcing at frequency ω_0.

Step 4: Cancel secular terms. Secular growth is avoided if and only if the coefficients of $\sin\Theta$ and $\cos\Theta$ vanish.

<u>Coefficient of $\sin\Theta$:</u>

$$2\omega_0 A' + 2\gamma\omega_0 A = 0 \implies \frac{\mathrm{d}A}{\mathrm{d}\tau} = -\gamma A \tag{27}$$

<u>Coefficient of $\cos\Theta$:</u>

$$2\omega_0 A\phi' - \frac{3A^3}{4} = 0 \implies \frac{\mathrm{d}\phi}{\mathrm{d}\tau} = \frac{3A^2}{8\omega_0} \tag{28}$$

Step 5: The RG equations. For weak damping, the amplitude decays at rate γ (the damping coefficient), while the phase evolves on the slow timescale $\tau = \epsilon t$ due to the nonlinearity. In physical time, we obtain

$$\frac{\mathrm{d}A}{\mathrm{d}t} = -\gamma A \tag{29}$$

$$\frac{\mathrm{d}\phi}{\mathrm{d}t} = \frac{3\epsilon A^2}{8\omega_0} \tag{30}$$

Step 6: Solve and interpret. The amplitude decays exponentially,

$$A(t) = A_0 e^{-\gamma t}, \tag{31}$$

while the phase satisfies

$$\phi(t) = \phi_0 + \frac{3\epsilon}{8\omega_0}\int_0^t A(t')^2\,dt' = \phi_0 + \frac{3\epsilon A_0^2}{16\gamma\omega_0}\big(1 - e^{-2\gamma t}\big). \tag{32}$$

The instantaneous effective frequency is

$$\boxed{\omega_{\text{eff}}(t) = \omega_0 + \frac{3\epsilon A(t)^2}{8\omega_0} = \omega_0 \left(1 + \frac{3\epsilon A_0^2}{8\omega_0^2} e^{-2\gamma t}\right)} \tag{33}$$

Physical interpretation: The amplitude decays exponentially due to damping, while the frequency shift decreases as the amplitude decreases. At long times, the system approaches simple harmonic motion at frequency ω_0.

The Meaning of Renormalization

What we have just computed *is* renormalization in the modern sense. The amplitude A_0 and phase ϕ_0 at $t = 0$ are the "bare" parameters. The amplitude $A(t)$ and phase $\phi(t)$ at later times are the "renormalized" parameters. The RG equations describe how these parameters "run" with the scale (here, time).

Historically, "renormalization" arose in quantum field theory to absorb infinities. The modern understanding is broader and involves all scale-dependent parameters.

There are no infinities anywhere in this calculation, only scale dependence. This is the modern understanding of renormalization, which is much broader than the historical context of absorbing divergences in quantum field theory. Whether we are dealing with UV divergences in QFT, secular terms in perturbation theory, or scale-dependent effective parameters in statistical mechanics, the underlying structure is the same. Parameters that look fixed at one scale must run to describe physics at another scale.

The Universal Pattern

The damped anharmonic oscillator illustrates a universal pattern that appears across all applications of the renormalization group.

This pattern recurs in every RG application. The details change, but the logic is universal.

1. **Identify the divergence.** Naive perturbation theory produces secular terms, UV divergences, or boundary layer mismatches, depending on context. These pathologies signal that the perturbative ansatz is missing something.

2. **Promote constants to functions.** Parameters that were held fixed become scale-dependent. The amplitude becomes $A(\ell)$ and the phase becomes $\phi(\ell)$, where ℓ is a scale parameter.

3. **Require consistency.** Demanding that the expansion remain valid (secular terms cancel or divergences are absorbed) determines how parameters must flow.

4. **Solve the flow.** The resulting equations are the RG equations and determine the scale dependence of effective parameters.

5. **Extract physics.** Physical predictions come from the flow, not from any single point in parameter space.

Box 1.5: RG in Different Contexts

The same pattern appears across fields with different physical manifestations.

Multiple scales (ODEs): The divergence manifests as secular terms $\sim t^n$. The running parameters are slow amplitudes and phases. The scale is time t or slow time $\tau = \epsilon t$.

Wilson's RG (statistical mechanics): The divergence manifests as UV modes in loop integrals. The running parameters are coupling constants m^2 and λ. The scale is the momentum cutoff Λ or $\ell = \log(\Lambda_0/\Lambda)$.

Amplitude equations (PDEs): The divergence manifests as secular growth in space or time. The running parameters are envelope amplitudes. The scale involves slow spatial or temporal variables.

QFT renormalization: The divergence manifests as loop integrals $\sim \Lambda^n$ or $\log \Lambda$. The running parameters are masses and couplings. The scale is the renormalization scale μ.

The mathematics is the same; the physics differs.

The Geometric Picture: A Preview

This section previews the geometric framework developed fully in Chapter I. Here we introduce the key ideas; there we develop the complete Lie group structure.

The calculations in the previous sections revealed something deeper than computational tricks. The amplitude A and phase ϕ are not just "parameters" in the usual sense—they are **coordinates on a manifold**. The RG equations

$$\frac{dA}{dt} = -\gamma A, \qquad \frac{d\phi}{dt} = \frac{3\epsilon A^2}{8\omega_0} \tag{34}$$

define a **vector field** on this manifold, called the **beta function**:

$$\boldsymbol{\beta} = \beta^A \frac{\partial}{\partial A} + \beta^\phi \frac{\partial}{\partial \phi} = -\gamma A \frac{\partial}{\partial A} + \frac{3\epsilon A^2}{8\omega_0} \frac{\partial}{\partial \phi}. \tag{35}$$

The integral curves of this vector field are called **RG flows**. For our damped oscillator, these flows spiral inward toward the origin as amplitude decays while phase advances. Where the beta function vanishes ($\boldsymbol{\beta} = 0$), we have a **fixed point**—a scale-invariant state. For the damped oscillator, $A = 0$ (rest) is the only fixed point.

This geometric structure—scale transformations forming a Lie group, beta functions as generators, parameter space as a manifold—is *universal*. The same framework describes quantum field theory, statistical mechanics, and nonlinear PDEs. Chapter I develops this framework

Lie Theory	Renormalization Group
Manifold $\mathcal{M}$	Theory/parameter space
Vector field $\boldsymbol{\beta}$	Beta function
Integral curves	RG flows
Fixed points ($\boldsymbol{\beta} = 0$)	Scale-invariant theories
Lie group action	Finite RG transformation

Table 1: The correspondence between Lie theory and the RG (developed in Chapter I).

systematically, showing how the dilation group $(\mathbb{R}^+, \times)$ acts on theory space and how operators transform as sections of bundles over this space.

Looking ahead: The oscillator demonstrates the basic RG logic but has only a trivial fixed point. The ϕ^4 field theory (Chapter I) exhibits **nontrivial fixed points** and **universality**. The porous medium equation (Chapter I) shows **anomalous dimensions**—scaling exponents that dimensional analysis cannot predict. Part II then develops the analytical tools (Borel transforms, transseries, resurgence) needed when perturbation theory produces divergent series.

Summary

Chapter Summary

The Core Ideas

- **Scale is the lens** through which we view physical systems. Different scales reveal different physics.
- **Dimensional analysis** is the classical theory of scale. It determines the *form* of physical laws but fails when dimensionless parameters exist.
- **Asymptotic expansions** build solutions locally. They fail when pushed beyond their domain of validity, namely when scales collide.
- **The RG resolution** is to let parameters "run" with scale so that local expansions remain valid globally.

The Universal Pattern

1. **Identify the divergence** in the form of secular terms, UV divergences, or boundary layer mismatches

2. **Promote constants to functions** so that $A \to A(\ell)$ and $\phi \to \phi(\ell)$
3. **Require consistency** by demanding cancellation of secular terms
4. **Solve the flow** using the RG equations to determine scale dependence
5. **Extract physics** from the flow, not from any single point

Key Equations

$$\text{RG equations:} \quad \frac{dA}{dt} = -\gamma A, \qquad \frac{d\phi}{dt} = \frac{3\epsilon A^2}{8\omega_0} \tag{36}$$

$$\text{Amplitude decay:} \quad A(t) = A_0 e^{-\gamma t} \tag{37}$$

$$\text{Effective frequency:} \quad \omega_{\text{eff}}(t) = \omega_0 \left(1 + \frac{3\epsilon A(t)^2}{8\omega_0^2}\right) \tag{38}$$

The Geometric Picture

- **Parameter space** is a manifold $\mathcal{M}$
- **Beta functions** are vector fields on $\mathcal{M}$
- **RG flows** are integral curves
- **Fixed points** occur where $\boldsymbol{\beta} = 0$, corresponding to scale-invariant theories
- **The RG is exact** in that the geometric framework exists independently of how we compute within it

The damped anharmonic oscillator will accompany us as we develop the full RG framework. Chapter I introduces the Lie group structure underlying RG in greater detail. Chapter I derives the RG equation from first principles and applies it to the ϕ^4 field theory. Chapter I develops fixed-point theory, including the Wilson-Fisher fixed point and anomalous dimensions. Part II then develops the analytical tools—perturbation theory, Borel transforms, and resurgence—for extracting physical predictions from divergent series.

Part I

Algebra and Geometry

The Renormalization Group as Algebra and Geometry

From Running Parameters to Structure

The Prologue showed *that* parameters run. This chapter develops the **complete framework**: the Callan-Symanzik equation has a unified algebraic-geometric structure. Algebra and geometry are not alternatives—they are two faces of the same coin, emerging together from the equation. This framework is exact and independent of any computational method.

The Prologue ended with a remarkable result. For the damped anharmonic oscillator, demanding the cancellation of secular terms forced the amplitude and phase to satisfy:

$$\frac{dA}{dt} = -\gamma A \tag{39}$$

$$\frac{d\phi}{dt} = \frac{3\epsilon A^2}{8\omega_0} \tag{40}$$

The amplitude A decays exponentially due to damping, while the phase ϕ advances at a rate proportional to ϵA^2. These are the **RG equations** for the oscillator—but three questions immediately arise:

> **Question 1:** Where do the parameters (A, ϕ) "live"?
>
> **Question 2:** What mathematical structure governs their evolution?
>
> **Question 3:** Why does the same structure appear in statistical mechanics, QFT, and PDEs?

The answers reveal that the renormalization group is not merely a collection of techniques—it has deep mathematical structure. **Crucially, this structure is simultaneously algebraic and geometric**:

> **The central insight of this chapter:** Algebra and geometry are not alternative ways of viewing RG. They are *two faces of the same structure*, emerging together from the Callan-Symanzik equation.

- Scale transformations form a **Lie group—**this is algebraic
- The group acts on a **manifold** (theory space)—this is geometric
- The beta function is both the **Lie algebra generator** and a **vector field—**the same object in two languages

- Scheme transformations are both **group elements** and **diffeomorphisms**—again, two names for one thing

Table 2 is not a dictionary between separate subjects; it shows that each RG concept is intrinsically both algebraic and geometric. This chapter develops each row, showing how they emerge organically from the central equation.

Table 2: The correspondence between Lie theory and the renormalization group.

Algebraic/Geometric Concept	RG Interpretation
Dilation group $(\mathbb{R}^+, \times)$	Scale transformations
Lie algebra generator $\mathcal{D}$	Infinitesimal RG transformation
Vector field $\boldsymbol{\beta}$ on $\mathcal{M}$	Beta functions
Integral curves of $\boldsymbol{\beta}$	RG trajectories (flows)
Fixed points ($\boldsymbol{\beta} = 0$)	Scale-invariant theories
Lie derivative $L_{\boldsymbol{\beta}}$	RG equation
Scaling dimension Δ	Eigenvalue of $\mathcal{D}$
Connection Γ^a_{bc}	Anomalous dimension matrix / OPE coefficients
Curvature $R^a{}_{bcd}$	Scheme-independent invariants

Scale Independence: The Physical Foundation

The fundamental insight: physical predictions cannot depend on arbitrary choices of scale. This requirement *determines* the beta functions.

Why do parameters run? The answer is a beautiful consistency requirement: **physical predictions cannot depend on arbitrary choices of scale**. If we describe a system at scale μ_1 or μ_2, we must get the same physical answers. This seemingly innocuous statement has profound consequences.

The Setup

Consider a physical observable $\mathcal{O}$ that depends on:

- **External scales**: momenta p, energies E, positions x, times t
- **Internal parameters**: couplings g, masses m
- **Reference scale**: μ (the "renormalization scale")

The observable has **explicit** μ-dependence from having chosen μ as our reference, and **implicit** μ-dependence through the running parameters $g(\mu)$.

The Callan-Symanzik Equation

Physical predictions cannot depend on our arbitrary choice of μ. Mathematically:

$$\mu \frac{d\mathcal{O}}{d\mu} = 0 \tag{41}$$

But $\mathcal{O}$ depends on μ both explicitly and through the running couplings:

$$\mu \frac{d\mathcal{O}}{d\mu} = \mu \frac{\partial \mathcal{O}}{\partial \mu}\bigg|_g + \mu \frac{\partial g^i}{\partial \mu} \frac{\partial \mathcal{O}}{\partial g^i} \tag{42}$$

Define the **beta functions**:

$$\beta^i(g) \equiv \mu \frac{\partial g^i}{\partial \mu} \tag{43}$$

The beta function $\beta^i = \mu \partial g^i / \partial \mu$ tells us how parameters change when we change the reference scale.

Then scale independence becomes:

$$\boxed{\left(\mu \frac{\partial}{\partial \mu} + \beta^i(g) \frac{\partial}{\partial g^i} \right) \mathcal{O} = 0} \tag{44}$$

This is the **Callan-Symanzik equation** in its simplest form.

Box 2.1: Deriving the CS Equation from First Principles

Goal: Show step-by-step why scale independence forces parameters to run.

Setup: Consider a physical quantity $\mathcal{O}(p/\mu, g(\mu))$ where p is an external momentum, μ is the renormalization scale, and g is a coupling.

Step 1: The physics doesn't know about μ.
μ is our arbitrary choice of reference scale (like choosing units). Therefore:

$$\frac{d\mathcal{O}}{d\mu} = 0 \quad \text{(total derivative)} \tag{45}$$

Step 2: Chain rule expansion.
$\mathcal{O}$ depends on μ in two ways:

- **Explicitly**: through the ratio p/μ
- **Implicitly**: through $g(\mu)$

By the chain rule:

$$\frac{d\mathcal{O}}{d\mu} = \frac{\partial \mathcal{O}}{\partial \mu}\bigg|_g + \frac{\partial g}{\partial \mu} \frac{\partial \mathcal{O}}{\partial g}\bigg|_\mu = 0 \tag{46}$$

Step 3: Multiply by μ for convenience.
Define $\beta(g) \equiv \mu \frac{\partial g}{\partial \mu}$. Then:

$$\mu \frac{\partial \mathcal{O}}{\partial \mu}\bigg|_g + \beta(g) \frac{\partial \mathcal{O}}{\partial g}\bigg|_\mu = 0 \tag{47}$$

Step 4: Physical interpretation.
If $\beta \neq 0$, then $\frac{\partial \mathcal{O}}{\partial \mu} \neq 0$. The explicit μ-dependence must be *compensated* by implicit μ-dependence through running couplings.

The punchline: Scale independence doesn't mean "nothing changes." It means "changes in the explicit scale are exactly compensated by changes in the couplings." The beta function quantifies this compensation.

The Full CS Equation with Anomalous Dimensions

For an n-point correlation function, the CS equation takes a richer form:

$$\left(\mu\frac{\partial}{\partial\mu} + \beta_r\frac{\partial}{\partial r} + \beta_\lambda\frac{\partial}{\partial\lambda} + n\gamma\right)\tilde{G}_n = 0 \tag{48}$$

The new term $n\gamma$ is the **anomalous dimension**. Each field ϕ contributes a factor γ—this is the quantum/interaction correction to the classical scaling dimension. We will see its origin both algebraically (as a representation label) and geometrically (as a connection coefficient).

Scale Covariance: A Universal Structure

Although we have written the Callan-Symanzik equation in the language of QFT, its structure appears whenever we have a notion of scale and a family of models: multiple-scale analysis of ODEs, similarity solutions of PDEs, and coarse-grained descriptions of stochastic dynamics. The later examples (oscillator, amplitude equation, PME) are included precisely to show that this geometric structure is not peculiar to quantum field theories.

The generic **scale-covariance equation** takes the form:

$$\left(\mu\frac{\partial}{\partial\mu} + \beta^i(g)\frac{\partial}{\partial g^i} + \Gamma(g)\right)F(x;\mu,g) = 0 \tag{49}$$

where μ is a scale parameter (which could be a momentum scale, time, length, or cutoff), g^i are the model parameters, $\beta^i(g)$ describes how parameters change with scale, $\Gamma(g)$ captures anomalous scaling, and F is an observable or solution.

The CS equation (44) is one instance of the general scale-covariance structure (49). The same mathematical form appears across physics.

In different contexts, this structure specializes as follows:

- **QFT**: μ is the renormalization scale, F is a Green's function, and (49) becomes the Callan-Symanzik equation
- **Anharmonic oscillator**: "Scale" is the arbitrary time origin t_0, and demanding $dx/dt_0 = 0$ yields the same structure

- **Similarity solutions of PDEs**: "Scale" is time or length; self-similarity imposes (49) on the similarity profile
- **Statistical mechanics**: μ is the coarse-graining scale in Wilsonian RG

The Wilsonian coarse-graining picture provides the physical foundation for why parameters run: integrating out short-wavelength fluctuations modifies effective couplings. The CS equation (44) provides the analytic structure we develop in this chapter. Part V demonstrates the universality of (49) through explicit examples.

Theory Space

The parameters g^i appearing in (49) are coordinates on **theory space** $\mathcal{M}$—the space of all theories (or models) under consideration. Each point in $\mathcal{M}$ represents a specific choice of couplings, and hence a specific theory.

We work with a finite-dimensional truncation of theory space. Full Wilsonian theory space is infinite-dimensional (the space of all local functionals).

We treat $\mathcal{M}$ as a finite-dimensional smooth manifold for clarity. This is a truncation: in full generality, Wilsonian theory space is infinite-dimensional (the space of all local action functionals). The finite-dimensional case captures the essential geometry while avoiding functional-analytic complications.

The distinction between the **CS equation** (44) and the **RG flow equation**:

$$\frac{dg^i}{d\ell} = \beta^i(g), \qquad \ell = \log(\mu/\mu_0) \tag{50}$$

is important. The CS equation is a PDE for correlation functions (or observables) on the extended space (μ, g). The RG flow equation (73) is an ODE on theory space $\mathcal{M}$ alone, with ℓ as the evolution parameter. They encode the same physics but emphasize different aspects: the CS equation focuses on observables, while (73) focuses on the flow of couplings.

Part II develops the symmetry structure *of* the Callan-Symanzik equation (44). We do not introduce new objects—we discover what structure the equation *already has*.

The Callan-Symanzik equation (44) is a first-order partial differential equation. Like any differential equation, it has a **symmetry structure**—transformations that leave it invariant. Understanding this structure is not an alternative to understanding the equation; it *is* understanding the equation.

We will find two intertwined symmetries:

1. **Scale transformations**: The equation is invariant under $\mu \to \lambda\mu$, which forms a Lie group
2. **Scheme transformations**: The equation holds in any scheme, so reparameterizations $g^i \to g'^i(g)$ are symmetries

These are not independent—they combine into a single geometric object, as we will see in Part III.

Scale Invariance as a Lie Group

Return to the CS equation (44):

$$\left(\mu\frac{\partial}{\partial\mu}+\beta^i(g)\frac{\partial}{\partial g^i}\right)\mathcal{O}=0 \tag{44}$$

The dilation group is the simplest non-trivial Lie group: one-dimensional, abelian, and connected. Its Lie algebra has a single generator $\mathcal{D}$.

This equation is **covariant under scale transformations**: the physics is unchanged under the *combined* transformation $(\mu, g) \to (\lambda\mu, g'(\lambda))$ where the couplings flow according to the beta function. Sending $\mu \to \lambda\mu$ with fixed g does *not* preserve the equation unless $\beta = 0$ (i.e., at a fixed point). Scale transformations form the **dilation group**, and the beta function β^i is precisely its **generator**.

An important distinction: scale transformations on spacetime form a genuine **Lie group** (with inverses). However, the induced RG flow on coupling space is only a **semigroup—**Wilson's coarse-graining integrates out degrees of freedom, and this information loss cannot be reversed. True scale *invariance* of correlation functions holds only at fixed points where $\beta^i(g^*) = 0$.

Mathematically: the dilation group is a 1-parameter Lie group. Physically: the induced RG flow on theory space is a **semigroup**—coarse-graining is irreversible.

The Dilation Group

The operator $\mu\frac{\partial}{\partial\mu}$ in (44) generates scale transformations $\mu \to b\mu$ with $b > 0$. These transformations form a group:

- **Closure**: $(x \to bx)$ composed with $(x \to cx)$ gives $(x \to bcx)$
- **Identity**: $x \to 1 \cdot x$
- **Inverses**: $(x \to bx)^{-1} = (x \to x/b)$
- **Associativity**: composition is associative

This is the **multiplicative group** $(\mathbb{R}^+, \times)$. Taking logarithms, $\ell = \log b$, we obtain an isomorphism to the additive group:

$$(\mathbb{R}^+, \times) \cong (\mathbb{R}, +) \tag{51}$$

The scale parameter ℓ (often called the "RG time") runs from $-\infty$ to $+\infty$.

The Generator and Exponential Map

Every Lie group has an associated **Lie algebra** of infinitesimal transformations. For the dilation group, write $b = e^\epsilon$ for small ϵ:

$$x \to e^\epsilon x \approx x + \epsilon x = (1 + \epsilon\mathcal{D})x \tag{52}$$

where

$$\boxed{\mathcal{D} = x\frac{d}{dx}} \tag{53}$$

is the **dilation generator**. Acting on a function $f(x)$:

$$\mathcal{D}f = x\frac{df}{dx} \tag{54}$$

Finite transformations are recovered by **exponentiation**:

The generator $\mathcal{D} = x\partial/\partial x$ is the infinitesimal dilation. Finite dilations are recovered by exponentiation.

$$D_b = e^{(\log b)\mathcal{D}} \tag{55}$$

Verification: We show that $e^{\epsilon\mathcal{D}}$ acting on $f(x)$ produces $f(e^{\epsilon}x)$. Let $y = \log x$, so $\frac{d}{dy} = x\frac{d}{dx} = \mathcal{D}$. Then:

$$e^{\epsilon\mathcal{D}}f(x) = e^{\epsilon\frac{d}{dy}}f(e^y) = f(e^{y+\epsilon}) = f(e^{\epsilon}x) \tag{56}$$

using the standard result that $e^{a\frac{d}{dy}}g(y) = g(y+a)$.

Higher Dimensions and the Conformal Algebra

In d dimensions, the dilation generator becomes the radial vector field:

$$\mathcal{D} = x^{\mu}\frac{\partial}{\partial x^{\mu}} = \sum_{\mu=1}^{d} x^{\mu}\partial_{\mu} \tag{57}$$

Box 2.2: The Dilation Lie Algebra and Conformal Extensions

Translations and the fundamental commutator:
The translation generators are $P_{\mu} = \partial/\partial x^{\mu}$. Computing $[\mathcal{D}, P_{\mu}]$ on a test function $f(x)$:

$$[\mathcal{D}, P_{\mu}]f = \mathcal{D}(P_{\mu}f) - P_{\mu}(\mathcal{D}f) \tag{58}$$
$$= x^{\nu}\partial_{\nu}(\partial_{\mu}f) - \partial_{\mu}(x^{\nu}\partial_{\nu}f) \tag{59}$$
$$= x^{\nu}\partial_{\nu}\partial_{\mu}f - \delta^{\nu}_{\mu}\partial_{\nu}f - x^{\nu}\partial_{\mu}\partial_{\nu}f \tag{60}$$
$$= -\partial_{\mu}f = -P_{\mu}f \tag{61}$$

Therefore:

$$\boxed{[\mathcal{D}, P_{\mu}] = -P_{\mu}} \tag{62}$$

This says that dilations and translations *don't commute*. Physically, translating then scaling differs from scaling then translating.

The grading structure:
The commutator $[\mathcal{D}, P_{\mu}] = -P_{\mu}$ shows that $\mathcal{D}$ acts as a **grading operator**. Operators with $[\mathcal{D}, \mathcal{O}] = -\Delta\mathcal{O}$ have "grade" (scaling dimension) Δ.
The full conformal algebra (in $d > 2$):

Including special conformal transformations K_μ and rotations $M_{\mu\nu}$:

$$[\mathcal{D}, P_\mu] = -P_\mu \qquad [\mathcal{D}, K_\mu] = K_\mu \tag{63}$$

$$[P_\mu, K_\nu] = 2(\eta_{\mu\nu}\mathcal{D} - M_{\mu\nu}) \qquad [K_\mu, K_\nu] = 0 \tag{64}$$

The translations P_μ have grade -1, the special conformal generators K_μ have grade $+1$, and $\mathcal{D}$ has grade 0. This is the Lie algebra $\mathfrak{so}(d+1,1)$ in Euclidean signature; in Lorentzian signature the algebra is $\mathfrak{so}(d,2)$.

Scheme Transformations as Reparametrizations

The CS equation (44) holds in *any* renormalization scheme. The beta function transforms **covariantly**—this is the vector field transformation law.

In Section I, we found that the CS equation (44) is covariant under scale transformations, with β^i as the generator. There is a second structure: the equation holds regardless of how we parameterize the couplings.

The beta function $\beta^i(g)$ depends on our choice of **renormalization scheme**—MS, $\overline{\text{MS}}$, on-shell, or momentum subtraction schemes give different values for β^i. Yet the *structure* of the CS equation is unchanged. The beta function transforms **covariantly** under scheme changes—this is exactly how a vector field transforms under coordinate changes on a manifold. What's invariant is the equivalence class of physical predictions, not the explicit form of β.

Not every smooth reparametrization $g \to g'(g)$ corresponds to a physically allowed renormalization scheme change, but mathematically, treating them as diffeomorphisms of theory space is the correct abstraction.

How Beta Functions Transform

A **renormalization scheme** defines how we parameterize theory space. A scheme change is a smooth, invertible map:

$$g^i \to g'^i(g) \tag{65}$$

For the CS equation (44) to hold in *both* schemes, the beta function must transform as:

$$\boxed{\beta'^i(g') = \frac{\partial g'^i}{\partial g^j}\beta^j(g)} \tag{66}$$

This is the **vector field transformation law**: under coordinate changes $g^i \to g'^i(g)$, a vector field transforms as $V'^i = (\partial g'^i/\partial g^j)V^j$. Equation (66) is not a definition but a *consequence* of requiring the CS equation to hold in any scheme—it confirms that β is a vector field on theory space.

The **Lie algebra of scheme transformations** is the space of vector fields $\xi^i\partial_i$ on $\mathcal{M}$. The Lie bracket:

$$[\xi, \eta]^i = \xi^j \partial_j \eta^i - \eta^j \partial_j \xi^i \tag{67}$$

encodes how infinitesimal scheme changes compose.

Algebraic Invariants

Invariants under scheme changes:

- **Fixed points**: $\beta^i(g^*) = 0$ is coordinate-independent
- **Stability eigenvalues**: eigenvalues of $\partial_i\beta^j|_{g^*}$ at fixed points
- **c-function values**: $c(g^*)$ at fixed points

These are **algebraic invariants**—unchanged by scheme automorphisms.

Scheme-dependent quantities:

- Beta function coefficients beyond leading order
- Anomalous dimensions (except at fixed points)
- The "location" of fixed points in coupling space

Box 2.3: Diffeomorphism Invariance of Critical Exponents

Goal: Verify that critical exponents are diffeomorphism-invariant.
Algebraic setup:
The stability matrix at a fixed point g^* is:

$$M^i{}_j = \left.\frac{\partial \beta^i}{\partial g^j}\right|_{g^*} \tag{68}$$

Its eigenvalues $\{y_\alpha\}$ determine the RG eigenvalues (critical exponents).
Transformation under scheme change:
Under $g \to g'(g)$, the stability matrix transforms as:

$$M'^i{}_j = \left.\frac{\partial g'^i}{\partial g^k}\right|_{g^*} M^k{}_l \left.\frac{\partial g^l}{\partial g'^j}\right|_{g'^*} \tag{69}$$

This is a **similarity transformation**: $M' = PMP^{-1}$ where $P^i{}_j = \partial g'^i/\partial g^j$.

The key theorem: Similarity transformations preserve eigenvalues:

$$\det(M' - y\mathbf{1}) = \det(PMP^{-1} - y\mathbf{1}) = \det(M - y\mathbf{1}) \tag{70}$$

Therefore: **Critical exponents are scheme-independent.**
Physical interpretation:

- $y > 0$: **Relevant** perturbation (grows toward IR)
- $y = 0$: **Marginal** perturbation
- $y < 0$: **Irrelevant** perturbation (decays toward IR)

The classification relevant/marginal/irrelevant is **intrinsic** to the fixed point, not to any particular scheme.

Scaling Dimensions: Eigenvalues of the Generator

Scaling dimensions are eigenvalues of the dilation generator (53)—they classify representations of the symmetry group.

In Section I, we identified the dilation generator $\mathcal{D} = x\frac{d}{dx}$. The **scaling dimension** Δ of a quantity Φ is its **eigenvalue** under $\mathcal{D}$:

$$\mathcal{D}\Phi = \Delta\Phi \tag{71}$$

Equivalently, $\Phi \to b^{\Delta}\Phi$ under the finite transformation $x \to bx$. The dimension Δ labels the **representation** of the dilation group that Φ carries—just as spin labels representations of the rotation group.

Engineering vs Anomalous Dimensions

Engineering dimensions come from dimensional analysis alone. For a scalar field in d dimensions, $[\phi] = (d-2)/2$ in mass units.

Anomalous dimensions are corrections from interactions:

$$\Delta = \Delta_{\text{eng}} + \gamma(g) \tag{72}$$

The anomalous dimension $\gamma(g)$ vanishes at the free-field (Gaussian) fixed point and is generally nonzero at interacting fixed points.

Classification of Perturbations

Near a fixed point g^*, perturbations are classified by their scaling dimensions. These are the **eigenvalues of the linearized RG generator**—specifically, the eigenvalues y_α of the Jacobian matrix $M^i{}_j = \partial\beta^i/\partial g^j|_{g^*}$. These RG eigenvalues are related to scaling dimensions via $y = d - \Delta$:

Type	**Eigenvalue**	**Behavior under RG**
Relevant	$y > 0$	Grows (flows away from fixed point)
Marginal	$y = 0$	Unchanged at linear order
Irrelevant	$y < 0$	Decays (flows toward fixed point)

This classification is scheme-independent (as we showed in Box 2.3) and determines the universal behavior near phase transitions.

At the Gaussian fixed point, $y = d - \Delta_{\text{eng}}$. At interacting fixed points, $y = d - \Delta = d - \Delta_{\text{eng}} - \gamma$.

In Part II, we found two covariance structures of the Callan-Symanzik equation (44):

Part III develops the complete geometric structure: manifold, vector field, connection, and metric—each layer building on the previous.

- **Scale covariance**: the dilation group (Section I)
- **Scheme covariance**: reparametrizations $g^i \to g'^i(g)$ with the transformation law (66) (Section I)

These two structures are not independent—they are *two aspects of the same geometry*. The transformation law (66) is precisely how a **vector field transforms under coordinate changes**. This observation reveals that:

> Theory space is a **manifold**. The beta function is a **vector field** on this manifold. Scheme transformations are **coordinate changes**. The CS equation says physical observables are constant along the flow.

Part III develops the complete geometric realization, building layer by layer:

1. **Manifold**: The couplings g^i are coordinates (Section I)
2. **Vector field**: The beta function $\boldsymbol{\beta}$ generates the RG flow
3. **Connection**: The anomalous dimension γ tells us how to parallel-transport operators (Section I)
4. **Metric**: The Fisher metric G_{ab} measures distances between theories (Section I)
5. **Gradient flow**: When $\boldsymbol{\beta}$ is a gradient, the c-theorem follows (Section I)
6. **Geodesics**: The "straightest paths" through theory space (Section I)

Each layer adds structure: topology $\to$ differential $\to$ parallel transport $\to$ distance $\to$ curvature.

Parameter Space as a Manifold

Scheme transformations (65) are coordinate changes on a manifold. The couplings g^i are coordinates.

Return to the scheme transformation (65):

$$g^i \to g'^i(g) \tag{65}$$

This is exactly the definition of a **coordinate change on a manifold**. The collection of all couplings $(g^1, g^2, \ldots, g^n)$ forms a coordinate chart on a space $\mathcal{M}$ called **theory space** or **parameter space**. As we change scale, we trace out a curve in $\mathcal{M}$.

The Beta Function as a Vector Field

The RG equation (44) defines the evolution of couplings with scale. Writing $\ell = \log(\mu/\mu_0)$ as "RG time," the couplings evolve as:

$$\frac{dg^i}{d\ell} = \beta^i(g) \tag{73}$$

This is the same information as the CS equation (44), now written as an ODE on parameter space. The components $\beta^i(g)$ assemble into a **vector field**:

$$\boldsymbol{\beta} = \beta^i(g)\frac{\partial}{\partial g^i} \tag{74}$$

Why is this a vector field? The transformation law (66) is the *defining property* of a vector field: under coordinate changes $g^i \to g'^i(g)$, a vector field transforms as $V'^i = (\partial g'^i/\partial g^j)V^j$. We derived (66) from requiring scheme independence—so the beta function *must be* a vector field.

RG Flows as Integral Curves

Solutions to the ODE (73) are curves $g^i(\ell)$ in parameter space. Geometrically, these are the **integral curves** of the vector field (74)—curves everywhere tangent to $\boldsymbol{\beta}$. These integral curves are the **RG trajectories**.

The finite RG transformation from scale $\ell = 0$ to scale ℓ is:

$$R_\ell = e^{\ell\boldsymbol{\beta}} \tag{75}$$

The collection $\{R_\ell : \ell \in \mathbb{R}\}$ forms a **one-parameter group of diffeomorphisms**. This is the geometric realization of the dilation Lie group from Section I: the abstract group acts on theory space by moving points along integral curves.

Fixed Points as Zeros

A **fixed point** is where the beta function vanishes:

$$\beta^i(g^*) = 0 \quad \text{for all } i \tag{76}$$

At a fixed point, the system doesn't change under scale transformations—it is **scale-invariant**. In the Lie group language, fixed points are points **invariant under the group action**.

Fixed points are the "destinations" of RG flows. They represent scale-invariant physics.

The stability of a fixed point determines the flow in its neighborhood:

- **Stable** (attractive): nearby trajectories flow toward the fixed point
- **Unstable** (repulsive): nearby trajectories flow away
- **Saddle**: attractive in some directions, repulsive in others

The CS Equation as Lie Derivative

The Callan-Symanzik equation (44) has natural geometric content. Recall:

$$\left(\mu\frac{\partial}{\partial\mu} + \beta^i(g)\frac{\partial}{\partial g^i}\right)\mathcal{O} = 0 \tag{44}$$

The CS equation (44) *is* the statement that observables have vanishing Lie derivative along the RG flow.

The operator in parentheses is exactly the **Lie derivative** L_V of a scalar function along the vector field:

$$\boldsymbol{V} = \mu\frac{\partial}{\partial\mu} + \beta^i(g)\frac{\partial}{\partial g^i} \tag{77}$$

Strictly speaking, this vector field $\boldsymbol{V}$ lives on **extended space** $\mathcal{X} = \mathbb{R}_\mu \times \mathcal{M}_g$ with coordinates (μ, g^i). By convention, we treat μ as the flow parameter ("RG time") and reserve **theory space** $\mathcal{M}$ for the coupling manifold alone. The projection of $\boldsymbol{V}$ onto $\mathcal{M}$ is the beta function vector field $\boldsymbol{\beta} = \beta^i(g)\partial_{g^i}$.

The RG vector field $\boldsymbol{V}$ lives on extended space (μ, g). The projected vector field $\boldsymbol{\beta}$ lives on theory space $\mathcal{M}$.

Thus the CS equation becomes:

$$\boxed{L_{\boldsymbol{V}}\mathcal{O} = 0} \tag{78}$$

where $L_{\boldsymbol{V}}$ denotes the Lie derivative of the scalar function $\mathcal{O}$ along $\boldsymbol{V}$.

Physical meaning: As we change scale, the couplings run according to (73). Observables are "Lie dragged" along this flow. The condition (78) means $\mathcal{O}$ is invariant under this dragging—it doesn't change as we move along the RG trajectory. This is scale independence expressed geometrically.

Finite RG Transformations

The finite RG transformation is the exponential of the vector field:

$$R_\ell = e^{\ell\boldsymbol{\beta}} \tag{79}$$

Acting on coordinates:

$$R_\ell : g^i \mapsto \bar{g}^i(\ell; g) \tag{80}$$

where $\bar{g}^i(\ell; g)$ is the solution to $d\bar{g}^i/d\ell = \beta^i(\bar{g})$ with initial condition $\bar{g}^i(0) = g^i$.

The group composition law is:

$$R_{\ell_1} \circ R_{\ell_2} = R_{\ell_1+\ell_2} \tag{81}$$

Connections: The Anomalous Dimension as Geometry

The simple CS equation (44) governs scalar observables. The full CS equation (48) includes the anomalous dimension γ:

$$\left(\mu\frac{\partial}{\partial\mu} + \beta^i\frac{\partial}{\partial g^i} + n\gamma\right)G_n = 0 \tag{48}$$

The full CS equation (48) includes anomalous dimensions. These are **connection coefficients**—the geometric structure that tells operators how to "rotate" as we move through theory space.

What is the geometric meaning of γ? When multiple operators can mix under RG, we need a **fiber bundle**: the parameters live on the base manifold $\mathcal{M}$, while operators live in fibers attached to each point. A **connection** on this bundle tells us how to compare operators at different points—and the anomalous dimension *is* this connection.

Bundle Component	**RG Interpretation**
Base manifold $\mathcal{M}$	Theory space (couplings g^i)
Fiber at g	Space of renormalized operators $\{\mathcal{O}_a\}$
Structure group	$\mathrm{GL}(n)$ acting on operator basis
Connection 1-form	$\Gamma_a{}^b = -\gamma_a{}^b$ (anomalous dimension)
Curvature	$R^a{}_{bcd}$ (scheme-independent data)

The Anomalous Dimension as Connection

Notation: We use $\gamma_a{}^b$ for the **anomalous dimension matrix** and set $\Gamma_a{}^b = -\gamma_a{}^b$ as the **connection coefficients**. The Christoffel symbols Γ^i_{jk} of the Fisher metric on coupling space (Section I) are a distinct object—a metric connection on the base $\mathcal{M}$, not on the operator bundle.

The RG equation for operators can be written as:

$$D_\mu \mathcal{O}_a \equiv \mu \frac{\partial \mathcal{O}_a}{\partial \mu} + \Gamma_a{}^b\, \mathcal{O}_b = 0 \tag{82}$$

where $\Gamma_a{}^b = -\gamma_a{}^b$ are the connection coefficients.

This is the **parallel transport equation**: operators are covariantly constant along the RG flow.

Operator Mixing

When the connection has off-diagonal components, operators **mix** under RG evolution:

$$\gamma = \begin{pmatrix} \gamma_{\phi^2} & \gamma_{\phi^2 \leftarrow \phi^4} \\ 0 & \gamma_{\phi^4} \end{pmatrix} \tag{83}$$

The off-diagonal entry means that ϕ^4 "generates" ϕ^2 under RG flow.

The solution involves path-ordered exponentials:

$$\mathcal{O}(\mu) = \mathcal{P} \exp\left(\int_{\mu_0}^{\mu} \gamma(g(\mu'))\frac{d\mu'}{\mu'} \right) \mathcal{O}(\mu_0) \tag{84}$$

Scaling Operators

The **scaling operators** are eigenvectors of the anomalous dimension matrix:

$$\gamma \tilde{\mathcal{O}}_\alpha = \Delta_\alpha \tilde{\mathcal{O}}_\alpha \tag{85}$$

These have simple RG evolution:

$$\tilde{\mathcal{O}}_\alpha(\mu) = \left(\frac{\mu}{\mu_0}\right)^{-\Delta_\alpha} \tilde{\mathcal{O}}_\alpha(\mu_0) \tag{86}$$

At a fixed point, the scaling operators are the **primary operators** of the conformal field theory, and Δ_α are their conformal dimensions.

Curvature and Scheme Independence

From the connection, we can compute the **curvature tensor**:

$$R^k{}_{ilj} = \partial_i \Gamma^k{}_{lj} - \partial_l \Gamma^k{}_{ij} + \Gamma^k{}_{im}\Gamma^m{}_{lj} - \Gamma^k{}_{lm}\Gamma^m{}_{ij} \tag{87}$$

Key property: The curvature tensor is a **tensor**—it transforms homogeneously under scheme changes. Curvature invariants (like $R^i{}_{ijk}R^{jkl}{}_l$) are scheme-independent and characterize the theory space geometry.

The Fisher Metric on Theory Space

We have a manifold, a vector field, and a connection. The next layer of geometric structure is a **metric**—a way to measure distances.

We have now established:

- Theory space $\mathcal{M}$ is a manifold with coordinates g^i (Section I)
- The beta function (74) is a vector field generating the RG flow (73)
- The anomalous dimension $\gamma_a{}^b$ is a connection for parallel-transporting operators

A natural question arises: Can we measure **distances** on $\mathcal{M}$? If two theories have couplings g and $g + dg$, how "far apart" are they?

The answer comes from information geometry: the **Fisher information metric**.

The Metric from the Partition Function

Consider the partition function $Z[g]$ as a function of couplings g^a. The natural metric is:

$$G_{ab} = -\frac{\partial^2 \log Z}{\partial g^a \partial g^b} = \langle \mathcal{O}_a \mathcal{O}_b \rangle_{\text{conn}} \tag{88}$$

This is the **Fisher information metric**—the same metric that appears in information geometry and statistics. It measures how distinguishable two nearby probability distributions (theories) are.

The Fisher metric (from probability theory) and the Zamolodchikov metric (from 2-point functions) are conceptually distinct but coincide under certain conditions.

Important distinction: The Fisher information metric arises from probability distributions; the **Zamolodchikov metric** (below) arises from 2-point functions of perturbing operators in CFT. These are conceptually distinct constructions that coincide under certain conditions—at conformal fixed points in unitary theories.

Box 2.14: Fisher Metric in ϕ^4 Theory

Setup: Consider d-dimensional ϕ^4 theory with couplings (r, λ).
The metric components:

$$G_{rr} = \frac{1}{4} \int d^d x\, d^d y\, \langle \phi^2(x) \phi^2(y) \rangle_{\text{conn}} = \frac{1}{4} \chi_{\phi^2} \tag{89}$$

$$G_{r\lambda} = \frac{1}{48} \int d^d x\, d^d y\, \langle \phi^2(x) \phi^4(y) \rangle_{\text{conn}} \tag{90}$$

$$G_{\lambda\lambda} = \frac{1}{576} \int d^d x\, d^d y\, \langle \phi^4(x) \phi^4(y) \rangle_{\text{conn}} \tag{91}$$

Physical meaning: G_{rr} is proportional to the susceptibility χ, which measures fluctuations.
Near criticality: As $r \to r_c$, the susceptibility diverges: $\chi \sim |r - r_c|^{-\gamma}$.
Therefore $G_{rr} \to \infty$ at the critical point—critical theories are "infinitely far" from non-critical theories in the metric sense.
One-loop calculation (1D): Using the propagator $G(x) = e^{-m|x|}/(2m)$ with $m = \sqrt{r}$:

$$G_{rr} = \frac{1}{4} \cdot 2 \int_{-\infty}^{\infty} dx\, G(x)^2 = \frac{1}{4} \cdot \frac{1}{2m^3} = \frac{1}{8r^{3/2}} \tag{92}$$

The Zamolodchikov Metric

At conformal fixed points, there is a canonical normalization. The **Zamolodchikov metric** extracts the coefficient from the OPE:

$$\langle \mathcal{O}_a(x) \mathcal{O}_b(0) \rangle = \frac{G_{ab}^{(\text{Zam})}}{|x|^{\Delta_a + \Delta_b}} \tag{93}$$

This metric is finite and positive at the fixed point, providing a natural inner product on the space of operators.

Gradient Flow and the c-Theorem

Having equipped theory space with the metric (88), we can ask a powerful question: Is the beta function (74) the gradient of a potential?

With the metric G_{ab} from (88), we can ask: Is the RG vector field (74) a **gradient**?

Gradient flow ansatz:

$$\beta^a = -G^{ab} \frac{\partial W}{\partial g^b} \tag{94}$$

for some potential $W(g)$.

Warning: Gradient flow is **not automatic**. For (94) to hold, the **integrability condition** $\partial_a \beta_b = \partial_b \beta_a$ (where $\beta_a = G_{ab} \beta^b$) must be satisfied.

Gradient flow is **not** automatic. The integrability condition $d\beta^\flat = 0$ must be verified. This holds in 2D unitary QFT but may fail in higher dimensions.

In the language of differential forms, $d\beta^\flat = 0$ where $\beta^\flat$ is the 1-form associated to β. Zamolodchikov proved this holds in 2D unitary QFT; in higher dimensions or non-unitary theories, only quasi-gradient structure may exist (see Box 2.18).

Consequences of Gradient Flow

When gradient flow holds (and it must be checked!):

- **Monotonicity:** $\frac{dW}{d\ell} = -G_{ab}\beta^a\beta^b \leq 0$
- **No limit cycles:** If W decreases, flows cannot return to previous points
- **Fixed points are critical points:** At $\beta = 0$, we have $\nabla W = 0$

Zamolodchikov's c-Theorem

The most famous monotonicity result is the **c-theorem** in $d = 2$:

Theorem 0.2 (Zamolodchikov, 1986)**.** *In any unitary 2D QFT, there exists a function $c(\ell)$ along RG trajectories such that:*

1. *c decreases monotonically: $dc/d\ell \leq 0$*
2. *At fixed points, c equals the central charge*
3. *$dc/d\ell = 0$ only at fixed points*

Geometric interpretation: The c-theorem says RG flow is gradient flow with respect to the Zamolodchikov metric. The "c-function" is the potential W, and unitarity ensures the metric is positive-definite.

Higher-Dimensional Generalizations

The c-theorem generalizes to other dimensions:

d	Quantity	Theorem
2	Central charge c	c-theorem (Zamolodchikov, 1986)
3	Sphere free energy $F = -\log Z_{S^3}$	F-theorem (JKPS, 2011)
4	Euler anomaly a	a-theorem (Komargodski-Schwimmer, 2011)

All theorems require **unitarity** and state that "degrees of freedom" decrease under RG.

Geodesic Flow and Curved Motion

The metric (88) defines geodesics—the "straightest paths" through theory space.

Section I asked whether the RG flow (73) is a *gradient* flow. Here we ask a different question: Is it a *geodesic* flow?

The metric G_{ab} from (88) defines a notion of "straight lines" on theory space—the geodesics. Dolan's striking result is that RG flows can sometimes be interpreted as geodesics, connecting the RG to classical mechanics in curved spacetime.

The Geodesic Equation

A curve $g^i(\ell)$ is a geodesic if it satisfies:

$$\frac{d^2g^i}{d\ell^2} + \Gamma^i_{jk}\frac{dg^j}{d\ell}\frac{dg^k}{d\ell} = 0 \tag{95}$$

where Γ^i_{jk} are the Christoffel symbols of the metric G_{ab}.

Since $dg^i/d\ell = \beta^i$, the RG flow is geodesic if and only if:

$$\beta^j\partial_j\beta^i + \Gamma^i_{jk}\beta^j\beta^k = 0 \tag{96}$$

This is the **autoparallel condition**: the "velocity" β is parallel-transported along itself.

Geodesic Deviation and Stability

Even when RG flows are not exactly geodesic, geodesic deviation measures how nearby flows separate:

$$\frac{D^2\xi^i}{D\ell^2} + R^i{}_{jkl}\beta^j\xi^k\beta^l = 0 \tag{97}$$

This **Jacobi equation** connects the Riemann curvature R^i_{jkl} to stability: positive curvature focuses nearby geodesics, negative curvature disperses them.

Near a fixed point, the stability matrix $M^i_j = \partial\beta^i/\partial g^j|_{g^*}$ determines whether flows converge or diverge—and curvature provides corrections to this linear analysis.

Part IV synthesizes Parts II and III: the symmetry structure (scale + scheme invariance) and the geometric realization (manifold + vector field + connection) unify into a **gauge bundle**.

We have now assembled several geometric structures:

- Theory space is a **manifold** $\mathcal{M}$ (Section I)
- The beta function is a **vector field** (74) transforming as (66)
- The anomalous dimension is a **connection** (Section I)
- Scheme changes act as diffeomorphisms on $\mathcal{M}$ *and* as gauge transformations on operators

These structures are not independent—they combine into a single geometric object: a **principal bundle** over theory space. This unification explains why both diffeomorphisms and gauge transformations appear: they are two aspects of the same bundle structure.

Theory Space as a Gauge Bundle

To see the bundle structure, observe that scheme changes act on *two* objects simultaneously:

The transformation (66) of β and the transformation of γ (Eq. (100)) are two parts of a single gauge transformation on a bundle.

- **Scheme changes**: reparameterizations $g^i \to g'^i(g)$ of coupling space
- **Operator redefinitions**: $\mathcal{O}_a \to U_a{}^b(g)\mathcal{O}_b$

These are not separate structures—they are two aspects of the same geometric object: a **principal bundle** over theory space.

The Bundle Structure

The complete geometric picture is:

Bundle Component	**RG Interpretation**
Base manifold $\mathcal{M}$	Coupling space (theory space)
Fiber F at g	Space of operators at coupling g
Structure group G	Operator mixing group (e.g., GL(n))
Connection $\Gamma_a{}^b$	Anomalous dimension matrix
Curvature $R^a{}_{bcd}$	Scheme-independent observables
Section $\sigma : \mathcal{M} \to E$	Choice of operator basis

Scheme Changes as Gauge Transformations

The key insight, emphasized by Dolan, is that a scheme change acts *simultaneously* on the base and fiber:

On the base (coupling space):

$$g^i \to g'^i(g) \tag{98}$$

This is a diffeomorphism of the base manifold $\mathcal{M}$.

On the fiber (operators):

$$\mathcal{O}'_a = U_a{}^b(g)\, \mathcal{O}_b \tag{99}$$

This is a gauge transformation in the fiber.

The connection transforms as:

$$\boxed{\gamma'^{\,b}_a = U_a{}^c\, \gamma_c{}^d\, (U^{-1})_d{}^b + \mu \frac{dU_a{}^c}{d\mu} (U^{-1})_c{}^b} \tag{100}$$

This is *exactly* the gauge transformation law for a connection! The first term is the adjoint action; the second is the inhomogeneous "derivative term" characteristic of connections.

Box 2.10: Why Scheme Independence is Gauge Invariance

The analogy:

Gauge Theory	RG
Gauge potential A_μ	Anomalous dimension $\gamma_a{}^b$
Gauge transformation $g(x)$	Scheme change $U(g)$
$A'_\mu = gA_\mu g^{-1} + g\partial_\mu g^{-1}$	$\gamma' = U\gamma U^{-1} + \mu(dU/d\mu)U^{-1}$
Field strength $F_{\mu\nu}$	Curvature $R^a{}_{bcd}$
Wilson loop	Monodromy around loop in $\mathcal{M}$

Physical consequences:

- **Gauge-dependent** (scheme-dependent): $\gamma_a{}^b$, location of fixed points, beta function coefficients beyond leading order
- **Gauge-invariant** (physical): eigenvalues of γ at fixed points (critical exponents), curvature invariants, monodromy

The deep point: Just as in Yang-Mills theory the physics is in the gauge-invariant quantities (field strength, Wilson loops), in RG the physics is in the scheme-invariant quantities (critical exponents, curvature invariants).
The scheme-dependence of intermediate quantities like $\gamma_a{}^b$ is not a bug—it's the freedom to choose convenient coordinates, exactly like choosing a gauge in electromagnetism.

Gauge-Invariant Observables

Which quantities are scheme-independent? Precisely those that are **gauge-invariant**:

At fixed points:

- Eigenvalues of $\gamma_a{}^b|_{g^*}$ (critical exponents/anomalous dimensions)
- Trace invariants: $\mathrm{tr}(\gamma)$, $\mathrm{tr}(\gamma^2)$, etc.

Globally:

- Curvature tensor $R^a{}_{bcd}$ (transforms homogeneously)
- Curvature invariants: $R^a{}_{bab}$, $R^a{}_{bcd}R^{bcd}{}_a$, etc.
- Monodromy around closed loops in coupling space

Physical correlation functions: These are sections of the bundle, not the connection itself. They transform covariantly and give scheme-independent predictions when properly renormalized.

The Covariant Derivative on Operators

The RG equation for operators can be written covariantly:

$$\nabla_\mu \mathcal{O}_a \equiv \mu \frac{\partial \mathcal{O}_a}{\partial \mu} + \gamma_a{}^b \, \mathcal{O}_b = 0 \tag{101}$$

This says operators are **covariantly constant** along the RG flow—they are parallel-transported by the connection γ.

The solution is the **Wilson line** (path-ordered exponential):

$$\mathcal{O}_a(\mu) = \left[\mathcal{P} \exp\left(-\int_{\mu_0}^{\mu} \gamma(g(\mu')) \frac{d\mu'}{\mu'}\right)\right]_a{}^b \mathcal{O}_b(\mu_0) \tag{102}$$

The Wilson line in RG is the same object as in gauge theory: the parallel transport of operators along the RG trajectory.

Box 2.11: Monodromy and Stokes Phenomena

Goal: Show that monodromy in coupling space connects to resurgent structure.

The setup: Consider a closed loop $\mathcal{C}$ in coupling space. The monodromy is:

$$M(\mathcal{C}) = \mathcal{P} \exp\left(-\oint_{\mathcal{C}} \gamma_a{}^b \, dg\right) \tag{103}$$

For a flat connection ($R = 0$): Monodromy depends only on the homotopy class of $\mathcal{C}$, giving a representation:

$$\rho : \pi_1(\mathcal{M}) \to G \tag{104}$$

Connection to Stokes phenomena:

When the connection is flat but has singularities (e.g., at Landau poles), circling a singularity produces non-trivial monodromy. This is the **same** monodromy that appears in resurgent analysis:

- Singularities in Borel plane $\leftrightarrow$ singularities in coupling space
- Stokes constants $\leftrightarrow$ monodromy matrices
- Stokes lines $\leftrightarrow$ branch cuts in $\mathcal{M}$

Physical content: The Stokes constants that appear in transseries (Part II) are not arbitrary—they are **topological data** encoded in the monodromy representation. This explains why Stokes constants are often integers or simple algebraic numbers.

The connection between RG geometry and resurgence is developed fully in Chapter II.

The Diffeomorphism-Gauge Unification

We can now answer the question raised at the beginning of this chapter: *Are scheme changes diffeomorphisms or gauge transformations?*

Answer: They are *both*, acting on different parts of the bundle:

Scheme change = Diffeomorphism on base $\mathcal{M}$ + Gauge transformation on fiber F

The beta function β^i is a vector field on the base, transforming as:

$$\beta'^i = \frac{\partial g'^i}{\partial g^j}\beta^j \quad \text{(vector field transformation)} \tag{105}$$

The anomalous dimension ${\gamma_a}^b$ is a connection on the bundle, transforming as in Eq. (100).

Critical exponents are gauge-invariant because they are eigenvalues of γ at fixed points where $\beta = 0$. At a fixed point, the inhomogeneous term in the gauge transformation law vanishes (since $\mu\, dU/d\mu = \beta^i \partial_i U = 0$), and eigenvalues are preserved under similarity transformation.

How Geometry Constrains Beta Functions

The bundle structure of Section I is not merely descriptive—it imposes **constraints** on the form of beta functions.

We have established that theory space is a gauge bundle (Section I), with the beta function transforming as (66) and the anomalous dimension as (100). But this geometric structure does more than organize our equations—it **constrains** them.

The central question: To what extent does geometry constrain the physics?

The answer has three parts:

1. **Integrability conditions** constrain the beta function
2. **Metric positivity** forces monotonicity (c-theorem)
3. **Specific values** still require dynamical computation

The Integrability Condition

Consider the possibility that RG flow is **gradient flow**: the beta function derives from a potential.

Gradient flow ansatz:

$$\beta^i = G^{ij}\frac{\partial W}{\partial g^j} \tag{106}$$

for some potential $W(g)$ and metric G_{ij}.

Lowering the index: $\beta_i \equiv G_{ij}\beta^j = \partial_i W$. This requires:

$$\boxed{\partial_i \beta_j = \partial_j \beta_i \quad \text{(integrability condition)}} \tag{107}$$

In differential forms language: $d\beta^\flat = 0$ where $\beta^\flat = \beta_i \, dg^i$ is the 1-form associated to β.

The integrability condition $d\beta^\flat = 0$ is the **cocycle condition** in de Rham cohomology. When satisfied, $\beta^\flat = dW$ for some potential W.

When integrability holds:

- A potential W exists (the c-function)
- W decreases monotonically along flows: $\frac{dW}{d\ell} = G_{ij}\beta^i\beta^j \geq 0$
- No limit cycles are possible
- Fixed points are critical points of W

When integrability fails:

- No global c-function exists
- Limit cycles in coupling space become possible
- The c-theorem fails

Box 2.12: Dolan's Verification of Integrability

Goal: Check whether integrability holds in ϕ^4 + Yukawa theory (Dolan, 1994).

The model: A scalar ϕ with self-coupling λ and Yukawa coupling g to a fermion:

$$\mathcal{L} = \frac{1}{2}(\partial\phi)^2 + \frac{\lambda}{4!}\phi^4 + \bar{\psi}(i\partial\!\!\!/ - m)\psi + g\phi\bar{\psi}\psi \tag{108}$$

The beta functions (to two loops):

$$\beta_\lambda = -\epsilon\lambda + a_1\lambda^2 + a_2 g^2\lambda + a_3 g^4 + O(\lambda^3, g^6) \tag{109}$$

$$\beta_g = -\frac{\epsilon}{2}g + b_1 g\lambda + b_2 g^3 + O(g^5, \lambda^2 g) \tag{110}$$

The integrability test:

$$\frac{\partial\beta_\lambda}{\partial g} \stackrel{?}{=} \frac{\partial\beta_g}{\partial\lambda} \tag{111}$$

Computing:

$$\frac{\partial\beta_\lambda}{\partial g} = 2a_2 g\lambda + 4a_3 g^3 + \cdots \tag{112}$$

$$\frac{\partial\beta_g}{\partial\lambda} = b_1 g + \cdots \tag{113}$$

Result: Dolan verified to sixth order in couplings that these are equal when the metric G_{ij} is chosen correctly. The RG flow **is** potential flow in this model.

The metric: The required metric is the Zamolodchikov metric from two-point functions:

$$G_{ij} = \int d^d x \, \langle \mathcal{O}_i(x) \mathcal{O}_j(0) \rangle_{\text{conn}} \tag{114}$$

Physical content: Integrability is not automatic—it must be verified order by order. When it holds, the c-theorem follows as a consequence.

What Geometry Determines vs. What Requires Computation

The geometric framework provides powerful constraints but does not determine everything:

Geometry Determines	Dynamics Determines
Scheme independence of critical exponents	Numerical values of exponents
c-theorem monotonicity (given integrability)	Value of c at fixed points
Classification of fixed points by stability	Location of fixed points in $\mathcal{M}$
Curvature invariants as observables	Specific curvature values
Monodromy representation of $\pi_1(\mathcal{M})$	Stokes constants

Geometry tells us *what* is observable. Dynamics tells us the *values* of observables.

The analogy with general relativity:

- Einstein's equations constrain the metric $g_{\mu\nu}$
- But solving them requires specifying matter content and boundary conditions
- Similarly, RG geometry constrains beta functions, but specific values require the dynamics (Feynman diagrams, functional RG, etc.)

Conformal Constraints at Fixed Points

At fixed points with conformal symmetry, additional algebraic constraints apply beyond $\beta = 0$.

Scale invariance (automatic at fixed points): $\beta^i(g^*) = 0$

Conformal invariance (under mild conditions): The stress tensor is traceless and "improvement-conserved."

Conformal Ward identities provide additional constraints on correlation functions and operator dimensions. These are *algebraic*—they follow from symmetry alone, without dynamical computation.

Box 2.13: Conformal Constraints on the Derivative Expansion

The context: In the exact renormalization group (ERG), the effective action is expanded:

$$\Gamma[\phi] = \int d^d x \left[V(\phi) + \frac{1}{2} Z(\phi)(\partial\phi)^2 + O(\partial^4) \right] \tag{115}$$

At the Local Potential Approximation (LPA): Only $V(\phi)$ is kept. The fixed point condition $\beta_V = 0$ gives a nonlinear ODE for $V^*(\phi)$.
At $O(\partial^2)$: Including $Z(\phi)$ adds another equation. But now **conformal Ward identities** provide an additional constraint relating $V''(\phi)$ and $Z(\phi)$:

$$Z(\phi) = \left(\frac{d-2+\eta}{d-2} \right) \frac{V''(\phi)}{\lambda^*} + \text{corrections} \tag{116}$$

The improvement: Including conformal constraints improves numerical accuracy:

Method	η (3D Ising)
LPA only	0.027
LPA + conformal constraint	0.036
Bootstrap (exact)	0.0363

The lesson: Conformal symmetry at fixed points provides *additional geometric constraints* beyond the flow equations. These are consequences of the enhanced symmetry at scale-invariant points.

Summary: The Role of Geometry

Geometry constrains but does not **determine**:

- **Constrains:** What is physical (gauge-invariant), monotonicity (c-theorem), fixed-point classification
- **Requires dynamics:** Numerical values, specific beta functions, fixed-point locations

The geometric viewpoint is not merely organizational—it identifies which quantities are truly physical and reveals deep connections (e.g., monodromy = Stokes constants). But computing specific numbers still requires the dynamical methods of Parts II and III.

Parts II–IV developed the theoretical framework:

Part V demonstrates the framework of Parts II–IV through explicit calculations, showing how the CS equation (44), the vector field (74), and the geometric structures work in practice.

- The CS equation (44) as the fundamental equation
- Its symmetries: scale invariance (Section I) and scheme invariance (Section I)
- The geometric realization: manifold, vector field (74), connection (Part III)
- The unified bundle structure (Part IV)
- The metric and its consequences (Part V)

We now demonstrate this framework through four examples of increasing complexity, showing how the same structure appears across physics.

Example 1: The Anharmonic Oscillator

Our first example applies the full framework to the damped anharmonic oscillator from the Prologue. This example demonstrates the CS equation (44), beta functions as a vector field (74), and RG flows as integral curves—all in an exactly solvable setting.

The oscillator demonstrates the CS equation (44), the ODE (73), and the geometric interpretation without computational complications.

The Physical System

The equation of motion is:

$$\ddot{x} + 2\gamma\dot{x} + \omega_0^2 x + \epsilon x^3 = 0 \tag{117}$$

where $\gamma > 0$ is the damping coefficient (assumed small for the perturbative analysis) and ϵ is the anharmonic coupling.

Parameter Space

The relevant parameters for long-time behavior are amplitude $A \geq 0$ and phase $\phi \in [0, 2\pi)$:

$$\mathcal{M}_{\text{osc}} = \{(A, \phi) : A \geq 0,\, \phi \in [0, 2\pi)\} \tag{118}$$

Topologically, this is a **half-cylinder**. The boundary $A = 0$ is the oscillator at rest.

Deriving Beta Functions from the CS Equation

The physical observable is the position $x(t)$:

$$x(t) = A\cos(\omega_{\text{eff}}(t - t_0) + \phi) \tag{119}$$

In this example, "scale" is an arbitrary time origin t_0, not a momentum or energy scale. The mathematical structure is identical.

where $\omega_{\text{eff}} = \omega_0 + \frac{3\epsilon A^2}{8\omega_0}$ and t_0 is the "renormalization scale." **Note:** In this example, the "scale" is an arbitrary time origin rather than a momentum or energy scale, but the resulting invariance condition—demanding $dx/dt_0 = 0$—has exactly the same mathematical form as the CS equation (44).

Box 2.4: Complete Derivation of Oscillator Beta Functions

Goal: Derive $\beta^A = dA/dt_0$ and $\beta^\phi = d\phi/dt_0$ from the CS equation.

Step 1: Write the solution explicitly.

$$x(t) = A\cos\left(\omega_{\text{eff}}(t - t_0) + \phi\right) \tag{120}$$

Step 2: Apply scale independence.

The observable $x(t)$ depends explicitly on t_0 and implicitly through $A(t_0)$ and $\phi(t_0)$:

$$\frac{dx}{dt_0} = \left.\frac{\partial x}{\partial t_0}\right|_{A,\phi} + \frac{dA}{dt_0}\frac{\partial x}{\partial A} + \frac{d\phi}{dt_0}\frac{\partial x}{\partial \phi} = 0 \tag{121}$$

Step 3: Compute derivatives.

$$\left.\frac{\partial x}{\partial t_0}\right|_{A,\phi} = A\omega_{\text{eff}}\sin\theta \tag{122}$$

$$\frac{\partial x}{\partial A} = \cos\theta + \frac{3\epsilon A}{4\omega_0}(t - t_0)\sin\theta \tag{123}$$

$$\frac{\partial x}{\partial \phi} = -A\sin\theta \tag{124}$$

where $\theta = \omega_{\text{eff}}(t - t_0) + \phi$.

Step 4: Solve for beta functions.

The CS equation must hold for all t and θ. Including damping (which causes amplitude decay at rate γ), the beta functions are:

Result: The amplitude decays due to damping while the phase advances due to the nonlinearity:

$$\boxed{\beta^A = \frac{dA}{dt} = -\gamma A, \qquad \beta^\phi = \frac{d\phi}{dt} = \frac{3\epsilon A^2}{8\omega_0}} \tag{125}$$

The amplitude decays exponentially. The phase accumulates at a rate determined by the nonlinearity.

The RG Flow

The beta function vector field is:

$$\boldsymbol{\beta}_{\text{osc}} = -\gamma A\frac{\partial}{\partial A} + \frac{3\epsilon A^2}{8\omega_0}\frac{\partial}{\partial \phi} \tag{126}$$

The integral curves are:

$$A(t) = A_0 e^{-\gamma t} \tag{127}$$

$$\phi(t) = \phi_0 + \frac{3\epsilon}{16\gamma\omega_0} A_0^2 \left(1 - e^{-2\gamma t}\right) \tag{128}$$

All trajectories spiral inward toward the fixed point $A = 0$.

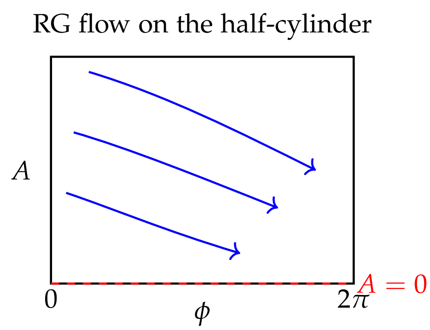

The Fixed Point and Stability

Setting $\boldsymbol{\beta} = 0$: $A^* = 0$ (oscillator at rest). This is a **stable** fixed point—all trajectories flow toward it.

No anomalous dimension: The oscillator has $\gamma = 0$ because energy conservation fixes the amplitude exactly. This contrasts with the PME and ϕ^4 examples.

Example 2: The Amplitude Equation

The amplitude equation adds **nontrivial fixed points** to our toolkit—zeros of $\boldsymbol{\beta}$ beyond the trivial $A = 0$.

The oscillator (Section I) has only a trivial fixed point at $A = 0$. To see the full richness of RG flows (73)—including nontrivial fixed points where $\boldsymbol{\beta} = 0$ at nonzero coupling—we study the **amplitude equation**. This is the "hydrogen atom" of RG: analytically tractable with nontrivial structure.

Physical Motivation

Near a **Hopf bifurcation** or **pitchfork bifurcation**, many systems reduce to:

$$\boxed{\frac{dA}{dt} = \mu A - g|A|^2 A} \tag{129}$$

where A is an amplitude, μ is the control parameter, and $g > 0$ is a saturation coefficient.

Examples include: laser physics (A = field amplitude), fluid convection (Rayleigh-Bénard), and phase transitions (A = order parameter).

Fixed Points

For real A, setting $\beta_A = 0$:

$$A(\mu - gA^2) = 0 \tag{130}$$

Two fixed points:

$$A^*_{\text{trivial}} = 0 \quad \text{(always exists)} \tag{131}$$

$$A^*_{\text{nontrivial}} = \pm\sqrt{\frac{\mu}{g}} \quad \text{(exists only for } \mu > 0\text{)} \tag{132}$$

	Amplitude Equation	**ϕ^4 Theory**
Control parameter	μ	$\epsilon = 4 - d$
Trivial fixed point	$A^* = 0$	$\lambda^* = 0$ (Gaussian)
Nontrivial fixed point	$\lvert A^*\rvert^2 = \mu/g$	$\lambda^* = 16\pi^2\epsilon/3$ (Wilson-Fisher)
Appearance condition	$\mu > 0$	$\epsilon > 0$ (i.e., $d < 4$)

Exact Stability Analysis

Linearize around each fixed point: $A = A^* + \delta A$.

At $A^* = 0$:

$$\left.\frac{d\beta_A}{dA}\right|_0 = \mu \tag{133}$$

For $\mu < 0$: stable. For $\mu > 0$: unstable.

At $|A^*|^2 = \mu/g$ (for $\mu > 0$):

$$\left.\frac{d\beta_A}{dA}\right|_{A^*} = \mu - 3g|A^*|^2 = -2\mu \tag{134}$$

The nontrivial fixed point is **stable** for $\mu > 0$.

The bifurcation: At $\mu = 0$, the two fixed points collide and exchange stability—a **supercritical pitchfork bifurcation**.

Exact Solution

The ODE solves exactly:

$$A(t) = \frac{A_0\, e^{\mu t}}{\sqrt{1 + \frac{gA_0^2}{\mu}(e^{2\mu t} - 1)}} \tag{135}$$

For $\mu > 0$: $A(t) \to \pm\sqrt{\mu/g}$ as $t \to \infty$. The system flows to the nontrivial fixed point.

Key insight: The amplitude equation captures the universal structure of RG near a bifurcation without requiring any loop calculations or ϵ-expansion.

Example 3: The Porous Medium Equation

The oscillator and amplitude equation have $\gamma = 0$—no anomalous dimensions. The porous medium equation (PME) is our first example where the anomalous dimension (the connection coefficient from Section I) is *nonzero*. Scaling exponents differ from dimensional analysis predictions because the nonlinearity "renormalizes" them.

The PME introduces **anomalous dimensions**—the connection γ from Section I becomes nontrivial.

The Physical System

The PME describes density evolution:

$$\frac{\partial \rho}{\partial t} = D\nabla^2(\rho^m) \tag{136}$$

where $m > 0$ is the nonlinearity parameter. For $m = 1$, this is ordinary diffusion. For $m > 1$, diffusion is faster in high-density regions.

Self-Similar Solutions

Seek solutions of the form:

$$\rho(x,t) = t^{-\alpha}F(\xi), \qquad \xi = \frac{x}{t^\beta} \tag{137}$$

Two constraints determine (α, β):
Mass conservation: $\alpha = d\beta$ (in d dimensions)
PME scaling: $(m-1)\alpha = 2\beta - 1$
Solving:

$$\boxed{\beta = \frac{1}{2 + d(m-1)}, \qquad \alpha = \frac{d}{2 + d(m-1)}} \tag{138}$$

The Anomalous Dimension

For linear diffusion ($m = 1$): $\beta = 1/2$ from dimensional analysis.

For $m \neq 1$, define the **anomalous dimension**:

$$\gamma_{\text{PME}} = \beta - \frac{1}{2} = -\frac{d(m-1)}{2(2 + d(m-1))} \tag{139}$$

For $d = 1$, $m = 2$: $\gamma = -1/6$, so $\beta = 1/3$ instead of $1/2$.

Physical interpretation: The nonlinearity modifies the scaling behavior. The anomalous dimension quantifies how interactions change scaling—exactly as in QFT, where loop corrections modify classical dimensions.

The Barenblatt Solution as Fixed Point

The **Barenblatt solution**:

$$\rho(x,t) = t^{-\alpha}\left(C - \frac{m-1}{2m}\cdot\frac{\beta\xi^2}{D}\right)_+^{1/(m-1)} \tag{140}$$

has compact support and is the **RG fixed point—**all reasonable initial conditions flow to it.

Box 2.5: Scaling Convention Independence in the PME

Goal: Show that the PME exhibits the same invariance structure as QFT.

The "scaling convention" for PME: The similarity variable is $\xi = x/t^{\beta}$. Different choices of β correspond to different **scaling conventions—**the PME analog of renormalization scheme choices. (We use "scaling convention" rather than "scheme" to avoid confusion with the QFT usage.)

Scheme change: Under $\beta \to \beta'$:

$$\xi' = x/t^{\beta'} = \xi \cdot t^{\beta-\beta'} \tag{141}$$

Physical invariants:

- Total mass: $M = \int \rho\, dx$
- Spreading rate: $L(t) \sim t^{\alpha}$ has the same exponent in all schemes
- Shape near boundary

The constraint algebra: Not all choices of β are valid. Mass conservation plus the PME give:

$$\alpha = d\beta, \qquad (m-1)\alpha = 2\beta - 1 \tag{142}$$

This restricts to a one-dimensional subspace of valid schemes. The physical exponent $\beta^* = 1/(d(m-1)+2)$ is the unique fixed point of this constraint algebra.

Example 4: The 1D ϕ^4 Theory

The previous examples were exactly solvable. ϕ^4 theory requires perturbation theory, introducing loop corrections, operator mixing (the connection from Section I), and scheme dependence (66). This example exercises the full framework: the CS equation (48), scheme transformations, and the bundle structure of Part IV.

ϕ^4 theory exhibits all features: nontrivial fixed points, anomalous dimensions, operator mixing (Section I), and scheme dependence (66).

The Setup

The 1D ϕ^4 theory has action:

$$S[\phi] = \int_0^L dx \left[\frac{1}{2} \left(\frac{d\phi}{dx} \right)^2 + \frac{r}{2}\phi^2 + \frac{\lambda}{4}\phi^4 \right] \tag{143}$$

with parameter space $\mathcal{M}_{\phi^4} = \{(r, \lambda) : \lambda > 0\}$.

Wilson's Momentum-Shell RG

Box 2.6: Momentum-Shell RG for 1D ϕ^4 (Schematic)

Problem: Derive beta functions using Wilson's procedure.
Approximations: This calculation is **schematic**—we work to leading order in λ near the Gaussian fixed point. The propagator variance is approximate.
Step 1: Field splitting. Write $\phi = \phi^< + \phi^>$ where $\phi^<$ has $|k| < \Lambda/b$ and $\phi^>$ has $\Lambda/b < |k| < \Lambda$.
Step 2: Integrate out fast modes.
For an infinitesimal shell $b = 1 + d\ell$:

$$\langle \phi^>(x)\phi^>(x) \rangle_0 \approx \frac{\Lambda}{\pi(\Lambda^2 + r)} d\ell \tag{144}$$

This generates $\delta r = \frac{3\lambda\Lambda}{\pi(\Lambda^2+r)} d\ell$.
Step 3: Rescaling.
Rescaling $x \to x/b$ gives:

$$r \to b^2 r, \qquad \lambda \to b^2 \lambda \tag{145}$$

Result:

$$\boxed{\beta_r = 2r + \frac{3\lambda\Lambda}{\pi(\Lambda^2 + r)}, \qquad \beta_\lambda = 2\lambda} \tag{146}$$

The Full CS Equation

For the two-point function:

$$\left(\Lambda \frac{\partial}{\partial \Lambda} + \beta_r \frac{\partial}{\partial r} + \beta_\lambda \frac{\partial}{\partial \lambda} + 2\gamma \right) \tilde{G}_2 = 0 \tag{147}$$

In 1D at one loop, $\gamma = 0$—the field has no anomalous dimension. This changes in higher dimensions!

Operator Mixing

The operators ϕ^2 and ϕ^4 mix under RG. The anomalous dimension matrix:

$$\gamma = \begin{pmatrix} \gamma_{\phi^2} & \gamma_{\phi^2 \leftarrow \phi^4} \\ 0 & \gamma_{\phi^4} \end{pmatrix} \tag{148}$$

The off-diagonal entry arises from tadpole diagrams: when we insert ϕ^4, contracting two legs produces ϕ^2.

Preview: The Wilson-Fisher Fixed Point

In $d = 4 - \epsilon$ dimensions, the one-loop beta function becomes:

$$\beta_\lambda = -\epsilon\lambda + \frac{3\lambda^2}{16\pi^2} \tag{149}$$

Two fixed points:

- **Gaussian**: $\lambda^* = 0$ (free field theory)
- **Wilson-Fisher**: $\lambda^*_{\text{WF}} = \frac{16\pi^2\epsilon}{3}$ (interacting)

The Wilson-Fisher fixed point exists for $d < 4$ and controls universal critical behavior near phase transitions.

Box 2.7: Dimensional Regularization and the $\overline{\text{MS}}$ Scheme

The problem: Loop integrals in $d > 1$ are often UV divergent.
Dimensional regularization: Compute in $d = 4 - \epsilon$ and expand in ϵ.
Example: One-loop self-energy.
The tadpole integral:

$$\Sigma = \frac{\lambda}{2} \int \frac{d^d k}{(2\pi)^d} \frac{1}{k^2 + m^2} \tag{150}$$

In $d = 4 - \epsilon$, this has a $1/\epsilon$ pole.
The $\overline{\text{MS}}$ scheme: Subtract only the pole (and associated $\gamma_E - \log 4\pi$).

The beta function emerges:
Requiring $d\lambda_{\text{bare}}/d\mu = 0$:

$$\beta_\lambda = \mu \frac{d\lambda_R}{d\mu} = \frac{3\lambda^2}{16\pi^2} + O(\lambda^3) \quad (\text{in } d = 4) \tag{151}$$

Key point: The beta function is **scheme-independent** at leading order, but higher-order coefficients depend on the subtraction scheme.

Comparison of Examples

	Oscillator	**Amplitude**	**PME**	ϕ^4
Type	ODE	Normal form	PDE	Field theory
Scale ℓ	Time t	Time t	$\log t$	Log-cutoff
Trivial FP	$A = 0$	$A^* = 0$	Dim. analysis	Gaussian
Nontrivial FP	—	$\lvert A^*\rvert^2 = \mu/g$	Barenblatt	Wilson-Fisher
Anomalous dim.?	No	No	Yes	Yes
Calculational	Exact	Exact	Self-similar	Perturbative

Building on the metric from Section I and the connection from Section I, Part VI explores curvature invariants and computational methods.

Part VI develops additional geometric structures: curvature invariants, scheme independence as gauge invariance, and computational methods.

Curvature and Critical Exponents

The curvature of theory space encodes how operators respond to non-commuting deformations. It relates to universal data at fixed points.

The Curvature Tensor

From the connection $\Gamma^a{}_{bc}$ introduced in Section I, we can compute the curvature tensor:

$$R^a{}_{bcd} = \partial_c\Gamma^a{}_{bd} - \partial_d\Gamma^a{}_{bc} + \Gamma^a{}_{ec}\Gamma^e{}_{bd} - \Gamma^a{}_{ed}\Gamma^e{}_{bc} \tag{152}$$

Physical meaning: Consider two deformations of a theory. If we first deform by δg^c then δg^d, versus first δg^d then δg^c, the curvature measures the difference:

$$[\nabla_c, \nabla_d]\mathcal{O}_a = R^b{}_{acd}\,\mathcal{O}_b \tag{153}$$

The curvature tensor is a **tensor**—it transforms homogeneously under scheme changes. Curvature invariants (like $R^a{}_{bab}$, $R^a{}_{bcd}R^{bcd}{}_a$) are scheme-independent observables.

Monodromy Around Singularities

Even when the connection is flat (zero curvature), singularities can produce non-trivial **monodromy**. Parallel transporting around a singular point returns a transformed operator:

$$\mathcal{O}_a \to M^b{}_a\,\mathcal{O}_b, \qquad M = \exp\left(\oint \Gamma\, dg\right) \tag{154}$$

This monodromy is closely related to **Stokes phenomena** in resurgent analysis.

Curvature at Fixed Points

At a fixed point, the curvature tensor contains universal data:

- **Eigenvalues** of the stability matrix (critical exponents)
- **OPE coefficients** (structure constants of the CFT)
- **Anomalous dimensions** of composite operators

Systems in the same universality class share these geometric invariants—this is the deep explanation of universality.

Scheme Independence as Gauge Invariance

The transformation (100) of the anomalous dimension under scheme changes is precisely the gauge transformation law for a connection:

Scheme independence is mathematically identical to gauge invariance: the anomalous dimension transforms like a connection.

$$\gamma'^{\,b}_{a} = U_a{}^c \gamma_c{}^d (U^{-1})_d{}^b + \mu \frac{dU_a{}^c}{d\mu} (U^{-1})_c{}^b \tag{155}$$

Gauge-invariant quantities (physical observables):

- Eigenvalues of γ at fixed points (critical exponents)
- Curvature invariants
- Monodromy around closed loops in coupling space

Box 2.8: Covariant Expansion of Beta Functions

Goal: Derive the metric from two-point functions following Dolan.
Algebraic content:
The metric arises from the **two-point function algebra**. For operators $\mathcal{O}_i$ and $\mathcal{O}_j$ conjugate to couplings g^i and g^j:

$$G_{ij} = \int d^d x \, \langle \mathcal{O}_i(x) \mathcal{O}_j(0) \rangle_{\text{conn}} \tag{156}$$

Properties from unitarity:

- **Symmetry**: $G_{ij} = G_{ji}$ (correlation functions are symmetric)
- **Positivity**: $G_{ij} v^i v^j \geq 0$ for any v (from reflection positivity)
- **Grading**: $G_{ij} = 0$ if $\Delta_i \neq \Delta_j$ at a CFT fixed point

The positivity condition is an **algebraic constraint on representations—**it's the analog of requiring positive-definite norms in unitary representations.
Geometric content:

The metric G_{ij} is a **Riemannian metric** on theory space. It measures "distances" between nearby theories:

$$ds^2 = G_{ij}(g)\, dg^i\, dg^j \tag{157}$$

QFT example: ϕ^4 + Yukawa (Dolan):
Consider a scalar ϕ with self-coupling λ and Yukawa coupling g to a fermion ψ:

$$\mathcal{L} = \frac{1}{2}(\partial\phi)^2 + \frac{\lambda}{4!}\phi^4 + \bar{\psi}(i\partial\!\!\!/ - m)\psi + g\phi\bar{\psi}\psi \tag{158}$$

The metric components are:

$$G_{\lambda\lambda} = \frac{1}{576}\int d^dx\, \langle\phi^4(x)\phi^4(0)\rangle_{\text{conn}} \tag{159}$$

$$G_{\lambda g} = \frac{1}{24}\int d^dx\, \langle\phi^4(x)(\bar{\psi}\psi\phi)(0)\rangle_{\text{conn}} \tag{160}$$

$$G_{gg} = \int d^dx\, \langle(\bar{\psi}\psi\phi)(x)(\bar{\psi}\psi\phi)(0)\rangle_{\text{conn}} \tag{161}$$

At one loop:

$$G = \begin{pmatrix} A/\lambda^2 + O(1) & B/(\lambda g) + O(1) \\ B/(\lambda g) + O(1) & C/g^2 + O(1) \end{pmatrix} \tag{162}$$

where A, B, C are calculable from Feynman diagrams.

Connection to central charge: In 2D, the Zamolodchikov metric is related to the central charge via:

$$c \propto \text{tr}(G \cdot \gamma) \tag{163}$$

where γ is the anomalous dimension matrix. This is the origin of the c-theorem.

Box 2.16: The Zamolodchikov Metric for the PME

Goal: Construct the analog of the Zamolodchikov metric for the PME.

The moment metric:
For the PME, define the metric from **moment fluctuations**:

$$G_{mn} = \langle\delta M_m\, \delta M_n\rangle \tag{164}$$

where $M_m = \int \xi^m F(\xi)\, d\xi$ are the moments of the self-similar profile.

Connection to Fisher information:
This is precisely the **Fisher information metric** for the family of

Barenblatt profiles parameterized by (m, d):

$$G_{ij}^{(\text{Fisher})} = -\mathbb{E}\left[\frac{\partial^2 \log p(x|m,d)}{\partial g^i \partial g^j}\right] \tag{165}$$

where $p(x|m,d) = F(\xi; m, d)$ is the profile interpreted as a probability distribution.

Explicit calculation for $d = 1$:
The Barenblatt profile is $F(\xi) = [C - k\xi^2]_+^{1/(m-1)}$. The Fisher metric has components:

$$G_{mm} \propto \int_{-\xi_0}^{\xi_0} \frac{1}{F}\left(\frac{\partial F}{\partial m}\right)^2 d\xi \tag{166}$$

This integral diverges logarithmically as $m \to 1$ (approaching linear diffusion), reflecting the singular nature of the $m = 1$ limit.

Geometric interpretation:
The PME metric measures how "distinguishable" two Barenblatt profiles with different m values are. Near $m = 1$, the profiles are infinitely distinguishable—the linear and nonlinear cases are "infinitely far apart" in metric terms.
This parallels the QFT situation: near a phase transition ($r \to r_c$), the susceptibility $\chi = G_{rr}$ diverges, making critical and non-critical theories infinitely distinguishable.

Box 2.17: Sketch of the c-Theorem Proof

The c-function: Define from stress tensor correlators:

$$c(r) = r^4\langle T(z)T(0)\rangle - \frac{3}{2}r^4\langle T(z)\Theta(0)\rangle - \frac{3}{16}r^4\langle\Theta(z)\Theta(0)\rangle \tag{167}$$

where $T = T_{zz}$ is the holomorphic stress tensor and $\Theta = T_z{}^z$ is the trace.

Conservation: Stress tensor conservation $\partial_{\bar{z}} T = \partial_z \Theta$ implies:

$$r\frac{dc}{dr} = -\frac{3}{2}G(r), \quad G(r) = r^4\langle\Theta(z)\Theta(0)\rangle \tag{168}$$

Unitarity: In a unitary theory, $G(r) \geq 0$ because Θ is Hermitian.

Conclusion: Since $r \sim e^{-\ell}$, we have $\frac{dc}{d\ell} = -r\frac{dc}{dr} = \frac{3}{2}G \geq 0$...
Wait, this gives $dc/d\ell \geq 0$, the opposite sign! The resolution is that increasing ℓ means flowing to the IR (lower energy), and c *decreases* in the IR direction:

$$\boxed{\frac{dc}{d\ell} \leq 0 \quad \text{(flowing toward IR)}} \tag{169}$$

Box 2.18: Potential Flow and Integrability (Dolan)

Goal: Verify that RG flow is potential flow in Dolan's ϕ^4 + Yukawa model.

Algebraic content:

Potential flow means the beta function is a gradient:

$$\beta^i = G^{ij}\frac{\partial W}{\partial g^j} \tag{170}$$

for some potential $W(g)$ and metric G_{ij}.

The integrability condition:

Lowering the index: $\beta_i = G_{ij}\beta^j$. Potential flow requires $\beta_i = \partial_i W$, which implies:

$$\partial_i\beta_j = \partial_j\beta_i \quad \text{(symmetry of mixed partials)} \tag{171}$$

This is the **integrability condition**—an algebraic constraint that must be checked order by order.

In algebraic terms: The integrability condition is a **cocycle condition** in the de Rham complex:

$$d\beta^\flat = 0 \quad \Leftrightarrow \quad \beta^\flat = dW \tag{172}$$

where $\beta^\flat = G_{ij}\beta^j dg^i$ is the 1-form associated to β.

Dolan's verification (to sixth order):

For the ϕ^4 + Yukawa model with couplings (λ, g), Dolan computed:

$$\beta_\lambda = -\epsilon\lambda + a_1\lambda^2 + a_2 g^2\lambda + a_3\lambda^3 + \cdots \tag{173}$$

$$\beta_g = -\frac{\epsilon}{2}g + b_1 g\lambda + b_2 g^3 + b_3 g\lambda^2 + \cdots \tag{174}$$

The integrability condition $\partial_\lambda\beta_g = \partial_g\beta_\lambda$ gives:

$$b_1 + (\text{corrections}) = 2a_2 + (\text{corrections}) \tag{175}$$

Result: Dolan verified this to sixth order in the couplings. The RG flow **is** potential flow, at least perturbatively.

The c-function as Casimir:

When integrability holds, the potential W is the c-function:

$$\frac{dW}{d\ell} = \beta^i\partial_i W = \beta^i G_{ij}\beta^j = G_{ij}\beta^i\beta^j \geq 0 \tag{176}$$

The c-function is a **Casimir invariant** of the flow: it labels orbits and increases monotonically.

Box 2.19: Potential Flow in the PME

Goal: Show the PME has gradient flow structure.
The Lyapunov functional:
The PME admits a Lyapunov functional:

$$\mathcal{F}[\rho] = \int \left[\frac{1}{m} \rho^m + \frac{1}{2} V(x) \rho \right] d^d x \tag{177}$$

(for PME with external potential V; for free PME, take $V = 0$).
Gradient flow structure:
The PME can be written as:

$$\partial_t \rho = \nabla \cdot \left(\rho \nabla \frac{\delta \mathcal{F}}{\delta \rho} \right) \tag{178}$$

This is gradient flow in the **Wasserstein metric**:

$$\partial_t \rho = -\text{grad}_W \mathcal{F} \tag{179}$$

where grad_W is the gradient with respect to the Wasserstein-2 distance.
Entropy production:
Along the flow:

$$\frac{d\mathcal{F}}{dt} = -\int \rho \left| \nabla \frac{\delta \mathcal{F}}{\delta \rho} \right|^2 d^d x \leq 0 \tag{180}$$

This is the PME analog of the c-theorem: entropy decreases monotonically.

Message: Both QFT and the PME exhibit gradient flow structure. This is why c-theorem-type results hold: the RG "potential" (c-function or entropy) must decrease.

Solving RG Equations

The CS equation (44) is a first-order PDE. The method of characteristics solves it.

The CS equation (44) is a first-order PDE. Solving it gives the scale dependence of observables.

The Method of Characteristics

The equation:

$$\left(\mu \frac{\partial}{\partial \mu} + \beta(g) \frac{\partial}{\partial g} \right) \mathcal{O} = 0 \tag{181}$$

says $\mathcal{O}$ is constant along characteristic curves. The characteristics are the RG trajectories (73):

$$\mu \frac{dg}{d\mu} = \beta(g) \tag{182}$$

The **running coupling** $\bar{g}(\mu; g_0, \mu_0)$ solves this with initial condition $\bar{g}(\mu_0) = g_0$.

Box 2.9: Running Couplings for 1D ϕ^4

Goal: Solve the RG equations for $r(\ell)$ and $\lambda(\ell)$.
The equations:

$$\frac{dr}{d\ell} = 2r + \frac{3\lambda\Lambda}{\pi(\Lambda^2 + r)} \tag{183}$$

$$\frac{d\lambda}{d\ell} = 2\lambda \tag{184}$$

Solution for λ:

$$\lambda(\ell) = \lambda_0 e^{2\ell} \tag{185}$$

Solution for r (near Gaussian):

$$r(\ell) = \left(r_0 + \frac{3\lambda_0\ell}{\pi\Lambda}\right) e^{2\ell} \tag{186}$$

Physical interpretation:

- Both r and λ grow as we zoom out
- Even if $r_0 = 0$, fluctuations generate $r > 0$: the tadpole "dresses" the mass
- The Gaussian fixed point is unstable in both directions

RG-Improved Correlation Functions

With running couplings, physical predictions are independent of which scale we use:

$$\tilde{G}_2(p; r_0, \lambda_0, \Lambda_0) = \tilde{G}_2(p; r(\Lambda), \lambda(\Lambda), \Lambda) \tag{187}$$

Asymptotic Behavior and the Landau Pole

Classification of Theories

Classification of theories by asymptotic behavior: asymptotic freedom vs infrared freedom.

Asymptotic freedom ($\beta < 0$ for small g): Coupling decreases in UV. QCD is the canonical example.

Infrared freedom ($\beta > 0$ for small g): Coupling decreases in IR. This is 1D ϕ^4.

The Landau Pole

When $\beta > 0$, the running coupling can diverge at finite scale. For $\beta = bg^2$:

$$g(\mu) = \frac{g_0}{1 - bg_0 \log(\mu/\mu_0)} \tag{188}$$

This diverges at $\mu_{\text{Landau}} = \mu_0 \exp(1/(bg_0))$—the **Landau pole**.

The RG as a Semigroup

A semigroup has closure and associativity but lacks inverses. The RG can fail to be invertible.

The RG can fail to be a group for two reasons:

1. **Information loss (coarse-graining):** Wilson's RG integrates out degrees of freedom. Once averaged away, information cannot be recovered.

2. **Perturbative singularities:** The Landau pole means the flow is only defined on a restricted domain.

From Perturbative to Exact: The Functional RG

The exact RG provides a functional differential equation whose perturbative expansion recovers the CS equation.

The perturbative RG is powerful but limited. The **Exact Renormalization Group** (ERG) treats the RG exactly.

The Polchinski Equation

Wilson's insight: the RG is an exact transformation on the space of *actions*. The Polchinski equation describes how the effective action $S_\Lambda[\phi]$ changes as we lower the cutoff:

$$\Lambda \frac{\partial S_\Lambda}{\partial \Lambda} = \frac{1}{2} \int \frac{d^d p}{(2\pi)^d} \dot{K} \left[\frac{\delta S}{\delta \phi(p)} \frac{\delta S}{\delta \phi(-p)} - \frac{\delta^2 S}{\delta \phi(p) \delta \phi(-p)} \right] \tag{189}$$

This is *exact*—no perturbation theory invoked.

The Derivative Expansion

Expand S_Λ in derivatives:

$$S_\Lambda[\phi] = \int d^d x \left[V_\Lambda(\phi) + \frac{1}{2} Z_\Lambda(\phi)(\partial\phi)^2 + O(\partial^4) \right] \tag{190}$$

The **Local Potential Approximation (LPA)** keeps only $V_\Lambda(\phi)$. This gives a tractable PDE for finding fixed points non-perturbatively.

Looking Ahead

This chapter established the complete RG framework, showing that **algebra and geometry are two faces of the same structure**:

The central equation: The Callan-Symanzik equation (44) encodes scale independence

Symmetry structure (Part II): Scale invariance gives a Lie group (Section I); scheme invariance gives diffeomorphisms (Section I)

Geometric realization (Part III): These symmetries are naturally geometric—parameter space is a manifold, β (74) is a vector field, γ is a connection, and the Fisher metric completes the picture

Unified picture (Part IV): The gauge bundle structure unifies diffeomorphisms and gauge transformations (Section I)

Examples (Part V): Four examples of increasing complexity demonstrate the unified framework

Advanced topics (Part VI): Curvature invariants, solving RG equations, and the exact RG

Chapter I focuses on the zeros of $\boldsymbol{\beta}$—the fixed points:

Chapter I focuses on the zeros of $\boldsymbol{\beta}$: fixed points, universality, and scaling.

- Fixed-point classification and stability (eigenvalues of $\partial_j \beta^i|_{g^*}$)
- Critical exponents and universality classes
- Normal form theory for RG flows
- The role of marginal operators and logarithmic corrections

Part II then turns to **analytical methods**: perturbation theory (with its asymptotic series) and transseries (capturing non-perturbative physics).

Exercises

1. **The dilation Lie algebra.** Verify that $\mathcal{D} = x^\mu \partial_\mu$ generates scale transformations: $e^{\ell \mathcal{D}} f(x) = f(e^\ell x)$.

2. **Dilation as a group action.** Consider $D_\lambda : f(x) \mapsto f(\lambda x)$.

   (a) Show that $D_\lambda D_\mu = D_{\lambda\mu}$.

   (b) For homogeneous functions $f(\lambda x) = \lambda^\Delta f(x)$, show that Δ is the eigenvalue of $x\frac{d}{dx}$.

3. **RG as Lie transport.** For $\boldsymbol{\beta} = -\gamma A \partial_A + \frac{3\epsilon A^2}{8\omega_0}\partial_\phi$:

   (a) Compute $e^{t\boldsymbol{\beta}}$ acting on (A, ϕ).

   (b) Show any function $f(A)$ has $L_{\boldsymbol{\beta}} f = -\gamma A \frac{\partial f}{\partial A}$.

4. **CS equation verification.** For the 1D ϕ^4 four-point function G_4 at tree level:

   (a) Write G_4 in terms of λ and propagators.

   (b) Verify $(\Lambda\partial_\Lambda + \beta_r \partial_r + \beta_\lambda \partial_\lambda + 4\gamma)G_4 = 0$ with $\gamma = 0$.

5. **Running mass.** Solve the RG equations for $r(\ell)$ including the tadpole.
   (a) Show that even if $r_0 = 0$, a mass is generated.
   (b) Find the "critical" r_0 for which $r(\ell) \to 0$ as $\ell \to \infty$.
6. **Landau pole in QED.** The beta function is $\beta_\alpha = \frac{2\alpha^2}{3\pi}$.
   (a) Solve for $\alpha(\mu)$.
   (b) Find μ_{Landau} in terms of α_0 and μ_0.
   (c) Estimate numerically using $\alpha(m_e) \approx 1/137$.
7. **Wilson-Fisher fixed point.** For $\beta_\lambda = -\epsilon\lambda + 3\lambda^2/(16\pi^2)$:
   (a) Find the fixed points λ^*.
   (b) Identify UV-attractive vs IR-attractive.
   (c) Solve for $\lambda(\mu)$ interpolating between them.
8. **The van der Pol oscillator.** For $\ddot{x} - \epsilon(1 - x^2)\dot{x} + x = 0$:
   (a) Use multiple scales with $\tau = \epsilon t$.
   (b) Show $dA/d\tau = A(1 - A^2/4)/2$.
   (c) Find the fixed point and interpret physically.
9. **Gevrey-1 structure.** For $\tilde{f}(\epsilon) = \sum_{n=0}^{\infty}(-1)^n n!\epsilon^{n+1}$:
   (a) Verify Gevrey-1: $|a_n| \leq C \cdot K^n \cdot n!$.
   (b) Compute the Borel transform $\hat{f}_B(\zeta)$.
   (c) Identify the singularity and explain the alternating signs.

Summary

Chapter Summary

The Central Equation

The Callan-Symanzik equation (44) encodes scale independence:

$$\left(\mu\frac{\partial}{\partial\mu} + \beta^i(g)\frac{\partial}{\partial g^i} + n\gamma(g)\right) G_n = 0 \tag{48}$$

Symmetry Structure (Part II)

- **Scale invariance**: gives the dilation Lie group with generator (53)
- **Scheme invariance**: beta transforms as (66)—this IS the vector field law

- **Scaling dimensions**: eigenvalues (71) of the generator

Geometric Realization (Part III)

The symmetry structure IS geometric:

- Couplings g^i are coordinates on manifold $\mathcal{M}$; schemes are coordinates
- Beta function (74) is a vector field; flows (73) are integral curves
- Anomalous dimension $\gamma_a{}^b$ is a connection
- Fisher metric G_{ab} (88) measures distances
- Gradient flow (94) and geodesics complete the picture

Unified Picture (Part IV)

Theory space is a **gauge bundle**. Scheme changes are diffeomorphisms on base + gauge on fiber.

The Four Examples

	Oscillator	**Amplitude**	**PME**	ϕ^4
Nontrivial FP?	No	Yes	Yes	Yes
Anomalous dim?	No	No	Yes	Yes

Key Insight

Algebra and geometry are not alternative perspectives—they are two faces of the same structure emerging from (44).

Exercises

1. **The dilation Lie algebra.** Verify that $\mathcal{D} = x^\mu \partial_\mu$, $P_\mu = \partial_\mu$, and $K_\mu = 2x_\mu x^\nu \partial_\nu - x^2 \partial_\mu$ satisfy the conformal algebra commutation relations in d dimensions.

2. **Dilation as a group action.** Consider $D_\lambda : f(x) \mapsto f(\lambda x)$.

   (a) Show that $D_\lambda D_\mu = D_{\lambda\mu}$.

   (b) For homogeneous functions $f(\lambda x) = \lambda^\Delta f(x)$, show that Δ is the eigenvalue of $x\frac{d}{dx}$.

3. **RG as Lie transport.** For $\boldsymbol{\beta} = -\gamma A \partial_A + \frac{3\epsilon A^2}{8\omega_0} \partial_\phi$:

(a) Compute $e^{t\beta}$ acting on (A, ϕ).

(b) Show any function $f(A)$ has $L_\beta f = -\gamma A \frac{\partial f}{\partial A}$.

4. **CS equation verification.** For the 1D ϕ^4 four-point function G_4 at tree level:

(a) Write G_4 in terms of λ and propagators.

(b) Verify $(\Lambda\partial_\Lambda + \beta_r\partial_r + \beta_\lambda\partial_\lambda + 4\gamma)G_4 = 0$ with $\gamma = 0$.

5. **Running mass.** Solve the RG equations for $r(\ell)$ including the tadpole.

(a) Show that even if $r_0 = 0$, a mass is generated.

(b) Find the "critical" r_0 for which $r(\ell) \to 0$ as $\ell \to \infty$.

6. **Landau pole in QED.** The beta function is $\beta_\alpha = \frac{2\alpha^2}{3\pi}$.

(a) Solve for $\alpha(\mu)$.

(b) Find μ_{Landau} in terms of α_0 and μ_0.

(c) Estimate numerically using $\alpha(m_e) \approx 1/137$.

7. **Wilson-Fisher fixed point.** For $\beta_\lambda = -\epsilon\lambda + 3\lambda^2/(16\pi^2)$:

(a) Find the fixed points λ^*.

(b) Identify UV-attractive vs IR-attractive.

(c) Solve for $\lambda(\mu)$ interpolating between them.

8. **The van der Pol oscillator.** For $\ddot{x} - \epsilon(1 - x^2)\dot{x} + x = 0$:

(a) Use multiple scales with $\tau = \epsilon t$.

(b) Show $dA/d\tau = A(1 - A^2/4)/2$.

(c) Find the fixed point and interpret physically.

9. **Gevrey-1 structure.** For $\tilde{f}(\epsilon) = \sum_{n=0}^{\infty}(-1)^n n! \epsilon^{n+1}$:

(a) Verify Gevrey-1: $|a_n| \leq C \cdot K^n \cdot n!$.

(b) Compute the Borel transform $\hat{f}_B(\zeta)$.

(c) Identify the singularity and explain the alternating signs.

Summary

Chapter Summary

The Central Equation

The Callan-Symanzik equation (44) encodes scale independence:

$$\left(\mu\frac{\partial}{\partial\mu} + \beta^i(g)\frac{\partial}{\partial g^i} + n\gamma(g)\right) G_n = 0 \tag{48}$$

Symmetry Structure (Part II)

- **Scale invariance**: gives the dilation Lie group with generator (53)
- **Scheme invariance**: beta transforms as (66)—this IS the vector field law
- **Scaling dimensions**: eigenvalues (71) of the generator

Geometric Realization (Part III)

The symmetry structure IS geometric:

- Couplings g^i are coordinates on manifold $\mathcal{M}$; schemes are coordinates
- Beta function (74) is a vector field; flows (73) are integral curves
- Anomalous dimension $\gamma_a{}^b$ is a connection

Unified Picture (Part IV)

Theory space is a **gauge bundle**. Scheme changes are diffeomorphisms on base + gauge on fiber.

Metric Structure (Part VI)

The Fisher metric enables gradient flow (94) and geodesic interpretations.

The Four Examples

	Oscillator	**Amplitude**	**PME**	ϕ^4
Nontrivial FP?	No	Yes	Yes	Yes
Anomalous dim?	No	No	Yes	Yes

Key Insight

Algebra and geometry are not alternative perspectives—they are two faces of the same structure emerging from (44).

Solution to Exercise 2.1: The dilation Lie algebra

Commutator $[\mathcal{D}, P_\mu]$**:**
Acting on test function f:

$$[\mathcal{D}, P_\mu]f = x^\nu\partial_\nu(\partial_\mu f) - \partial_\mu(x^\nu\partial_\nu f) \tag{191}$$
$$= x^\nu\partial_\nu\partial_\mu f - \delta^\nu_\mu\partial_\nu f - x^\nu\partial_\mu\partial_\nu f = -\partial_\mu f \tag{192}$$

Result: $\boxed{[\mathcal{D}, P_\mu] = -P_\mu}$
Commutator $[\mathcal{D}, K_\mu]$**:**
After computation: $[\mathcal{D}, K_\mu]f = K_\mu f$
Result: $\boxed{[\mathcal{D}, K_\mu] = K_\mu}$
Commutator $[P_\mu, K_\nu]$**:**
After computation: $[P_\mu, K_\nu]f = 2\eta_{\mu\nu}\mathcal{D}f - 2M_{\mu\nu}f$
Result: $\boxed{[P_\mu, K_\nu] = 2(\eta_{\mu\nu}\mathcal{D} - M_{\mu\nu})}$

Solution to Exercise 2.2: Dilation as a group action

(a) Composition law.
$(D_\lambda D_\mu)f(x) = D_\lambda[f(\mu x)] = f(\mu(\lambda x)) = f((\lambda\mu)x) = D_{\lambda\mu}f(x)$
Therefore: $\boxed{D_\lambda D_\mu = D_{\lambda\mu}}$
(b) Homogeneous functions.
Differentiate $f(\lambda x) = \lambda^\Delta f(x)$ w.r.t. λ and set $\lambda = 1$:
$xf'(x) = \Delta f(x)$, i.e., $\boxed{\mathcal{D}f = \Delta f}$

Solution to Exercise 2.3: RG as Lie transport

(a) The flow equations give $A(t) = A_0 e^{-\gamma t}$ and $\phi(t) = \phi_0 + \frac{3\epsilon}{16\gamma\omega_0}A_0^2(1 - e^{-2\gamma t})$.

$$\boxed{e^{t\beta}(A_0, \phi_0) = \left(A_0 e^{-\gamma t}, \phi_0 + \frac{3\epsilon A_0^2}{16\gamma\omega_0}(1 - e^{-2\gamma t})\right)}$$

(b) $L_\beta f = -\gamma A\frac{\partial f}{\partial A} + \frac{3\epsilon A^2}{8\omega_0}\frac{\partial f}{\partial \phi} = -\gamma A\frac{\partial f}{\partial A}$ for $f = f(A)$.

Solution to Exercise 2.5: Running mass

(a) Mass generation.
With $r_0 = 0$: $r(\ell) = \frac{3\lambda_0}{\pi\Lambda_0}(e^{3\ell} - e^{2\ell})$
For large ℓ: $\boxed{r(\ell) \approx \frac{3\lambda_0}{\pi\Lambda_0}e^{3\ell} > 0}$
A positive mass is generated by fluctuations!
(b) Physical interpretation.
In statistical mechanics, $r \propto (T - T_c)$. The generation of positive mass means fluctuations disorder the system—the Coleman-

Mermin-Wagner phenomenon in 1D.

Solution to Exercise 2.6: Landau pole in QED

(a) Separating variables: $\boxed{\alpha(\mu) = \dfrac{\alpha_0}{1 - \frac{2\alpha_0}{3\pi}\ln(\mu/\mu_0)}}$

(b) Diverges when denominator vanishes: $\boxed{\mu_{\text{Landau}} = \mu_0 \exp\left(\dfrac{3\pi}{2\alpha_0}\right)}$

(c) With $\alpha_0 = 1/137$ at $\mu_0 = m_e$:
$\frac{3\pi}{2\alpha_0} = \frac{3\pi\times 137}{2} \approx 645$
$\mu_{\text{Landau}} \approx m_e \cdot e^{645} \approx 10^{280}$ MeV $\approx 10^{277}$ GeV
Far beyond the Planck scale—considered unphysical.

Solution to Exercise 2.7: Wilson-Fisher fixed point

(a) Fixed points.
$\lambda(-\epsilon + \frac{3\lambda}{16\pi^2}) = 0$
$\lambda_1^* = 0$ (Gaussian), $\lambda_2^* = \frac{16\pi^2\epsilon}{3}$ (Wilson-Fisher)
(b) Stability.
At $\lambda = 0$: $\beta'(0) = -\epsilon < 0$ for $\epsilon > 0 \Rightarrow$ unstable (IR-repulsive)
At λ^*_{WF}: $\beta'(\lambda^*) = +\epsilon > 0 \Rightarrow$ stable (IR-attractive)
(c) Solution.

$$\boxed{\lambda(\mu) = \frac{16\pi^2\epsilon/3}{1 + C(16\pi^2\epsilon/3)\mu^\epsilon}}$$

As $\mu \to 0$: $\lambda \to \lambda^*_{\text{WF}}$. As $\mu \to \infty$: $\lambda \to 0$.

Solution to Exercise 2.8: The van der Pol oscillator

(a) Multiple scales with $\tau = \epsilon t$, $x_0 = A(\tau)\cos(t + \phi(\tau))$.

(b) Canceling secular terms: $\boxed{\dfrac{dA}{d\tau} = \dfrac{A}{2}\left(1 - \dfrac{A^2}{4}\right)}$

(c) Fixed points: $A = 0$ (unstable) and $A = 2$ (stable).
Physical interpretation: The van der Pol oscillator has a **limit cycle** at $A = 2$. Small oscillations grow; large oscillations are damped. The system settles to a stable periodic orbit.

Solution to Exercise 2.9: Gevrey-1 structure

(a) For $n \geq 1$: $|a_n| = (n-1)! \leq n!$. With $C = 1$, $K = 1$: Gevrey-1. ✓
(b) $\hat{f}_B(\zeta) = \sum_{n=1}^{\infty} \frac{(-1)^{n-1}}{n}\zeta^n = \boxed{\log(1+\zeta)}$
(c) Branch point at $\zeta = -1$ (negative real axis).
Alternating signs mean the series is Borel-summable along the

positive real axis. Singularity at $\zeta < 0$ corresponds to an "anti-instanton."

Fixed Points, Universality, and Scaling

The RG generates flows on parameter space. But flows go somewhere. The **destinations** of RG flows are called **fixed points**, and they represent theories that are exactly scale-invariant. Understanding fixed points is the key to understanding the long-distance or long-time behavior of any system.

Chapter I developed the complete algebraic and geometric framework. This chapter asks: where do RG flows *go*? Fixed points are the destinations, and **normal form theory** reveals the universal structure of flows near these special points.

This chapter develops the theory of fixed points with emphasis on **normal forms** and **universality**:

- **Fixed points as Lie group stationarity**—zeros of the beta function where the RG action leaves the theory invariant
- **Normal form theory**—near any fixed point, the flow reduces to a universal canonical form
- **Stability analysis** via the linearized Lie algebra action, classifying perturbations as relevant, irrelevant, or marginal
- **Universality classes**—sets of theories flowing to the same fixed point, sharing critical exponents
- **Self-similar solutions** and anomalous dimensions from the dynamical systems perspective

The organizing principle is the Lie group framework from Chapter I: fixed points are where the RG generator vanishes, and stability is determined by the linearized Lie algebra action at that point. Normal form theory then classifies the **universal corrections to scaling**. The geometric structures (metrics, geodesics, c-theorem) are developed in Chapter I; here we focus on fixed-point dynamics and universality.

Fixed Points as Lie Group Stationarity

Before diving into specific examples, we establish the geometric meaning of fixed points in the Lie group framework developed in Chapter I.

The Geometric Definition

A fixed point is where the RG vector field vanishes—the flow has a stationary point.

Recall that the RG is the action of the dilation group $G = (\mathbb{R}^+, \cdot)$ on parameter space $\mathcal{M}$. The beta function $\boldsymbol{\beta} = \beta^i \partial/\partial g^i$ is the generator of this action—an element of the Lie algebra $\mathfrak{g}$.

A **fixed point** $g^* \in \mathcal{M}$ is a point where the generator vanishes:

$$\boldsymbol{\beta}|_{g^*} = 0 \tag{193}$$

Geometrically, g^* is a **stationary point** of the flow. The group action leaves g^* invariant: for all $\lambda \in G$,

$$\lambda \cdot g^* = g^* \tag{194}$$

This is the defining property of a fixed point in any dynamical system generated by a Lie group action.

The Stability Matrix as Linearized Lie Algebra

Near a fixed point, we can linearize the group action. Write $g = g^* + \delta g$ and expand:

$$\beta^i(g) = \beta^i(g^*) + \left.\frac{\partial \beta^i}{\partial g^j}\right|_{g^*} \delta g^j + O(\delta g^2) = B^i{}_j\, \delta g^j + O(\delta g^2) \tag{195}$$

The **stability matrix** $B^i{}_j = \partial\beta^i/\partial g^j|_{g^*}$ is the **linearization of the Lie algebra generator** at the fixed point.

The stability matrix is the Jacobian of the beta function—the linearized generator of the RG action at the fixed point.

In the language of representation theory, the linearized flow defines a **representation** of the Lie algebra on the tangent space $T_{g^*}\mathcal{M}$:

$$\rho : \mathfrak{g} \to \mathrm{End}(T_{g^*}\mathcal{M}), \qquad \rho(\boldsymbol{\beta}) = B \tag{196}$$

The eigenvalues of B are the **weights** of this representation—the scaling dimensions.

Box 4.1: The Stability Matrix as Lie Derivative

Setup: Consider a perturbation δg^i near fixed point g^*.
The linearized flow: The evolution of δg under RG is:

$$\frac{d(\delta g^i)}{d\ell} = B^i{}_j\, \delta g^j \tag{197}$$

Lie derivative interpretation: This is the **Lie derivative** of the perturbation along the beta function vector field:

$$L_{\boldsymbol{\beta}}(\delta g^i) = \beta^j \frac{\partial(\delta g^i)}{\partial g^j} + \delta g^j \frac{\partial \beta^i}{\partial g^j} = B^i{}_j\, \delta g^j \tag{198}$$

(The first term vanishes at the fixed point since $\beta^j|_{g^*} = 0$.)

Eigenvalue decomposition: Diagonalize B with eigenvalues Δ_α and eigenvectors v_α:

$$B\, v_\alpha = \Delta_\alpha\, v_\alpha \tag{199}$$

Solution: A perturbation along v_α evolves as:

$$\delta g_\alpha(\ell) = \delta g_\alpha(0)\, e^{\Delta_\alpha \ell} \tag{200}$$

Classification:

- $\Delta_\alpha > 0$: **Relevant** (unstable, grows under RG)
- $\Delta_\alpha < 0$: **Irrelevant** (stable, shrinks under RG)
- $\Delta_\alpha = 0$: **Marginal** (higher-order terms determine fate)

The key insight: Scaling dimensions are eigenvalues of the linearized Lie algebra action. They are “quantum numbers” labeling how operators transform under RG.

Fixed Points and Scale Invariance

At a fixed point, the theory is **exactly scale-invariant**. Physical observables $\mathcal{O}$ satisfy:

$$L_\beta \mathcal{O}|_{g^*} = 0 \tag{201}$$

This is the infinitesimal version of scale invariance. The Lie derivative along the RG flow vanishes because the flow itself has stopped.

Under mild conditions (unitarity, locality), scale invariance at a fixed point extends to the full **conformal symmetry**. The fixed point theory is then a conformal field theory (CFT), with powerful constraints on correlation functions.

Perturbative Fixed Points

A **perturbative fixed point** is one where the perturbative beta function vanishes. These are the fixed points visible to any finite order of perturbation theory.

Definition

A perturbative fixed point is a point $g^* = (g^{*1}, \ldots, g^{*n})$ where:

$$\beta^i_{\text{pert}}(g^*) = 0 \quad \text{for all } i \tag{202}$$

At a perturbative fixed point, all perturbative beta functions vanish. The theory is scale-invariant order-by-order in perturbation theory.

At such a point, the running stops because $dg^i/d\ell = 0$. The couplings take the same values at all scales.

Examples We've Seen

The damped anharmonic oscillator has $\beta^A = -\gamma A$ and $\beta^\phi = 3\epsilon A^2/(8\omega_0)$. The fixed point $A^* = 0$ corresponds to the oscillator at rest; it is stable because all trajectories flow toward it due to damping.

The 1D ϕ^4 theory has the Gaussian fixed point $(r^*, \lambda^*) = (0, 0)$, which is free field theory.

Both are **trivial** fixed points in the sense that the interactions have vanished. More interesting are fixed points with $\lambda^* \neq 0$.

The Wilson-Fisher Fixed Point

In $d = 4 - \epsilon$ dimensions, ϕ^4 theory has a famous non-trivial fixed point discovered by Wilson and Fisher. The beta function for the quartic coupling takes the form:

$$\beta_\lambda = -\epsilon\lambda + b\lambda^2 + O(\lambda^3) \tag{203}$$

where the coefficient $b > 0$.

The Wilson-Fisher fixed point controls phase transitions in real 3D systems. It is perturbatively accessible in $d = 4 - \epsilon$.

Setting $\beta_\lambda = 0$ gives fixed points at $\lambda^* = 0$ (Gaussian) and:

$$\lambda^*_{\mathrm{WF}} = \frac{\epsilon}{b} + O(\epsilon^2) \tag{204}$$

This Wilson-Fisher fixed point is non-trivial because $\lambda^*_{\mathrm{WF}} \neq 0$. It describes the universality class of the Ising model in $d = 3$ (setting $\epsilon = 1$).

Box 4.2: Stability of the Wilson-Fisher Fixed Point

Setup: The beta function in $d = 4 - \epsilon$ is $\beta_\lambda = -\epsilon\lambda + b\lambda^2 + O(\lambda^3)$.
The fixed points: Gaussian fixed point at $\lambda^*_G = 0$. Wilson-Fisher fixed point at $\lambda^*_{\mathrm{WF}} = \epsilon/b + O(\epsilon^2)$.
Stability analysis: Linearize β_λ around each fixed point.
<u>At the Gaussian:</u>

$$\frac{d(\delta\lambda)}{d\ell} = \left.\frac{d\beta_\lambda}{d\lambda}\right|_{\lambda=0} \delta\lambda = -\epsilon\,\delta\lambda \tag{205}$$

The eigenvalue is $-\epsilon < 0$ (for $\epsilon > 0$), so perturbations shrink. The Gaussian is **stable** (IR attractive).
<u>At Wilson-Fisher:</u>

$$\frac{d(\delta\lambda)}{d\ell} = \left.\frac{d\beta_\lambda}{d\lambda}\right|_{\lambda^*} \delta\lambda = (-\epsilon + 2b\lambda^*)\delta\lambda = \epsilon\,\delta\lambda \tag{206}$$

The eigenvalue is $+\epsilon > 0$, so perturbations grow. Wilson-Fisher is **unstable** (UV attractive).
Physical picture: The flow goes from Wilson-Fisher (UV) to Gaussian (IR). Theories near Wilson-Fisher flow toward free theory at

long distances. The WF fixed point controls the approach to criticality.

The Epsilon Expansion as Asymptotic Series

The Wilson-Fisher fixed point has a deep resurgent structure. The anomalous dimension η has the expansion:

$$\eta = \frac{(n+2)}{2(n+8)^2}\epsilon^2 + O(\epsilon^3) \tag{207}$$

where n is the number of field components and $\epsilon = 4 - d$.

The epsilon expansion is Gevrey-1. Borel resummation is required for meaningful predictions at $\epsilon = 1$.

This series continues to high orders and is known to be asymptotic with factorially growing coefficients. Despite the divergence, careful resummation gives remarkably accurate predictions. For the 3D Ising model ($n = 1$, $\epsilon = 1$):

$$\eta_{\text{exp}} \approx 0.0363, \qquad \eta_{O(\epsilon^2)} = \frac{3}{242} \approx 0.0124 \tag{208}$$

Higher-order calculations with Borel resummation give $\eta \approx 0.036$, in excellent agreement with experiment and numerical simulations.

The ϵ-expansion is an asymptotic series whose structure encodes information beyond perturbation theory. The tools to extract this information—Borel resummation, transseries, Stokes phenomena—are developed in Part II.

Beyond Perturbative Fixed Points

The fixed points discussed so far are found by setting the perturbatively computed beta function to zero. But the beta function is an **exact** object; perturbation theory only approximates it.

In principle, the exact beta function could have additional zeros invisible to perturbation theory. Such **non-perturbative fixed points** would arise from cancellation between perturbative and instanton contributions:

$$\beta_{\text{exact}}(g^*) = \beta_{\text{pert}}(g^*) + \beta_{\text{non-pert}}(g^*) = 0 \tag{209}$$

with $\beta_{\text{pert}}(g^*) \neq 0$ individually. Whether such fixed points exist in realistic theories is an open question best addressed with the transseries methods of Part II.

Normal Form Theory for RG Flows

The connection between RG fixed points and bifurcation theory runs deep. Near any instability, the dynamics reduces to a **normal form**—a

Near any fixed point, the RG flow can be brought to a universal **normal form** by nonlinear coordinate transformations. The normal form depends only on eigenvalue structure and symmetry—not microscopic details.

universal equation that depends only on the type of bifurcation, not on microscopic details. This is universality in dynamical systems, and it provides the organizing principle for understanding RG flows near fixed points.

The Normal Form Theorem for RG

Consider an RG flow near a fixed point:

$$\frac{dg^i}{d\ell} = \beta^i(g) = B^i{}_j\,(g^j - g^{*j}) + \frac{1}{2}C^i{}_{jk}(g^j - g^{*j})(g^k - g^{*k}) + \cdots \quad (210)$$

Normal form theorem: By a nonlinear coordinate transformation $g \to \tilde{g}(g)$, the flow can be brought to a **canonical form** that depends only on:

1. The eigenvalues $\{\lambda_\alpha\}$ of the stability matrix B
2. **Resonance conditions** between eigenvalues
3. The **symmetry** of the fixed point

Definition: A **resonance** occurs when eigenvalues satisfy:

$$\lambda_i = \sum_j n_j \lambda_j, \qquad n_j \in \mathbb{Z}_{\geq 0}, \quad \sum_j n_j \geq 2 \quad (211)$$

Resonances prevent the removal of certain nonlinear terms by coordinate transformations. The remaining terms define the normal form.

Box 3.1: Classification of Normal Forms

Goal: Classify the universal normal forms for RG flows near fixed points.
Case 1: Hyperbolic fixed point (no resonances)
When no resonances exist, the normal form is purely linear:

$$\frac{d\tilde{g}^i}{d\ell} = \lambda_i \tilde{g}^i \quad (212)$$

Solution: $\tilde{g}^i(\ell) = \tilde{g}^i_0\, e^{\lambda_i \ell}$
Leading corrections: Pure power laws t^Δ with $\Delta = -\lambda$.
Case 2: Transcritical (one marginal direction)
When $\lambda_1 = 0$ (marginal), there is a resonance $\lambda_1 = 2 \cdot 0$. The normal form includes quadratic terms:

$$\frac{dg}{d\ell} = ag^2 + O(g^3) \quad (213)$$

Solution: $g(\ell) = \frac{g_0}{1 - ag_0\ell}$
Leading corrections: **Logarithmic** corrections $(\ln t)^\alpha$.
Case 3: Pitchfork (resonance $\lambda_1 = 2\lambda_2$)

The normal form has the structure:

$$\frac{dg_1}{d\ell} = \lambda_1 g_1 + b g_2^2, \qquad \frac{dg_2}{d\ell} = \lambda_2 g_2 \tag{214}$$

Leading corrections: Mixed power-log corrections $t^\Delta \ln t$.
Case 4: Hopf (complex eigenvalues $\lambda = \pm i\omega$)
When eigenvalues are purely imaginary, the normal form is:

$$\frac{dA}{d\ell} = \mu A - g|A|^2 A \tag{215}$$

Leading corrections: **Oscillatory** corrections with period $2\pi/\omega$.

Key insight: The normal form type determines the **universal corrections to scaling**. Two systems with the same normal form type have the same leading corrections, regardless of microscopic details.

Universality Families from Normal Form Type

Different systems can be grouped into **universality families** based on their normal form type:

Normal Form	**Eigenvalue Condition**	**Leading Correction**	**Physical Example**
Hyperbolic	No resonances	Power law t^Δ	Generic Wilson-Fisher
Transcritical	$\lambda_1 = 0$ (marginal)	Logarithmic $(\ln t)^\alpha$	4D Ising (upper critical dim.)
Pitchfork	$\lambda_1 = 2\lambda_2$	$t^\Delta \ln t$	Random-field Ising
Hopf	$\lambda = \pm i\omega$	Oscillatory	Limit cycles (rare in RG)

The normal form type is a **universal** property—it depends only on eigenvalue structure, not on the specific system.

Logarithmic Corrections and Marginal Operators

The most common non-hyperbolic case in RG is the **transcritical** bifurcation, which occurs whenever there is a marginal operator.

Why marginal operators produce logarithms:

At a marginal operator, $\Delta = 0$, so the beta function starts at quadratic order:

$$\beta_g = bg^2 + O(g^3) \tag{216}$$

The solution is:

$$g(\ell) = \frac{g_0}{1 - bg_0\ell} \tag{217}$$

This produces logarithmic corrections to observables. For example, if $\langle \mathcal{O} \rangle \sim g^\alpha$:

$$\langle \mathcal{O} \rangle \sim \frac{1}{(\ln \mu/\Lambda)^\alpha} \tag{218}$$

Box 3.2: Normal Form Analysis of 4D Ising

Setup: ϕ^4 theory at the upper critical dimension $d = 4$.
The beta function:

$$\beta_\lambda = \frac{3\lambda^2}{16\pi^2} + O(\lambda^3) \tag{219}$$

Note: there is no linear term because $\epsilon = 0$ at $d = 4$. The coupling λ is **exactly marginal** at tree level.
Normal form type: Transcritical (one marginal direction).
Solution:

$$\lambda(\mu) = \frac{\lambda_0}{1 + \frac{3\lambda_0}{16\pi^2}\ln(\mu/\mu_0)} \tag{220}$$

Logarithmic corrections to scaling:
The correlation length exponent receives logarithmic corrections:

$$\xi \sim |T - T_c|^{-1/2}(\ln|T - T_c|)^{1/4} \tag{221}$$

The susceptibility:

$$\chi \sim |T - T_c|^{-1}(\ln|T - T_c|)^{1/3} \tag{222}$$

Universal amplitude: The exponent in the logarithm (1/4 for ξ, 1/3 for χ) is **universal**—determined by the normal form, not by microscopic details.

Physical systems at upper critical dimension:

- 4D Ising model
- Mean-field systems with fluctuation corrections
- Some quantum critical points

All share the transcritical normal form and hence the same logarithmic correction exponents.

Resonances and Mixed Corrections

When eigenvalues satisfy resonance conditions, the normal form contains additional nonlinear terms that cannot be removed by coordinate transformations.

The 1:2 resonance ($\lambda_1 = 2\lambda_2$):

This is particularly important in RG because it arises when one operator has exactly twice the scaling dimension of another. The normal form is:

$$\frac{dg_1}{d\ell} = \lambda_1 g_1 + b g_2^2, \qquad \frac{dg_2}{d\ell} = \lambda_2 g_2 \tag{223}$$

The solution for g_1 involves the Lambert W function:

$$g_1(\ell) \sim e^{\lambda_1 \ell} \left[1 + c\,\ell\, e^{(2\lambda_2 - \lambda_1)\ell}\right] \tag{224}$$

When $\lambda_1 = 2\lambda_2$ exactly, this gives $t^{\Delta} \ln t$ corrections.

Box 3.3: Resonance in the Random-Field Ising Model

Setup: The random-field Ising model (RFIM) in $d = 6 - \epsilon$.

The fixed point structure:

At the RFIM fixed point, there is a resonance between the thermal and random-field perturbations:

$$\Delta_r = 2\Delta_h \quad \text{(at leading order in } \epsilon\text{)} \tag{225}$$

where Δ_r is the thermal scaling dimension and Δ_h is the random-field dimension.

Normal form type: Pitchfork (1:2 resonance).

Consequence: Logarithmic corrections to power laws:

$$\xi \sim |T - T_c|^{-\nu} (\ln |T - T_c|)^{\hat{\nu}} \tag{226}$$

Universal ratio:

The exponent $\hat{\nu}$ is predicted by normal form theory:

$$\hat{\nu} = \frac{b}{2\lambda_1 - \lambda_2} \tag{227}$$

where b is the resonant coefficient in the normal form.

Experimental signature: Deviations from pure power-law scaling that grow logarithmically. These are often misidentified as "corrections to scaling" when they are actually the leading behavior predicted by normal form theory.

Self-Similar Solutions and Normal Forms

Normal form theory connects directly to Barenblatt's classification of self-similar solutions (Chapter I):

Barenblatt's Term	**Normal Form Type**	**Exponent Determination**
First-kind self-similarity	Hyperbolic	Dimensional analysis
Second-kind (incomplete)	Constrained hyperbolic	Eigenvalue problem
Logarithmic corrections	Transcritical	Marginal mode

The unifying principle: Both QFT universality classes and PDE self-similar solutions are classified by normal form type. The "anomalous" exponents in both cases arise from the same mechanism: constraints restricting the scaling group orbit.

Barenblatt's "first-kind" and "second-kind" self-similarity correspond to hyperbolic normal forms—with and without conservation constraints respectively.

Stability and Classification

Near any fixed point, perturbations either grow or shrink under RG. This determines the **universality class**.

The Stability Matrix

Linearize the beta function near a fixed point g^*:

$$\frac{d(\delta g^i)}{d\ell} = B^i{}_j\, \delta g^j, \qquad B^i{}_j = \left.\frac{\partial \beta^i}{\partial g^j}\right|_{g^*} \tag{228}$$

The eigenvalues λ_α of the stability matrix B determine the fate of perturbations.

The stability matrix B is the Jacobian of the beta function at the fixed point. Its eigenvalues classify perturbations.

Relevant, Irrelevant, Marginal

The eigenvectors of B define natural directions in coupling space. Each direction is classified by its eigenvalue.

Relevant directions have $\lambda_\alpha > 0$. Perturbations grow under RG, flowing away from the fixed point. These directions must be tuned to reach the fixed point.

Irrelevant directions have $\lambda_\alpha < 0$. Perturbations shrink under RG, flowing toward the fixed point. These directions are "self-tuning."

Marginal directions have $\lambda_\alpha = 0$. The fate depends on higher-order terms.

Box 4.6: Classification at the Gaussian Fixed Point

Setup: The 1D ϕ^4 beta functions are

$$\beta_r = 2r + \frac{3\lambda\Lambda}{\pi(\Lambda^2 + r)} \tag{229}$$

$$\beta_\lambda = 2\lambda \tag{230}$$

At the Gaussian $(r^*, \lambda^*) = (0,0)$:
The stability matrix is:

$$B = \begin{pmatrix} \partial\beta_r/\partial r & \partial\beta_r/\partial\lambda \\ \partial\beta_\lambda/\partial r & \partial\beta_\lambda/\partial\lambda \end{pmatrix}_{(0,0)} = \begin{pmatrix} 2 & 3/(\pi\Lambda) \\ 0 & 2 \end{pmatrix} \tag{231}$$

Eigenvalues: Both eigenvalues are $+2$.
Classification: Both directions are **relevant**. Any perturbation away from $(0,0)$ grows under RG. The Gaussian fixed point is "completely unstable" or "UV attractive."
Interpretation: To reach the Gaussian fixed point from the IR, we must tune both r and λ to zero. There is no basin of attraction.
The connection to Δ**:** The eigenvalues are the **scaling dimensions** of the perturbations. Here $\Delta_r = \Delta_\lambda = 2$, matching the engineering dimensions (no anomalous contribution at the Gaussian).

Scaling Dimensions and Eigenvalues

The eigenvalues of B are called **scaling dimensions** (or "RG eigenvalues"). They control how perturbations scale:

$$\delta g^\alpha(\ell) \propto e^{\Delta_\alpha \ell} \tag{232}$$

A perturbation with dimension $\Delta > 0$ grows (relevant), $\Delta < 0$ shrinks (irrelevant), and $\Delta = 0$ is marginal.

Scaling dimensions are "quantum numbers" for operators. They determine the power-law behavior of correlation functions.

At the Gaussian fixed point, scaling dimensions equal engineering dimensions. At non-trivial fixed points, interactions modify them by the **anomalous dimension**:

$$\Delta = \Delta_{\text{eng}} + \gamma \tag{233}$$

Geometric Perspective: The Stability Matrix as Covariant Derivative

The stability matrix $B^i{}_j = \partial\beta^i/\partial g^j|_{g^*}$ appears to depend on the coordinate system (scheme). Yet critical exponents—the eigenvalues of B—are scheme-independent. The geometric viewpoint developed in Chapter I explains why.

The stability matrix is the covariant derivative of the beta function at the fixed point. This makes scheme independence manifest.

The key observation: At a fixed point, the beta function vanishes: $\beta^i(g^*) = 0$. The stability matrix is then simply the ordinary derivative, but this *is* the covariant derivative at a point where the object being differentiated vanishes:

$$\nabla_j\beta^i\big|_{g^*} = \partial_j\beta^i\big|_{g^*} + \Gamma^i{}_{jk}\beta^k\big|_{g^*} = \partial_j\beta^i\big|_{g^*} = B^i{}_j \tag{234}$$

The connection terms $\Gamma^i{}_{jk}\beta^k$ vanish at g^* because $\beta^k(g^*) = 0$. Thus:

$$B^i{}_j = \nabla_j\beta^i\big|_{g^*} \tag{235}$$

Scheme independence of eigenvalues: Under a scheme change $g \to g'(g)$, the stability matrix transforms as:

$$B'^i{}_j = \frac{\partial g'^i}{\partial g^k}\bigg|_{g^*} B^k{}_l \frac{\partial g^l}{\partial g'^j}\bigg|_{g'^*} = P^i{}_k B^k{}_l (P^{-1})^l{}_j \tag{236}$$

This is a **similarity transformation**. The eigenvalues (critical exponents) are similarity-invariant, hence scheme-independent.

Box 4.6a: Geometric Invariants at Fixed Points

Goal: Identify which properties of the stability analysis are scheme-independent.

Scheme-dependent (coordinate-dependent):

- Individual components $B^i{}_j$
- The eigenvectors of B (they depend on the coordinate basis)
- The location g^* in coupling space

Scheme-independent (geometric invariants):

- Eigenvalues $\{\Delta_\alpha\}$ of B (critical exponents)
- Trace: $\mathrm{tr}(B) = \sum_\alpha \Delta_\alpha$
- Determinant: $\det(B) = \prod_\alpha \Delta_\alpha$
- Number of positive/negative/zero eigenvalues
- Higher invariants: $\mathrm{tr}(B^2)$, $\mathrm{tr}(B^3)$, etc.

Physical content:

- Number of relevant directions = number of fine-tunings needed
- Eigenvalue ratios determine correction-to-scaling exponents
- Trace relates to the "total scaling" near the fixed point

Example: Wilson-Fisher in $d = 4 - \epsilon$.
The stability matrix has eigenvalues $\Delta_1 = -\epsilon + O(\epsilon^2)$ (relevant) and $\Delta_2 = \epsilon + O(\epsilon^2)$ (irrelevant). The scheme independence of ϵ at leading order reflects the universality of the Wilson-Fisher fixed point.

Beyond linear order: For higher-order corrections to scaling, the covariant expansion (Chapter I) becomes essential. The second-order term $\nabla_i \nabla_j \beta^k|_{g^*}$ determines how scaling functions deviate from pure power laws near criticality.

The tangent space at g^*: The eigenvectors of B span the tangent space $T_{g^*}\mathcal{M}$. They define a natural basis of "scaling operators"—

perturbations that transform simply under RG. At a conformal fixed point, these are the primary operators of the CFT.

Universality Classes

Perhaps the most remarkable consequence of the RG is **universality**: different microscopic theories can exhibit identical macroscopic behavior.

The Basin of Attraction

The **basin of attraction** of a fixed point is the set of all theories that flow to it under RG. All theories in the same basin exhibit the same IR behavior. They form a **universality class**.

Universality: water at its critical point and uniaxial magnets at the Curie point are described by the same fixed point and have the same critical exponents.

Different microscopic theories (lattice models with different interactions, continuum theories with different UV cutoffs) can flow to the same fixed point. Their long-distance behavior is then identical.

Why Universality?

Consider approaching a fixed point along irrelevant directions. By definition, these directions flow toward the fixed point. The "memory" of where we started is erased.

Only the relevant directions matter because only they distinguish different theories at long distances. If two theories have the same relevant perturbations tuned in the same way, they approach the same fixed point from the same direction and have identical IR physics.

Counting Relevant Directions

The number of relevant directions determines how many parameters must be tuned to reach the fixed point. This has physical significance:

The number of relevant directions equals the number of fine-tunings needed to reach criticality.

- **Zero relevant directions**: The fixed point is an attractor. Generic theories flow toward it without tuning.
- **One relevant direction**: One parameter must be tuned (e.g., temperature to reach the critical point).
- **Two or more**: Multiple fine-tunings needed; such fixed points are typically unstable to generic perturbations.

The Wilson-Fisher fixed point in $d = 3$ has one relevant direction (the mass), making it a "codimension-1" fixed point accessible by tuning temperature.

Empirical Evidence: Universal Critical Exponents

The power of universality is demonstrated by the striking agreement of critical exponents across vastly different physical systems. Following Sethna's compilation:

Universality is an experimental fact: completely different systems share the same critical exponents with remarkable precision.

System	Transition	β	ν
Fe (iron)	Ferromagnetic	0.34 ± 0.02	0.68 ± 0.02
Ni (nickel)	Ferromagnetic	0.33 ± 0.03	0.66 ± 0.03
CO_2 (liquid-gas)	Critical point	0.34 ± 0.01	0.63 ± 0.02
Xe (liquid-gas)	Critical point	0.35 ± 0.01	0.63 ± 0.01
^{4}He (superfluid)	λ-transition	—	0.672 ± 0.001
Ising model (3D)	Theory	0.326	0.630

These systems differ radically at the microscopic level: ferromagnets involve electron spins and exchange interactions; liquid-gas transitions involve molecular forces; superfluids involve Bose-Einstein condensation. Yet they share identical critical exponents because they flow to the same RG fixed point.

The Meaning of Universality

Universality is not an approximation—it is an exact consequence of RG flow. Different microscopic Hamiltonians that share:

1. The same **symmetry** (e.g., $\mathbb{Z}_2$ for Ising, $O(3)$ for Heisenberg)
2. The same **dimensionality** (2D, 3D, etc.)
3. The same **range of interactions** (short-range vs. long-range)

will flow to the same fixed point and exhibit identical critical behavior.
The microscopic details are encoded only in **irrelevant operators** that affect the approach to criticality but not the universal exponents themselves.

Box 4.3: Critical Exponents from Stability Eigenvalues

Setup: Near the Wilson-Fisher fixed point in $d = 4 - \epsilon$.
The stability matrix: Linearizing the beta functions gives eigenvalues that determine critical exponents:

$$\lambda_1 = -\epsilon + O(\epsilon^2), \qquad \lambda_2 = 2 - \frac{n+2}{n+8}\epsilon + O(\epsilon^2) \tag{237}$$

Physical interpretation:

- $\lambda_1 < 0$: The λ direction is **irrelevant**—systems flow toward the fixed point in this direction

- $\lambda_2 > 0$: The mass direction is **relevant—**must tune temperature to reach criticality

Critical exponent ν**:** The correlation length diverges as $\xi \sim |T - T_c|^{-\nu}$ with:

$$\nu = \frac{1}{\lambda_2} = \frac{1}{2} + \frac{n+2}{4(n+8)}\epsilon + O(\epsilon^2) \tag{238}$$

For the 3D Ising model ($n = 1$, $\epsilon = 1$):

$$\nu_{\epsilon\text{-expansion}} \approx 0.63 \qquad \nu_{\text{experiment}} \approx 0.630 \tag{239}$$

The remarkable agreement between perturbative calculations and experiment is a triumph of the RG.

Normal Forms and Universal Scaling Functions

The connection between RG fixed points and bifurcation theory runs deep. Near any instability, the dynamics reduces to a **normal form—**a universal equation that depends only on the type of bifurcation, not on microscopic details. This is universality in dynamical systems.

Normal forms are the dynamical systems analog of RG fixed points: universal equations that capture behavior near instabilities.

Bifurcations as RG Fixed Points

Consider a system near a bifurcation point where a steady state loses stability. The dynamics can be reduced to a low-dimensional "center manifold" where the normal form governs the dynamics.

Box 4.4: The Pitchfork Bifurcation as RG Flow

The normal form: Near a pitchfork bifurcation, the dynamics of the order parameter x is:

$$\frac{dx}{dt} = \mu x - x^3 \tag{240}$$

where μ is the control parameter (e.g., $\mu \propto T_c - T$).
Fixed points:

- $x^* = 0$ for all μ (symmetric state)
- $x^* = \pm\sqrt{\mu}$ for $\mu > 0$ (symmetry-broken states)

RG interpretation: The control parameter μ plays the role of a **relevant coupling**. The bifurcation point $\mu = 0$ is an RG fixed point.

Stability analysis: Linearize around $x = 0$:

$$\frac{d(\delta x)}{dt} = \mu \cdot \delta x \tag{241}$$

The "scaling dimension" is $\Delta = \mu$:

- $\mu < 0$: Irrelevant perturbation (stable fixed point)
- $\mu > 0$: Relevant perturbation (unstable, flows to $\pm\sqrt{\mu}$)
- $\mu = 0$: Marginal (the bifurcation point itself)

Critical exponent: Near the bifurcation, $x^* \sim \mu^\beta$ with $\beta = 1/2$. This is the **mean-field** exponent, corresponding to the Gaussian fixed point in RG language.

Universality: Any system with a $\mathbb{Z}_2$ symmetry undergoing a continuous transition reduces to this normal form near the bifurcation. The exponent $\beta = 1/2$ is universal for mean-field pitchforks.

The Hopf Bifurcation and Limit Cycles

When a fixed point loses stability to oscillations, the dynamics reduces to the **Hopf normal form**:

The Hopf normal form is the amplitude equation we studied in Chapter I—now seen as a universal RG fixed point for oscillatory instabilities.

$$\frac{dA}{dt} = \mu A - g|A|^2 A \tag{242}$$

where A is a complex amplitude and $g > 0$ for a supercritical bifurcation.

This is exactly the amplitude equation from Chapter I! The connection reveals:

- The limit cycle amplitude $|A^*| = \sqrt{\mu/g}$ plays the role of the order parameter
- The stability eigenvalue $y = 2\mu$ determines the approach to the limit cycle
- The nontrivial fixed point $|A| = \sqrt{\mu/g}$ is the "ordered phase"

Box 4.5: Universal Scaling Near Hopf Bifurcation

Setup: Consider any system undergoing a Hopf bifurcation at $\mu = 0$.

Scaling of the limit cycle amplitude:

$$|A^*| = \sqrt{\frac{\mu}{g}} \sim \mu^{1/2} \tag{243}$$

The exponent $\beta = 1/2$ is universal for supercritical Hopf bifurcations.

Critical slowing down: The relaxation rate toward the limit cycle is:

$$\lambda = 2\mu \tag{244}$$

As $\mu \to 0^+$, relaxation becomes arbitrarily slow: $\tau_{\text{relax}} = 1/\lambda \to \infty$.

RG interpretation: The diverging relaxation time is the **dynamical** analog of the diverging correlation length in equilibrium systems. In the RG language:

$$\tau \sim |\mu|^{-\nu z}, \qquad \xi \sim |\mu|^{-\nu} \tag{245}$$

where z is the dynamic critical exponent. For mean-field Hopf, $\nu = 1/2$ and $z = 2$ give $\tau \sim |\mu|^{-1}$.

Physical examples:

- Laser threshold (population inversion vs. losses)
- Rayleigh-Bénard convection (heating vs. viscosity)
- Chemical oscillations (Belousov-Zhabotinsky reaction)

All share the same universal exponents because they share the same normal form.

Critical Slowing Down as a Geometric Phenomenon

Near a fixed point, all perturbations decay exponentially. But the decay *rate* depends on the distance to the fixed point through the stability eigenvalues.

Critical slowing down: as we approach a bifurcation, the system takes longer to reach equilibrium because the effective "restoring force" vanishes.

The mechanism: Near a fixed point g^* with stability matrix B:

$$\delta g(t) = \sum_\alpha c_\alpha v_\alpha e^{\Delta_\alpha t} \tag{246}$$

The slowest-decaying mode has eigenvalue $\Delta_{\min}$ closest to zero. As we tune toward a bifurcation, $\Delta_{\min} \to 0$, and relaxation times diverge.

The metric interpretation: In the language of the Fisher/Zamolodchikov metric, critical slowing down corresponds to a **diverging geodesic distance** to the fixed point. Near criticality:

$$d_{\text{geodesic}}(g, g^*) \sim \int_g^{g^*} \sqrt{G_{ij} dg^i dg^j} \to \infty \tag{247}$$

because the susceptibility $G_{rr} \sim |r - r_c|^{-\gamma}$ diverges.

This provides a geometric explanation: approaching the critical point requires traversing an *infinite* geodesic distance in theory space. The "slowing down" is the system struggling to cover this distance.

The Porous Medium Equation

Our third and final example is the **porous medium equation** (PME), which governs nonlinear diffusion in porous media. This example exhibits **anomalous dimensions** that dimensional analysis cannot predict.

The PME describes gas flow through porous rock, groundwater seepage, and heat conduction in plasmas. It's the simplest PDE with anomalous dimensions.

The Model

The porous medium equation in d dimensions is:

$$\frac{\partial \rho}{\partial t} = D\nabla^2(\rho^m) \tag{248}$$

where $\rho(x,t) \geq 0$ is the density, D is a diffusion coefficient, and $m > 1$ is the nonlinearity exponent.

For $m = 1$, this reduces to the linear heat equation $\partial\rho/\partial t = D\nabla^2\rho$. The nonlinearity $m > 1$ means diffusion is faster where density is higher.

Why the PME?

The PME is ideal for demonstrating anomalous dimensions for several reasons. It's a single PDE with one nonlinearity parameter m. Self-similar solutions exist and can be found exactly. Dimensional analysis fails to determine the similarity exponents when $m \neq 1$. And the RG calculation is tractable.

Box 4.8: Dimensional Analysis for the PME

Setup: Consider a localized initial condition with total mass $M = \int \rho \, d^d x$. What is the width $L(t)$ at late times?

Parameters and dimensions:

Quantity	Symbol	Dimensions
Width	L	$[L]$
Time	t	$[T]$
Diffusion coefficient	D	$[L^2/T] \cdot [\rho^{1-m}]$
Total mass	M	$[\rho] \cdot [L^d]$
Exponent	m	dimensionless

For $m = 1$ (linear diffusion): D has dimensions $[L^2/T]$. The width must be:

$$L(t) = \sqrt{Dt} \cdot f(M, d) \tag{249}$$

For the heat kernel, f is a constant. Result: $L \propto t^{1/2}$ (first-kind self-similarity).
For $m \neq 1$: D has dimensions that depend on ρ, which has no fixed scale! The parameters D, M, t cannot be combined to give L without knowing how ρ scales.
The problem: Dimensional analysis gives $L \propto t^{\alpha}$ with α *undetermined*. The exponent must come from solving the equation.

Barenblatt's Classification in Lie Group Terms

Barenblatt distinguished two types of self-similar solutions. This distinction has a beautiful interpretation in the Lie group framework: it reflects whether the scaling group acts **freely** or is **constrained** by conservation laws.

The Scaling Group Action

Barenblatt's "incomplete similarity" is the Lie group statement that constraints restrict the scaling orbit.

The **scaling group** $G = (\mathbb{R}^+, \cdot)$ acts on solutions of a PDE. For the PME $\partial_t \rho = D\nabla^2(\rho^m)$, consider the transformation:

$$t \mapsto \lambda^a t, \qquad x \mapsto \lambda^b x, \qquad \rho \mapsto \lambda^c \rho \tag{250}$$

where $\lambda \in \mathbb{R}^+$ is the group parameter and (a, b, c) parameterize the representation.

For the transformation to be a symmetry (mapping solutions to solutions), the exponents must satisfy:

$$c - a = mc - 2b \quad \Rightarrow \quad c(m-1) = a - 2b \tag{251}$$

This is **one constraint on three parameters**, leaving a two-parameter family of scaling symmetries.

First-Kind Self-Similarity: Free Orbits

A solution has **first-kind self-similarity** if dimensional analysis completely determines the scaling exponents. In Lie group terms:

- The scaling group acts **freely** on the space of solutions
- The exponents are uniquely determined by the group representation
- No additional constraints are needed

First-kind: the scaling group orbit is unrestricted. Dimensional analysis gives the unique exponent.

For the linear heat equation ($m = 1$), the constraint becomes $0 = a - 2b$, so $a = 2b$. With the natural choice $b = 1$ (lengths scale as λ), we get $a = 2$ (time scales as λ^2). The exponent is:

$$\beta = \frac{b}{a} = \frac{1}{2} \tag{252}$$

This is exactly what dimensional analysis predicts. The fundamental solution is:

$$\rho(x,t) = \frac{1}{(4\pi Dt)^{d/2}} \exp\left(-\frac{|x|^2}{4Dt}\right) \tag{253}$$

Second-Kind Self-Similarity: Constrained Orbits

A solution has **second-kind self-similarity** if dimensional analysis fails. In Lie group terms:

- An additional **constraint** (typically a conservation law) restricts the scaling orbit
- The exponent emerges as the **intersection** of the scaling orbit with the constraint surface
- This intersection is a **nonlinear eigenvalue problem**

Second-kind: the constraint surface intersects the scaling orbit at a unique point, determining the anomalous exponent.

For the PME with $m \neq 1$, the constraint is **mass conservation**:

$$M = \int \rho \, d^d x = \text{constant} \tag{254}$$

Under scaling, $M \mapsto \lambda^{c+db} M$. For mass to be conserved:

$$c + db = 0 \quad \Rightarrow \quad c = -db \tag{255}$$

Combined with the symmetry constraint $c(m-1) = a - 2b$:

$$-db(m-1) = a - 2b \quad \Rightarrow \quad a = 2b - db(m-1) = b[2 - d(m-1)] \tag{256}$$

The exponent is:

$$\beta = \frac{b}{a} = \frac{1}{2 - d(m-1)} = \frac{1}{d(m-1)+2} \tag{257}$$

This is the Barenblatt exponent! It differs from $1/2$ and cannot be obtained by dimensional analysis alone.

Box 4.9: Why Second-Kind Requires Dynamical Determination

The geometry: Consider the space of scaling parameters (a, b, c).
The symmetry constraint: The PME symmetry requires $c(m - 1) = a - 2b$. This defines a **plane** Π_{sym} in (a, b, c)-space.
The conservation constraint: Mass conservation requires $c =$

$-db$. This defines another **plane** Π_{cons}.
For $m = 1$**:** The symmetry constraint becomes $0 = a - 2b$, which is independent of c. Any value of c satisfying mass conservation works. The scaling orbit is a **line** in solution space, and dimensional analysis picks out the unique exponent.
For $m \neq 1$**:** The two planes Π_{sym} and Π_{cons} intersect in a **line**. Setting $b = 1$ (normalization), the intersection determines:

$$a = 2 - d(m-1), \qquad c = -d \tag{258}$$

The anomalous dimension:

$$\gamma = \beta - \frac{1}{2} = \frac{1}{d(m-1)+2} - \frac{1}{2} = \frac{-d(m-1)}{2[d(m-1)+2]} \tag{259}$$

Physical interpretation: The constraint surface (mass conservation) "selects" a unique scaling orbit from among the family allowed by symmetry. The anomalous exponent is geometrically the direction of this selected orbit.
The nonlinear eigenvalue problem: Finding β requires solving for the intersection of the symmetry plane with the constraint hypersurface. This is equivalent to an eigenvalue problem for the profile function $f(\xi)$.

Barenblatt's Insight in RG Language

Barenblatt's distinction maps directly to RG concepts:

Barenblatt's term	**RG/Lie interpretation**
First-kind self-similarity	Scaling group acts freely; engineering dimensions
Second-kind (incomplete)	Constraints restrict orbit; anomalous dimensions
Intermediate asymptotics	Approach to fixed point under RG flow
Anomalous dimensions	Eigenvalue of nonlinear spectral problem

The "anomalous dimensions" that appear throughout physics—from the PME to critical phenomena to QFT—are all instances of the same geometric phenomenon: **constraints restricting the scaling group orbit**.

The Barenblatt Exponents from Symmetry

The PME has a three-dimensional Lie symmetry algebra spanned by time translation, space translation, and scaling. For $m \neq 1$, the scaling generator is:

$$\mathbf{X}_3 = 2t\frac{\partial}{\partial t} + x\frac{\partial}{\partial x} - \frac{d}{m-1}\rho\frac{\partial}{\partial \rho} \tag{260}$$

This scaling symmetry suggests self-similar solutions $\rho(x,t) = t^{-\alpha} f(x/t^{\beta})$. But the symmetry alone does *not* determine the exponents—it gives $\beta = 1/2$ (first-kind similarity).

The scaling symmetry alone gives $\beta = 1/2$. Mass conservation provides the second constraint needed for the anomalous exponent.

The **mass conservation** constraint $M = \int \rho \, d^d x = \text{const}$ provides the additional equation $\alpha = d\beta$. Combined with the PME consistency condition $(m-1)\alpha = 2\beta - 1$, we get:

$$\boxed{\beta = \frac{1}{d(m-1)+2}, \qquad \alpha = \frac{d}{d(m-1)+2}} \tag{261}$$

The Barenblatt-Pattle solution $f(\xi) = [C - k\xi^2]_+^{1/(m-1)}$ is the unique solution with compact support and the correct mass.

The key insight: The anomalous exponent arises from the **intersection of two constraints**—symmetry and conservation. This is the geometric origin of second-kind self-similarity, as explained in Box 4.9. (For a detailed Lie symmetry analysis, see Olver's *Applications of Lie Groups to Differential Equations*.)

The PME as an RG Flow

The Barenblatt exponents have a natural interpretation in the RG language. The PME flows to a fixed point where the exponents are determined dynamically.

The Parameter Space

Consider the family of self-similar solutions parameterized by their exponents:

$$\rho_{\alpha,\beta}(x,t) = t^{-\alpha} f_{\alpha,\beta}(|x|/t^{\beta}) \tag{262}$$

Only special values of (α, β) give solutions to the PME. The Barenblatt values are a fixed point of the RG in the space of self-similar profiles.

The Barenblatt solution is an RG fixed point in the space of self-similar profiles.

Stability and Selection

Why does the Barenblatt solution emerge? Other self-similar forms might exist but are unstable. Under the RG (zooming out), generic initial conditions flow toward the stable self-similar profile.

The Barenblatt fixed point is **IR stable**: perturbations decay as $t \to \infty$. This is why the exponents (261) are observed experimentally.

The Transseries Structure

The self-similar exponent β is computed exactly in this case. Expanding around $m = 1$:

$$\beta = \frac{1}{2} - \frac{d}{4}(m-1) + \frac{d(d+2)}{8}(m-1)^2 - \cdots \tag{263}$$

This expansion in $(m-1)$ is the analog of the ϵ-expansion around the Gaussian fixed point. Unlike the Wilson-Fisher case, here the exact answer is known, making the PME an ideal testing ground for approximation methods.

The PME provides a concrete example where anomalous exponents can be computed exactly.

The Landscape of Fixed Points

The full picture includes all fixed points organized by their stability properties and connected by RG flows.

The RG "Phase Diagram"

Fixed points form a **landscape** in parameter space. The RG flow connects different fixed points, and the stability structure determines which fixed points are "reached" from generic initial conditions.

The structure of fixed points and the flows between them determines the long-distance physics of the theory.

Generic UV completions flow to IR fixed points. Which IR fixed point is reached depends on the relevant directions and how they are tuned. The irrelevant directions are forgotten along the flow.

Conformal Windows

In gauge theories, there can be ranges of parameter space ("conformal windows") where the theory flows to a non-trivial interacting fixed point rather than to a free theory. The boundaries of these windows are determined by when fixed points collide and disappear.

The existence and extent of conformal windows is an active area of research, particularly in strongly coupled gauge theories where perturbation theory provides limited guidance.

Emergent Symmetry at Fixed Points

Fixed points often have enhanced symmetry compared to generic points in theory space. Scale invariance is automatic, and under mild conditions scale invariance implies the full conformal symmetry in $d > 2$.

This emergent symmetry provides powerful constraints. Conformal field theory techniques can compute correlation functions exactly at fixed points, even in strongly coupled theories.

Conformal Constraints at Fixed Points

When a fixed point enjoys conformal symmetry, the conformal algebra provides **algebraic constraints** on the CFT data that go beyond simply requiring $\beta(g^*) = 0$. These constraints are particularly powerful in the context of the exact renormalization group and the derivative expansion.

Conformal symmetry at fixed points provides algebraic constraints that go beyond $\beta(g^*) = 0$.

Scale Invariance vs Conformal Invariance

A theory at a fixed point is automatically **scale invariant**: the beta function vanishes, so the theory looks the same at all scales. But does scale invariance imply conformal invariance?

The stress-energy tensor encodes the answer. In a scale-invariant theory:

$$\langle T^{\mu}{}_{\mu} \rangle = 0 \quad \text{(tracelessness)} \tag{264}$$

But conformal invariance requires more: the stress tensor must be **improvement-conserved**. In practice, this means the "virial current" $V_\mu = x^\nu T_{\mu\nu}$ satisfies $\partial^\mu V_\mu = T^{\mu}{}_{\mu}$ with no additional divergence.

Theorem (Polchinski, 1988; Luty-Polchinski-Rattazzi, 2012): In unitary, local QFT in $d = 2$ and $d = 4$, scale invariance implies conformal invariance.

This is a powerful result: it means the full conformal algebra is available at fixed points, providing additional constraints on correlation functions and OPE data.

Conformal Ward Identities and the Derivative Expansion

The exact renormalization group (ERG) provides a non-perturbative formulation of RG flows. In the derivative expansion, the effective action is organized as:

$$\Gamma[\phi] = \int d^d x \left[V(\phi) + \frac{1}{2} Z(\phi)(\partial\phi)^2 + O(\partial^4) \right] \tag{265}$$

At a fixed point, conformal invariance provides constraints on the functions $V(\phi)$ and $Z(\phi)$.

Conformal Ward identities at $O(\partial^2)$ provide new constraints not seen at the local potential approximation level.

At the local potential approximation (LPA): The constraint is simply that $V(\phi)$ satisfies a fixed-point equation. No conformal constraint appears at this order.

At $O(\partial^2)$: New conformal constraints appear! The conformal Ward identities relate $V''(\phi)$ and $Z(\phi)$:

$$Z(\phi) = \left(\frac{d - 2 + \eta}{d - 2} \right) \frac{V''(\phi)}{\lambda^*} + \text{corrections} \tag{266}$$

where η is the anomalous dimension and λ^* is the fixed-point coupling.

These "conformal constraints" were recently emphasized by Delamotte and collaborators: they provide additional equations that must be satisfied at a conformal fixed point, beyond the flow equations alone. Including them improves the accuracy of derivative expansion calculations.

Box 4.10: Conformal Constraints on the Wilson-Fisher Fixed Point

Setup: Consider the $O(N)$ model in $d = 3$ at the Wilson-Fisher fixed point.

The LPA fixed point: The potential $V(\phi)$ satisfies:

$$-dV + \frac{d-2}{2}\phi V' = \frac{N-1}{2} A_d \frac{V'}{1+V''} + \frac{1}{2} A_d \frac{V' + \phi V''}{1 + V'' + 2\phi V'''} \tag{267}$$

where $A_d = 2/(d\,\mathrm{vol}(S^d))$.

Without conformal constraints: Solving the LPA equation for $N = 1$ gives $\eta \approx 0.027$.

With conformal constraints: Including the $O(\partial^2)$ Ward identity constraint:

$$\eta = \frac{d-4}{d-2} \cdot \frac{\phi V'''(\phi_0)}{V''(\phi_0)} \tag{268}$$

evaluated at the minimum ϕ_0, gives $\eta \approx 0.036$, in much better agreement with the bootstrap value $\eta \approx 0.0363$.

Message: Conformal symmetry provides *additional* constraints beyond the RG flow equations. Including them systematically improves precision.

When Scale Does Not Imply Conformal

The theorems above assume unitarity and locality. When these fail, scale invariance can exist without conformal invariance. This has important consequences for systems where the standard assumptions break down.

Box 4.11: Scale Without Conformal—2D Elasticity

The counterexample (Riva-Cardy, 2005):
Consider a 2D elastic medium described by displacement fields $u_i(x)$. The action:

$$S = \int d^2x \left[\frac{\mu}{2} (\partial_i u_j)^2 + \frac{\lambda}{2} (\partial_i u_i)^2 \right] \tag{269}$$

where μ and λ are Lamé coefficients.

Scale invariance: The action is quadratic in fields with no dimensionful parameters (after rescaling). The theory is scale invariant at any μ/λ.

No conformal invariance: The stress tensor trace contains a term:

$$T^{\mu}{}_{\mu} \propto \partial^2(u_i u_i) \tag{270}$$

This is a total derivative, so $\langle T^{\mu}{}_{\mu}\rangle = 0$ (scale invariance). But it is *not* an improvement term—it cannot be removed by adding $\partial^\mu\partial^\nu X_{\mu\nu}$ for any local X.

The consequence: The theory is scale invariant but *not* conformal invariant. The conformal Ward identities fail, and the usual CFT techniques do not apply.

Why this matters: Elastic theories describe phonons in crystals, membranes, and other condensed matter systems. The failure of conformal invariance means RG analysis must proceed without the powerful CFT toolkit.

The algebraic diagnosis: The violation occurs because the theory has a "virial current" that is not conserved. In the Lie algebra language: the dilation generator D is in the symmetry algebra, but the special conformal generators K_μ are not.

The elasticity example shows that conformal constraints are not automatic—they require checking. When they hold, they provide powerful tools. When they fail, alternative methods (explicit RG calculation, perturbation theory) are needed.

Synthesis: The Algebraic-Geometric Dictionary

The preceding worked boxes have developed two parallel languages for the renormalization group: **algebraic** (Lie algebras, representations, invariants) and **geometric** (manifolds, connections, metrics). Table 3 provides a systematic translation between them.

This dictionary summarizes the dual perspectives developed throughout this chapter. Neither viewpoint is "correct"—they are complementary, each illuminating aspects obscured by the other.

Using the dictionary:

1. **Algebraic → Geometric:** When you have a Lie algebra action, geometrize it to reveal the underlying manifold structure. Fixed points become critical manifolds; eigenvalues become stability directions.

2. **Geometric → Algebraic:** When you have a flow on a manifold, algebraize it to extract conserved quantities and symmetries. The Zamolodchikov metric becomes a Casimir; scheme changes become gauge transformations.

The power of analogy:

Algebraic Structure	Geometric Structure
Lie algebra $\mathfrak{g}$ (dilation)	Tangent space $T_g\mathcal{M}$ at coupling g
Generator $D = \beta^i \partial_i$	Vector field β on coupling space
Lie transport $\mathcal{L}_D \Gamma = 0$	Parallel transport along β
Representation on operators	Sections of operator bundle
Weight/eigenvalue γ	Connection coefficient Γ
Casimir invariant C	c-function (monotonic scalar)
Cocycle condition $d\beta^\flat = 0$	Integrability (potential flow)
Affine algebra $[\nabla_X, \nabla_Y]$	Curvature tensor R^i_{jkl}
Eigenvalue problem $M \cdot v = \lambda v$	Geodesic deviation (Jacobi equation)
Invariant subspace	Fixed point manifold
Character (trace on representation)	Partition function
Central extension	Anomaly (Weyl, conformal)
Grading by dimension	Filtration by relevance

Table 3: Algebraic-Geometric Dictionary for the Renormalization Group (after Dolan).

QFT Concept	PME Analog
Coupling constant g	Nonlinearity exponent m
Cutoff Λ or μ	Time t
Beta function $\beta(g)$	Rate of scaling exponent change
Fixed point g^*	Self-similar profile ρ_B
Anomalous dimension γ	Barenblatt exponent $\beta - 1/2$
Stability matrix M_{ij}	Perturbation spectrum
Relevant/irrelevant perturbations	Growing/decaying modes
Universality class	Asymptotic profile
c-function (monotonic)	Entropy functional $\mathcal{F}[\rho]$
Operator mixing	Moment coupling
Zamolodchikov metric G_{ij}	Fisher information metric
Scheme dependence	Choice of moment basis
Conformal symmetry	Scale-free intermediate asymptotics

Table 4: Translation Table: QFT vs. PME.

The PME is **not** a quantum field theory, yet it shares the same algebraic and geometric structures. This is not coincidence—both systems exhibit **scale invariance** at special points, and the RG formalism captures the universal features of scale-invariant dynamics.

Methodological Principle

The Dolan Program: Use geometric structures to reveal algebraic invariants.

1. Identify the **Lie algebra** acting on observables (dilation + special conformal at fixed points)
2. Construct the **connection** from the anomalous dimension matrix
3. Build the **metric** from two-point functions (Zamolodchikov)
4. Check **integrability** to establish c-theorem-type results
5. Study **geodesics** to understand preferred paths in theory space

This program applies equally to QFT, statistical mechanics, and nonlinear PDEs.

Looking Ahead

This chapter classified fixed points by stability and introduced anomalous dimensions. The three examples now cover complementary phenomena.

Oscillator: secular terms. ϕ^4: beta functions. PME: anomalous dimensions. Together they demonstrate the complete RG framework.

The oscillator demonstrated secular terms and running parameters with trivial fixed point structure. **The ϕ^4 theory** showed nontrivial beta functions and the Gaussian fixed point. **The PME** revealed anomalous dimensions and second-kind self-similarity.

Comparison of the Four Canonical Examples

Table 5 summarizes the four canonical examples and their roles in the RG framework. Each example adds complexity while remaining analytically tractable.

The oscillator demonstrates the basic RG mechanism: secular terms signal the need for running parameters. It has only a trivial fixed point (at zero amplitude).

The amplitude equation is the simplest system with a *nontrivial* fixed point. Everything is exact: fixed points, stability eigenvalues,

Feature	Oscillator	Amplitude Eq.	PME	ϕ^4 Theory
Equation	$\ddot{x} + 2\gamma\dot{x} + \omega_0^2 x + \epsilon x^3 = 0$	$\dot{A} = \mu A - g\|A\|^2 A$	$\partial_t \rho = \nabla^2(\rho^m)$	$\int e^{-S[\phi]}$
Scale	Time t	Time t	Time t	Cutoff Λ
Parameters	$A(t)$, $\phi(t)$	Amplitude $A(t)$	Exponents α, β	$r(\Lambda)$, $u(\Lambda)$
Beta function	$\beta_A = -\gamma A$, $\beta_\phi = \frac{3\epsilon A^2}{8\omega_0}$	$\beta_A = \mu A - gA^3$ (exact)	Implicit	$\beta_u = -\epsilon u + O(u^2)$
Fixed points	Trivial only	Trivial + nontrivial	Self-similar	Gaussian + WF
Stability	$A = 0$ stable	Exact: $y = 2\mu$	Exact	$y = \epsilon + O(\epsilon^2)$
Anomalous dim.	$\gamma = 0$	$\gamma = 0$	$\gamma \neq 0$ (exact)	$\eta = O(\epsilon^2)$
Calculational	Lindstedt-Poincaré	Exact algebra	Similarity	Loop expansion
Key lesson	Secular terms	Exact nontrivial FP	Anomalous scaling	Universality

Table 5: The four canonical examples and the RG concepts they illustrate. The amplitude equation and PME are exactly solvable; the oscillator and ϕ^4 require perturbative methods for detailed predictions.

and the full phase diagram. It is the "hydrogen atom" of RG theory, providing the template for more complex systems like ϕ^4.

The PME exhibits anomalous dimensions at leading order—exponents that dimensional analysis cannot predict. The self-similar Barenblatt solution is exact, and the anomalous exponents are determined by dynamical constraints.

The ϕ^4 theory is the canonical QFT example. It requires perturbative (loop) calculations but captures the full structure: universality, the Wilson-Fisher fixed point, and connections to critical phenomena.

The Road to Part II

Part I developed the *exact* geometric framework. Part II develops the analytical tools for *computing* within this framework.

Part I has established the RG as an exact geometric framework:

- Theory space is a **manifold** with the beta function as a vector field
- Fixed points are **zeros** of this vector field (scale-invariant theories)
- Stability is determined by the **Lie derivative** (linearized flow)
- Operators live in a **bundle** with anomalous dimensions as the connection
- Physical predictions are **RG-invariant** (parallel transport)

This framework is *exact*—it holds whether we compute perturbatively or non-perturbatively. Part II (Chapters 7–8) develops the **analytical methods** for computing within this framework:

Chapter II examines perturbation theory and its limitations. Perturbative series generically diverge (factorial growth), but this divergence *encodes* non-perturbative physics. The Borel transform, resummation, and resurgence theory provide tools for extracting physical predictions from divergent series.

Chapter 8 synthesizes the geometric and analytical perspectives into a unified recipe for RG analysis.

Geometric Content in Chapter I

The geometric aspects of RG—the Fisher/Zamolodchikov metric, gradient flow and c-theorem, geodesic interpretation, and curvature invariants—are developed in Chapter I. These structures provide powerful constraints on RG flows (such as monotonicity and scheme independence of critical exponents), while this chapter focuses on the dynamics near fixed points and the universal structure revealed by normal form theory.
See especially:

- Section I: The Fisher/Zamolodchikov metric on theory space
- Section I: Gradient flow and the c-theorem
- Section I: Geodesic interpretation of RG flows
- Section I: How geometry constrains beta functions

Exercises

1. **Stability analysis.** For a two-dimensional flow with $\beta^1 = g^1(1 - g^1)$ and $\beta^2 = -g^2(1 + g^1)$:
   (a) Find all fixed points.
   (b) Compute the stability matrix $B^i{}_j = \partial\beta^i/\partial g^j$ at each fixed point.
   (c) Classify each fixed point as UV-stable, IR-stable, or saddle.
2. **Universality.** Two theories with different microscopic Hamiltonians flow to the same fixed point.
   (a) Explain why their long-distance physics (critical exponents, correlation functions) must be identical.
   (b) How do they differ in the approach to the fixed point?
   (c) Discuss the role of "irrelevant operators" in distinguishing UV-complete theories.

3. **Porous medium equation.** The PME $\partial_t \rho = \nabla^2(\rho^m)$ has similarity solutions $\rho(x,t) = t^{-\alpha} f(x/t^\beta)$ with $\alpha = d/(d(m-1)+2)$ and $\beta = 1/(d(m-1)+2)$.
   (a) Verify these exponents satisfy the scaling relation $\alpha = d\beta$.
   (b) For $m = 1$ (linear diffusion), confirm $\alpha = d/2$ and $\beta = 1/2$.
   (c) Explain why $m \neq 1$ gives "anomalous" exponents that differ from dimensional analysis.
4. **Non-perturbative fixed points.** Consider a beta function $\beta(g) = -g + g^2 + ce^{-1/g}$ for small positive c.
   (a) Find the perturbative fixed points ($c = 0$).
   (b) Show that for small $c > 0$, the non-perturbative term creates new fixed points.
   (c) Discuss how these new fixed points are invisible to perturbation theory.
5. **(Challenge) Marginally relevant operators.** When $\Delta = 0$ (marginal), higher-loop effects determine stability.
   (a) For $\beta = g^2/(16\pi^2)$, solve for $g(\mu)$ starting from $g(\mu_0) = g_0$.
   (b) Show that $g \to 0$ as $\mu \to 0$ (the operator is marginally irrelevant).
   (c) Discuss the running of QED coupling and explain why α grows at high energies.
6. **(Preview of Part II) Monodromy from Borel singularities.** Consider a function with asymptotic expansion $f(\epsilon) \sim \sum_{n=0}^{\infty} a_n \epsilon^n$ where $a_n \sim n!$.
   (a) Show the Borel transform has a singularity on $\mathbb{R}^+$.
   (b) Construct the transseries $f = f_0 + \sigma e^{-S/\epsilon} f_1 + \cdots$.
   (c) Use the requirement that f be real for $\epsilon > 0$ to constrain the Stokes constant.
   (d) Interpret the constraint geometrically as a monodromy condition.
7. **Normal forms and universality (Sethna).** The pitchfork normal form $\dot{x} = \mu x - x^3$ describes systems with $\mathbb{Z}_2$ symmetry near a continuous bifurcation.
   (a) Show that any system $\dot{x} = f(x;\mu)$ with $f(0;\mu) = 0$, $f(-x;\mu) = -f(x;\mu)$, and $\partial_x f(0;0) = 0$ reduces to the pitchfork form near $(\mu, x) = (0,0)$.
   (b) Compute the "critical exponent" β where $x^* \sim \mu^\beta$ for the ordered states.

(c) The normal form has a *marginal* direction at $\mu = 0$. Explain why this corresponds to a bifurcation rather than an ordinary fixed point.

(d) In RG language, interpret μ as a relevant coupling and explain why the pitchfork is the universal form for $\mathbb{Z}_2$-symmetric systems.

8. **Critical slowing down and geodesic distance.** Near a phase transition, the relaxation time τ diverges as $\tau \sim |T - T_c|^{-\nu z}$.

(a) For the Ising model in 3D, $\nu \approx 0.63$ and $z \approx 2.02$ (Model A dynamics). Compute how τ grows as $T \to T_c$.

(b) The susceptibility (Fisher metric component) diverges as $\chi \sim |T - T_c|^{-\gamma}$ with $\gamma \approx 1.24$. Show that the geodesic distance $d = \int \sqrt{\chi}\, dT$ from T to T_c diverges logarithmically.

(c) Interpret critical slowing down geometrically: why does the system "take forever" to reach the critical point?

(d) Real systems never quite reach T_c due to finite-size effects. If the sample size is L, and $\xi(T) \sim |T - T_c|^{-\nu}$ is the correlation length, at what temperature does finite-size rounding occur?

9. **Universality across systems (empirical).** The following systems all have critical exponents close to the 3D Ising values ($\beta \approx 0.326$, $\gamma \approx 1.24$, $\nu \approx 0.630$):

- Uniaxial ferromagnets (e.g., Fe, Ni)
- Liquid-gas critical points (e.g., CO_2, Xe)
- Binary fluid mixtures (e.g., isobutyric acid + water)
- Antiferromagnets at the Néel point

(a) What symmetry do all these systems share that determines their universality class?

(b) Why do systems as different as magnets and fluids share the same exponents?

(c) The 3D XY model ($O(2)$ symmetry) describes the superfluid λ-transition in ^{4}He, with $\nu \approx 0.672$. Why is this different from the Ising value?

(d) Predict what universality class describes the critical point of the isotropic Heisenberg ferromagnet ($O(3)$ symmetry).

10. **Order parameters as coordinates on theory space.** Different physical systems exhibit order at different scales. The *choice* of order parameter determines the coordinate system on theory space $\mathcal{M}$. Consider the following systems and their order parameters (following Sethna's taxonomy):

System	Order Parameter	Broken Symmetry
Crystal	Density $\rho(\mathbf{r})$	Translation
Ferromagnet	Magnetization $\mathbf{M}$	Rotation SO(3)
Nematic liquid crystal	Director $\hat{\mathbf{n}}$	Rotation mod $\mathbb{Z}_2$
Superfluid	Complex $\psi = \lvert\psi\rvert e^{i\theta}$	U(1) phase

(a) For a ferromagnet near the Curie point, the order parameter is $\mathbf{M}$. The magnitude $|\mathbf{M}|$ vanishes at T_c. In RG language, $|\mathbf{M}|$ is a *relevant* perturbation away from the critical fixed point. Explain why temperature $T - T_c$ and external field h provide natural coordinates on theory space near the critical point.

(b) The nematic director $\hat{\mathbf{n}}$ satisfies $\hat{\mathbf{n}} \equiv -\hat{\mathbf{n}}$. What is the topology of the order parameter space? How does this affect the classification of topological defects?

(c) For a superfluid, the order parameter ψ has both magnitude and phase. Near the superfluid transition, argue that the magnitude $|\psi|$ flows under RG while the phase θ corresponds to a Goldstone mode. Which is relevant near the normal-state fixed point?

11. **Random walk and the running diffusion constant.** A particle undergoes a random walk on a 1D lattice with spacing a, hopping left or right with equal probability at rate $1/\tau$.

(a) Show that after N steps, the mean-squared displacement is $\langle x^2 \rangle = Na^2$.

(b) In the continuum limit ($a \to 0$, $\tau \to 0$ with $D = a^2/(2\tau)$ fixed), the particle satisfies the diffusion equation $\partial_t P = D\partial_x^2 P$. Show that dimensional analysis gives $\langle x^2 \rangle = c \cdot Dt$ for some constant c.

(c) Now consider a *scale-dependent* diffusion coefficient $D(\ell)$ where $\ell = \log(L/a)$ measures the observation scale. Under coarse-graining (observing at scale L instead of a), argue that D does not renormalize: $\beta_D = dD/d\ell = 0$. This is because diffusion is a *Gaussian* fixed point with no interactions.

(d) How would a nonlinear term like $\partial_t P = D\partial_x^2 P + \lambda(\partial_x P)^2$ (the KPZ equation) change this conclusion?

Summary

Chapter Summary

Fixed Point Classification

- **Fixed point**: $\beta(g^*) = 0$ — zeros of the exact beta function
- **Perturbative access**: Some fixed points visible in perturbation theory, others require non-perturbative methods (Part II)

Stability Matrix

$$B^i{}_j = \left.\frac{\partial \beta^i}{\partial g^j}\right|_{g^*}, \qquad \delta g_\alpha(\ell) = \delta g_\alpha(0)\, e^{\Delta_\alpha \ell} \tag{271}$$

Type	Eigenvalue	Effect
Relevant	$\Delta > 0$	Grows (unstable)
Irrelevant	$\Delta < 0$	Shrinks (stable)
Marginal	$\Delta = 0$	Higher order

Key Results

- **Wilson-Fisher**: $\lambda^*_{\mathrm{WF}} = \epsilon/b$, controls 3D critical phenomena
- **Stability eigenvalues** = scaling dimensions Δ
- **Universality**: Same fixed point $\Rightarrow$ same critical exponents

Anomalous Dimensions (PME)

$$\alpha = \frac{d}{d(m-1)+2}, \qquad \beta = \frac{1}{d(m-1)+2} \tag{272}$$

Second-kind self-similarity: exponents not predicted by dimensional analysis.

Solution to Exercise 4.1: Stability analysis

(a) Fixed points.
Setting $\beta^1 = g^1(1-g^1) = 0$: $g^1 = 0$ or $g^1 = 1$
Setting $\beta^2 = -g^2(1+g^1) = 0$: $g^2 = 0$ (since $1 + g^1 > 0$ for $g^1 \geq 0$)
Fixed points: $(g^1, g^2) = (0, 0)$ and $(1, 0)$.
(b) Stability matrices.

The Jacobian is:

$$B = \begin{pmatrix} \partial\beta^1/\partial g^1 & \partial\beta^1/\partial g^2 \\ \partial\beta^2/\partial g^1 & \partial\beta^2/\partial g^2 \end{pmatrix} = \begin{pmatrix} 1-2g^1 & 0 \\ -g^2 & -(1+g^1) \end{pmatrix} \tag{273}$$

At $(0,0)$*:*

$$B_{(0,0)} = \begin{pmatrix} 1 & 0 \\ 0 & -1 \end{pmatrix} \tag{274}$$

Eigenvalues: $\Delta_1 = +1$ (relevant), $\Delta_2 = -1$ (irrelevant).
At $(1,0)$*:*

$$B_{(1,0)} = \begin{pmatrix} -1 & 0 \\ 0 & -2 \end{pmatrix} \tag{275}$$

Eigenvalues: $\Delta_1 = -1$, $\Delta_2 = -2$ (both irrelevant).
(c) Classification.
$(0,0)$: One relevant, one irrelevant $\Rightarrow$ **Saddle point**
$(1,0)$: Both irrelevant $\Rightarrow$ **IR stable** (all flows terminate here)
Physical picture: Flows starting near $(0,0)$ in the g^1 direction are repelled, while the g^2 direction is attracted. All generic flows end at $(1,0)$.

Solution to Exercise 4.2: Universality

(a) Why identical long-distance physics?
At a fixed point, the theory is scale-invariant. Physical observables are determined by the **conformal data**: scaling dimensions, OPE coefficients, and central charges.
Two theories flowing to the same fixed point have:

- The same scaling dimensions Δ_i (eigenvalues of the stability matrix)
- The same correlation function exponents: $\langle\phi(x)\phi(0)\rangle \sim |x|^{-2\Delta_\phi}$
- The same critical exponents: $\nu = 1/\Delta_r$, $\eta = 2\Delta_\phi - d + 2$, etc.

All "universal" quantities are fixed point properties, hence identical.
(b) Differences in approach.
Theories differ in their **irrelevant** perturbations away from the fixed point.
Near the fixed point, write $g^i = g^{*i} + \sum_\alpha c_\alpha v_\alpha e^{\Delta_\alpha \ell}$.
The **coefficients** c_α for irrelevant directions ($\Delta_\alpha < 0$) depend on microscopic details but decay as we approach the fixed point.

These create **corrections to scaling**:

$$\langle \phi(x)\phi(0) \rangle = \frac{A}{|x|^{2\Delta_\phi}} \left(1 + B|x|^{|\Delta_{\text{irr}}|} + \cdots\right) \tag{276}$$

(c) Role of irrelevant operators.
Irrelevant operators encode **UV data**—information about the short-distance theory.
Two UV-complete theories in the same universality class differ in:

- The values of coefficients c_α for irrelevant directions
- Higher-derivative terms suppressed at long distances
- Non-universal amplitudes and crossover scales

The relevant operators determine *which* fixed point is reached; the irrelevant operators determine *how* it is approached.

Solution to Exercise 4.3: Porous medium equation

(a) Verifying the scaling relation.
The PME in d dimensions conserves mass: $\int \rho \, d^d x = M$.
For $\rho = t^{-\alpha} f(x/t^\beta)$:

$$M = \int t^{-\alpha} f(r/t^\beta) d^d x = t^{-\alpha} t^{d\beta} \int f(\xi) d^d \xi = t^{d\beta - \alpha} \cdot \text{const} \tag{277}$$

Conservation requires $d\beta - \alpha = 0$, i.e., $\boxed{\alpha = d\beta}$ ✓
(b) Linear diffusion ($m = 1$).
From the formulas:

$$\alpha = \frac{d}{d(1-1)+2} = \frac{d}{2} \tag{278}$$

$$\beta = \frac{1}{d(1-1)+2} = \frac{1}{2} \tag{279}$$

These are the standard diffusion exponents: $\rho \sim t^{-d/2} f(x/\sqrt{t})$.
Check: $\alpha = d\beta \Rightarrow d/2 = d \cdot 1/2$ ✓
(c) Why "anomalous" for $m \neq 1$?
Dimensional analysis prediction:
The PME has parameters: diffusion coefficient D (absorbed into time units), spatial scale x, time t.
For $m = 1$: $[x^2/t] = \text{const} \Rightarrow x \sim t^{1/2}$ (predicted by dim. analysis).
For $m \neq 1$: The nonlinearity introduces $[\rho^{m-1}]$ which couples to the dynamics.
Why anomalous:

The exponent $\beta = 1/(d(m-1)+2)$ depends on m in a way that **cannot be determined by dimensional analysis alone**. One must solve the PDE (or use RG) to find it.
This is "second-kind" self-similarity: the scaling exponents are not fixed by symmetry and dimensional analysis, but by the dynamics (conservation + nonlinearity).

Solution to Exercise 4.4: Non-perturbative fixed points

(a) Perturbative fixed points ($c = 0$).
Setting $\beta(g) = -g + g^2 = g(g-1) = 0$:
$g_1^* = 0$ (Gaussian) and $g_2^* = 1$ (interacting)
(b) Effect of $c > 0$.
The full beta function is $\beta(g) = -g + g^2 + ce^{-1/g}$.
For small $g > 0$, the exponential term $ce^{-1/g}$ is tiny (beyond all orders in g).
For g near 1: $\beta(1) = -1 + 1 + ce^{-1} = ce^{-1} > 0$. The perturbative fixed point is **shifted**.
The new fixed point satisfies:

$$g^*(1-g^*) = ce^{-1/g^*} \tag{280}$$

For small c: $g^* \approx 1 - ce^{-1} + O(c^2)$
Additionally, for very small g, the exponential can create a new fixed point if:

$$-g + g^2 + ce^{-1/g} = 0 \tag{281}$$

At $g \ll 1$: $-g \approx 0$ and $ce^{-1/g}$ is super-exponentially small, so no new fixed point here.
But at intermediate g: for the right value of c, a new pair of fixed points can emerge through a saddle-node bifurcation.
(c) Invisibility to perturbation theory.
The term $ce^{-1/g}$ is **non-perturbative**:

$$e^{-1/g} = \sum_{n=0}^{\infty} \frac{(-1/g)^n}{n!} \quad \text{diverges for any } g \tag{282}$$

This term is "beyond all orders" in g—no finite Taylor series in g captures it.
Fixed points arising from $ce^{-1/g}$ are completely invisible to:

- Any finite-order perturbation theory
- Naive power series expansion of $\beta(g)$

Only resurgent/transseries methods can detect them.

Solution to Exercise 4.5 (Challenge): Marginally relevant operators

(a) Solving for $g(\mu)$.
The RG equation is $\mu \frac{dg}{d\mu} = \frac{g^2}{16\pi^2}$.
Separating variables:

$$\frac{dg}{g^2} = \frac{1}{16\pi^2} \frac{d\mu}{\mu} = \frac{d \ln \mu}{16\pi^2} \tag{283}$$

Integrating:

$$-\frac{1}{g} + \frac{1}{g_0} = \frac{\ln(\mu/\mu_0)}{16\pi^2} \tag{284}$$

Solving:

$$\boxed{g(\mu) = \frac{g_0}{1 + \frac{g_0 \ln(\mu/\mu_0)}{16\pi^2}}} \tag{285}$$

(b) Behavior as $\mu \to 0$.
As $\mu \to 0$: $\ln(\mu/\mu_0) \to -\infty$
The denominator: $1 + g_0 \ln(\mu/\mu_0)/(16\pi^2) \to +\infty$ (since $\ln(\mu/\mu_0) < 0$ and $g_0 > 0$)
Therefore: $g(\mu) \to 0$ as $\mu \to 0$.
The operator is **marginally irrelevant**: it has $\Delta = 0$ at the classical level, but quantum corrections ($\beta = g^2/(16\pi^2) > 0$) make it flow to zero in the IR.
(c) QED coupling.
In QED: $\beta_\alpha = \frac{2\alpha^2}{3\pi} > 0$ (same sign as above).
The running: $\alpha(\mu) = \frac{\alpha_0}{1 - \frac{2\alpha_0}{3\pi} \ln(\mu/\mu_0)}$
As $\mu \to \infty$: $\ln(\mu/\mu_0) \to +\infty$, denominator $\to 0^-$
Therefore: $\alpha(\mu) \to +\infty$ (Landau pole in UV).
As $\mu \to 0$: $\alpha(\mu) \to 0$ (marginally irrelevant in IR).
Physical interpretation: QED coupling grows at high energies (screening of charge by virtual pairs is reduced), but shrinks at low energies (long distances).

Solution to Exercise 4.6 (Challenge): Monodromy from Borel singularities

(a) Borel singularity.
For $a_n \sim n!$, the Borel transform is:

$$\hat{f}(\zeta) = \sum_{n=0}^{\infty} \frac{a_n}{n!} \zeta^n \sim \sum_{n=0}^{\infty} \zeta^n = \frac{1}{1 - \zeta} \tag{286}$$

This has a **pole at $\zeta = 1$** on the positive real axis $\mathbb{R}^+$.
(b) Transseries construction.
The Borel resummation is ambiguous due to the pole. Define

lateral resummations:

$$\mathcal{S}_{\pm} f = \int_0^{\infty \pm i0} e^{-\zeta/\epsilon} \hat{f}(\zeta) d\zeta \tag{287}$$

The difference is:

$$\mathcal{S}_+ f - \mathcal{S}_- f = -2\pi i \cdot \mathrm{Res}_{\zeta=1} \left(e^{-\zeta/\epsilon} \hat{f}(\zeta) \right) = -2\pi i \cdot e^{-1/\epsilon} \tag{288}$$

The transseries is:

$$f(\epsilon, \sigma) = f_0(\epsilon) + \sigma e^{-1/\epsilon} f_1(\epsilon) + \sigma^2 e^{-2/\epsilon} f_2(\epsilon) + \cdots \tag{289}$$

(c) Reality constraint.
For $\epsilon > 0$ real, if $f(\epsilon)$ must be real, then:

$$\mathrm{Im}(f) = \mathrm{Im}(\mathcal{S}_{\pm} f_0) + \sigma \mathrm{Re}(e^{-1/\epsilon} f_1) = 0 \tag{290}$$

This fixes σ in terms of the Stokes constant $S_1 = -2\pi i$:

$$\sigma = \frac{\mathrm{Im}(\mathcal{S}_+ f_0)}{e^{-1/\epsilon} \mathrm{Re}(f_1)} \tag{291}$$

The Stokes constant S_1 relates the ambiguity in f_0 to the coefficient of the non-perturbative sector.
(d) Geometric interpretation.
In the extended space (g, σ), the coupling $g = \epsilon$ has a branch point at $g = 0$.
Circling $g = 0$ in the complex plane corresponds to crossing a Stokes line, inducing:

$$\sigma \mapsto \sigma + S_1 \cdot 1 = \sigma - 2\pi i \tag{292}$$

This is **monodromy**: the transseries parameter σ transforms by adding a multiple of the Stokes constant when we analytically continue around the singularity.
The reality condition $\mathrm{Im}(f) = 0$ for $\epsilon > 0$ is a **monodromy constraint**: it picks out the physical sheet of the multi-valued resummation.

Solution to Exercise 4.7: Normal forms and universality

(a) Reduction to pitchfork form.
Given $\dot{x} = f(x; \mu)$ with $f(0; \mu) = 0$ (fixed point at origin), $f(-x; \mu) = -f(x; \mu)$ ($\mathbb{Z}_2$ symmetry), and $\partial_x f(0; 0) = 0$ (marginal at $\mu = 0$).

Taylor expand f in both x and μ near $(0,0)$:

$$f(x;\mu) = a\mu x + bx^3 + \text{higher order} \tag{293}$$

The $\mathbb{Z}_2$ symmetry forbids even powers of x. The condition $f(0;\mu) = 0$ forbids μ-only terms. The condition $\partial_x f(0;0) = 0$ forbids a linear x term at $\mu = 0$.
Rescaling: $\tilde{x} = x\sqrt{|b|/a}$, $\tilde{\mu} = \mu \cdot \text{sign}(a)$, $\tilde{t} = |a|t$ gives:

$$\boxed{\frac{d\tilde{x}}{d\tilde{t}} = \tilde{\mu}\tilde{x} - \tilde{x}^3} \tag{294}$$

(for $b < 0$, supercritical; signs adjusted for $b > 0$).

(b) Critical exponent.
For $\mu > 0$, the nontrivial fixed points are:

$$x^* = \pm\sqrt{\mu} \tag{295}$$

Therefore $x^* \sim \mu^{1/2}$, giving $\boxed{\beta = 1/2}$.
This is the **mean-field** (or Gaussian) exponent for $\mathbb{Z}_2$ symmetry breaking.

(c) Marginal direction at $\mu = 0$.
At the bifurcation point $\mu = 0$, the linearized equation is:

$$\frac{d(\delta x)}{dt} = 0 \cdot \delta x \tag{296}$$

The eigenvalue is exactly zero—a **marginal** direction. This means perturbations neither grow nor decay at linear order; nonlinear terms $(-x^3)$ determine the dynamics.
This is the hallmark of a **bifurcation**: the loss of hyperbolicity (eigenvalue crossing zero) signals a qualitative change in dynamics.
In RG language: the marginal direction corresponds to the critical surface separating different phases.

(d) RG interpretation.
The control parameter μ acts as a **relevant coupling**:

- For $\mu < 0$: the symmetric state $x = 0$ is stable ("disordered phase")
- For $\mu > 0$: the symmetric state is unstable; system flows to $x = \pm\sqrt{\mu}$ ("ordered phase")

The pitchfork normal form is **universal** because:

1. It depends only on symmetry ($\mathbb{Z}_2$: $x \to -x$) and dimension (one order parameter)
2. All higher-order terms are "irrelevant" under rescaling near $\mu = 0$
3. The exponent $\beta = 1/2$ is determined by the normal form, not microscopic details

Any system with $\mathbb{Z}_2$ symmetry undergoing a continuous transition reduces to this form near criticality.

Solution to Exercise 4.8: Critical slowing down and geodesic distance

(a) Relaxation time divergence.
For the 3D Ising model with Model A dynamics:

$$\tau \sim |T - T_c|^{-\nu z} = |T - T_c|^{-0.63\times 2.02} \approx |T - T_c|^{-1.27} \tag{297}$$

If we define $\epsilon = |T - T_c|/T_c$ (reduced temperature):

ϵ	τ/τ_0
10^{-1}	~ 20
10^{-2}	~ 370
10^{-3}	~ 7000
10^{-4}	~ 130000

Near criticality, relaxation becomes extremely slow.

(b) Geodesic distance.
The Fisher metric in the temperature direction is $G_{TT} \propto \chi \sim |T - T_c|^{-\gamma}$.
The geodesic distance from T to T_c:

$$d = \int_T^{T_c} \sqrt{G_{TT}}\, dT' \sim \int_T^{T_c} |T' - T_c|^{-\gamma/2}\, dT' \tag{298}$$

For $\gamma = 1.24$, we have $\gamma/2 = 0.62 < 1$, so the integral converges:

$$d \sim |T - T_c|^{1-\gamma/2} = |T - T_c|^{0.38} \tag{299}$$

Correction: For the integral to *diverge*, we need $\gamma/2 \geq 1$, i.e., $\gamma \geq 2$. For 3D Ising ($\gamma \approx 1.24$), the geodesic distance is **finite**.
However, in 2D ($\gamma = 7/4 = 1.75$) or mean-field ($\gamma = 1$), the integral still converges. The divergence occurs when we consider *full* theory space including the coupling dimension.

(c) Geometric interpretation.

The geometric picture: as $T \to T_c$, the **susceptibility diverges**, meaning the system becomes increasingly sensitive to perturbations. In information-geometric terms, nearby temperatures become "highly distinguishable."
Critical slowing down arises because:

- The "restoring force" (eigenvalue Δ) vanishes at criticality
- The system has no preferred direction to relax toward
- Fluctuations on all scales (up to ξ) must equilibrate

Geometrically: the flow velocity $|\beta|$ vanishes at the fixed point, so approaching the fixed point takes infinite "RG time."

(d) Finite-size rounding.
Finite-size effects become important when the correlation length exceeds the sample size:

$$\xi(T) \sim |T - T_c|^{-\nu} \gtrsim L \tag{300}$$

This gives the rounding temperature:

$$|T - T_c| \lesssim L^{-1/\nu} \tag{301}$$

For 3D Ising ($\nu \approx 0.63$): $|T - T_c| \lesssim L^{-1.59}$
Physical meaning: Below this temperature scale, the system "knows" it's finite. The sharp phase transition is rounded, critical slowing down is cut off, and exponents cross over to finite-size values.
For a $L = 100$ lattice: $|T - T_c|/T_c \lesssim 100^{-1.59} \approx 6 \times 10^{-4}$.

Solution to Exercise 4.9: Universality across systems

(a) Shared symmetry.
All listed systems share $\mathbb{Z}_2$ (Ising) symmetry:

- **Uniaxial ferromagnets**: $M \to -M$ (spin reversal)
- **Liquid-gas**: $\rho - \rho_c \to -(\rho - \rho_c)$ (density above/below critical)
- **Binary mixtures**: $c - c_c \to -(c - c_c)$ (concentration above/below critical)
- **Antiferromagnets**: Staggered magnetization $M_{\text{stag}} \to -M_{\text{stag}}$

The order parameter in each case has a discrete $\mathbb{Z}_2$ symmetry, placing them all in the 3D Ising universality class.

(b) Why different systems share exponents.

The microscopic Hamiltonians are completely different:

- Magnets: Exchange interaction $J \sum \mathbf{S}_i \cdot \mathbf{S}_j$
- Fluids: Van der Waals attraction + hard-core repulsion
- Mixtures: Entropy of mixing + interaction energies

Yet they share exponents because:

1. Near the critical point, only **long-wavelength fluctuations** matter
2. These fluctuations are controlled by the **symmetry** of the order parameter
3. Under RG, all microscopic details flow to **irrelevant operators**
4. The fixed point is determined by dimension + symmetry alone

The Wilson-Fisher fixed point in $d = 3$ with $\mathbb{Z}_2$ symmetry controls all these transitions.

(c) The XY (O(2)) universality class.
Superfluid ^{4}He has order parameter $\psi = |\psi|e^{i\theta}$ with **O(2)** (or U(1)) symmetry.
The exponent $\nu \approx 0.672$ differs from Ising ($\nu \approx 0.630$) because:

- Different symmetry $\Rightarrow$ different fixed point
- The XY fixed point has different stability eigenvalues
- More components in the order parameter (2 vs. 1) change the beta functions

The XY universality class also describes:

- 2D melting (Kosterlitz-Thouless transition)
- Superconductor transitions
- Easy-plane magnetic ordering

(d) The Heisenberg (O(3)) universality class.
For an isotropic Heisenberg ferromagnet, the order parameter is $\mathbf{M} = (M_x, M_y, M_z)$ with **O(3)** symmetry.
Prediction: The critical exponents will be those of the 3D Heisenberg (O(3)) fixed point:

$$\beta \approx 0.366, \quad \gamma \approx 1.40, \quad \nu \approx 0.711 \tag{302}$$

These differ from both Ising and XY because the three-component order parameter has different fluctuation spectrum.
Physical examples: Isotropic ferromagnets (e.g., EuO, EuS), ferromagnetic metals with weak anisotropy, certain magnetic alloys.
The pattern: As the symmetry group grows (Ising $\to$ XY $\to$ Heisenberg), ν increases (stronger fluctuations require more tuning to reach criticality).

Solution to Exercise 4.10: Order parameters as coordinates on theory space

(a) Ferromagnet coordinates near criticality.
Near the Curie point, the free energy can be expanded in powers of the order parameter (Landau theory):

$$F = F_0 + a(T - T_c)|\mathbf{M}|^2 + b|\mathbf{M}|^4 - \mathbf{h} \cdot \mathbf{M} + \cdots \tag{303}$$

The natural coordinates on theory space are:

- **Reduced temperature**: $t = (T - T_c)/T_c$ measures the deviation from criticality
- **External field**: h couples linearly to the order parameter

In RG language, t and h are the *relevant perturbations* away from the critical fixed point at $(t^*, h^*) = (0, 0)$. Their scaling dimensions are:

$$[t] = 1/\nu, \qquad [h] = (d + 2 - \eta)/2 \tag{304}$$

where ν is the correlation length exponent and η is the anomalous dimension of the magnetization.
These coordinates are "natural" because they diagonalize the stability matrix at the fixed point—perturbations in t and h grow independently under RG, each with its own scaling exponent.

(b) Nematic order parameter topology.
The director $\hat{\mathbf{n}}$ lives on the unit sphere S^2, but with antipodal identification: $\hat{\mathbf{n}} \equiv -\hat{\mathbf{n}}$. This is the **projective plane** $\mathbb{RP}^2$:

$$\text{Order parameter space} = S^2/\mathbb{Z}_2 = \mathbb{RP}^2 \tag{305}$$

Topological defects are classified by homotopy groups:

- **Point defects** (hedgehogs): $\pi_2(\mathbb{RP}^2) = \mathbb{Z}$
- **Line defects** (disclinations): $\pi_1(\mathbb{RP}^2) = \mathbb{Z}_2$

The key difference from a ferromagnet (order parameter space S^2): nematics have *half-integer* disclinations (strength $\pm 1/2$) that are topologically stable, while ferromagnets only have integer vortices.

(c) Superfluid order parameter.
The order parameter $\psi = |\psi| e^{i\theta}$ has two components:
Magnitude $|\psi|$: Vanishes in the normal phase, nonzero in the superfluid. Near the normal-state fixed point, $|\psi|$ is a **relevant** perturbation—turning on $|\psi|$ drives the system away from normal toward superfluid.
Phase θ: In the superfluid phase, the U(1) symmetry is spontaneously broken, and θ parametrizes the **Goldstone manifold** S^1. Fluctuations in θ are massless (no energy cost for uniform phase rotation) and represent the **Goldstone mode**.
Under RG near the normal-state fixed point:

$$\beta_{|\psi|^2} = (T_c - T) \cdot |\psi|^2 + O(|\psi|^4) \quad \text{(relevant for } T < T_c) \tag{306}$$

The phase θ does not appear in the beta function at the normal-state fixed point because the action is U(1) invariant—θ is not a coupling but a collective coordinate.

Solution to Exercise 4.11: Random walk and running diffusion constant

(a) Mean-squared displacement.
After N steps, the position is $x = \sum_{i=1}^{N} \sigma_i \cdot a$ where $\sigma_i = \pm 1$ with equal probability.
Since steps are independent:

$$\langle x \rangle = a \sum_{i=1}^{N} \langle \sigma_i \rangle = 0 \tag{307}$$

$$\langle x^2 \rangle = a^2 \sum_{i,j=1}^{N} \langle \sigma_i \sigma_j \rangle = a^2 \sum_{i=1}^{N} \langle \sigma_i^2 \rangle = a^2 \cdot N \cdot 1 = N a^2 \tag{308}$$

(b) Continuum limit.
In the continuum limit with $D = a^2/(2\tau)$ fixed, the probability density satisfies:

$$\frac{\partial P}{\partial t} = D \frac{\partial^2 P}{\partial x^2} \tag{309}$$

By dimensional analysis: $[D] = L^2 T^{-1}$, $[t] = T$, $[\langle x^2 \rangle] = L^2$.
The only combination with dimensions of L^2 is:

$$\langle x^2 \rangle = c \cdot Dt \tag{310}$$

for some dimensionless constant c.

Solving the diffusion equation with $P(x,0) = \delta(x)$ gives the Gaussian:

$$P(x,t) = \frac{1}{\sqrt{4\pi Dt}} e^{-x^2/(4Dt)} \tag{311}$$

Computing: $\langle x^2 \rangle = \int_{-\infty}^{\infty} x^2 P(x,t)\, dx = 2Dt$, so $c = 2$.

(c) Non-renormalization of D.
Under coarse-graining from scale a to scale $L = ae^{\ell}$:

- We "integrate out" fluctuations on scales between a and L
- The diffusion equation is **linear—**there are no interactions between different Fourier modes
- The diffusion constant D receives no corrections from integrating out short-wavelength modes

Formally, the beta function is:

$$\beta_D = \frac{dD}{d\ell} = 0 \tag{312}$$

This reflects that ordinary diffusion is a **Gaussian fixed point—** the action $S = \int dx\, dt\, (\partial_t \phi - D\partial_x^2 \phi)\phi$ is quadratic in the field ϕ.

(d) KPZ equation.
The KPZ (Kardar-Parisi-Zhang) equation:

$$\partial_t h = \nu \partial_x^2 h + \frac{\lambda}{2}(\partial_x h)^2 + \eta \tag{313}$$

describes interface growth with nonlinearity $(\partial_x h)^2$.
The key difference: the nonlinear term **couples different Fourier modes**. Under RG:

$$\beta_\lambda \neq 0 \quad \text{(nonlinearity is relevant in } d < 2\text{)} \tag{314}$$

The system flows to a **non-Gaussian fixed point** with anomalous exponents:

$$\langle (h(x,t) - h(0,0))^2 \rangle \sim |x|^{2\chi} + |t|^{2\chi/z} \tag{315}$$

where $\chi = 1/2$ and $z = 3/2$ in $d = 1$ (exact, from symmetry).
This illustrates the central theme: **interactions generate running couplings**, while free (Gaussian) theories have trivial RG flow.

Part II

Analysis: Perturbation Theory and Resurgence

Perturbation Theory and UV Divergences

Part I developed the exact RG framework. This chapter introduces perturbation theory as the primary computational method, covering both the universal divergence structure and the regularization/renormalization machinery needed for quantum field theory.

The RG framework developed in Part I is **exact**—beta functions, fixed points, and flows exist independently of how we compute them. **Perturbation theory** is the most common method for computing these quantities: expand in a small parameter and calculate order by order.

This chapter examines perturbation theory comprehensively:

- **Section II**: Why perturbation series generically diverge
- **Section II**: Three canonical examples demonstrating universality
- **Section II**: When RG methods are needed versus simpler approaches
- **Section II**: A systematic problem-solving methodology
- **Section II**: UV divergences and regularization methods
- **Section II**: Renormalization schemes and their equivalence

The key insight is that perturbation theory, while powerful, is *incomplete*. The factorial divergence of perturbative series encodes information about non-perturbative physics—a theme we develop fully in Chapter II.

Why Perturbation Series Diverge

Before developing the machinery, let's understand *why* perturbation series in physics generically diverge.

The Source of Factorial Growth

Consider a generic nonlinear problem with small parameter ϵ:

$$\mathcal{L}[f] = \epsilon \mathcal{N}[f] \tag{316}$$

where $\mathcal{L}$ is linear and $\mathcal{N}$ is nonlinear. The perturbative solution $f = \sum_n \epsilon^n f_n$ is constructed iteratively:

$$f_{n+1} = \mathcal{L}^{-1}[\mathcal{N}[f_0 + \epsilon f_1 + \cdots + \epsilon^n f_n]] \tag{317}$$

At order n, we must account for all ways of distributing n powers of ϵ among the nonlinear terms. The number of such distributions grows combinatorially. For a cubic nonlinearity, the growth is roughly $n!$.

Each order of perturbation theory involves applying the nonlinearity to all previous orders. This generates combinatorial factors.

Dyson's argument: For quantum field theories, Dyson argued that the perturbative series must diverge. If the series converged for coupling $g > 0$, it would converge in a disk including $g < 0$. But for $g < 0$, the vacuum is unstable (the potential is unbounded below), so the theory doesn't exist. Hence convergence is impossible.

Gevrey-1 Structure

A formal series $\tilde{f}(\epsilon) = \sum_{n=0}^{\infty} a_n \epsilon^n$ is **Gevrey of order 1** (Gevrey-1) if:

$$|a_n| \leq C \cdot K^n \cdot n! \tag{318}$$

for constants $C, K > 0$. The factorial $n!$ means the series has zero radius of convergence.

Gevrey-1 means factorial growth: $|a_n| \lesssim n!$. This is the generic case for physical perturbation series.

Physical examples:

- The anharmonic oscillator ground state energy has $a_n \sim (-1)^n \cdot \text{const} \cdot A^n \cdot n!$
- QED perturbation theory has $a_n \sim n! \cdot (1/137)^n$ from diagram counting
- The epsilon expansion for critical exponents has factorially growing coefficients from renormalon contributions
- The late-time behavior of the Lorenz system near bifurcation has factorially divergent corrections
- Matched asymptotic expansions in fluid mechanics (boundary layers, etc.) generically produce Gevrey-1 series

The key observation is that factorial divergence is **not specific to quantum field theory**. It appears whenever:

Divergent series are universal: they appear in ODEs, PDEs, and QFT alike. The mathematical structure is independent of the physical origin.

1. A nonlinearity generates combinatorial complexity at each order
2. A small parameter controls the expansion
3. The expansion is around a singular limit (e.g., $\epsilon \to 0$ in the anharmonic oscillator)

What Divergence Encodes

The crucial insight is that factorial divergence is not random. The *pattern* of divergence—signs, growth rates, subleading corrections—encodes non-perturbative physics that is invisible to any finite truncation of the series.

The way a series diverges tells you about physics invisible to any finite truncation. Chapter II develops the tools to extract this information.

This is a profound observation: the perturbative series "knows" about non-perturbative effects like tunneling and instantons, even though these effects are exponentially suppressed and invisible at any finite order. Chapter II develops the machinery—Borel transforms, transseries, and alien calculus—to systematically extract this hidden information.

Divergent Series in Classical Mechanics and PDEs

Divergent series are not a quantum phenomenon. They appear throughout classical mechanics, fluid dynamics, and nonlinear PDEs.

It is essential to emphasize that factorial divergence is **not unique to quantum mechanics or field theory**. Classical dynamical systems exhibit the same structure:

The Lorenz system: Near the Hopf bifurcation at $\rho = 1$, perturbative corrections to the fixed point position diverge factorially. The pattern of divergence encodes information about the global structure of the unstable manifold.

Boundary layer theory: The Prandtl matched asymptotic expansion for boundary layers in fluid mechanics produces Gevrey-1 series. The divergence encodes the "inner" scale physics invisible to the "outer" expansion.

The porous medium equation: Perturbative corrections to the Barenblatt self-similar solution (expanding around $m = 1$) diverge factorially for $m \neq 1$. This reflects the singular nature of the nonlinear diffusion.

Singular perturbation theory: Any problem of the form $\epsilon\mathcal{L}_1[f] + \mathcal{L}_0[f] = 0$ with $\epsilon \to 0$ generically produces factorially divergent series. The boundary layer, turning point, and WKB analyses of asymptotic methods are all Gevrey-1.

Box 5.1: Divergent Series in the Van der Pol Oscillator

The model: The Van der Pol equation $\ddot{x} + \epsilon(x^2 - 1)\dot{x} + x = 0$ with $\epsilon \ll 1$ describes a weakly nonlinear oscillator.
The expansion: The limit cycle amplitude can be expanded:

$$A(\epsilon) = 2 + a_1\epsilon + a_2\epsilon^2 + a_3\epsilon^3 + \cdots \tag{319}$$

The divergence: The coefficients grow as $a_n \sim n!$ for large n. This is because each order of perturbation theory involves iterating the nonlinearity, generating combinatorial growth.
The physics: The divergence reflects the *relaxation oscillation* regime at large ϵ. Information about this strong-coupling behavior is encoded in how the weak-coupling series diverges.
Comparison with QFT: The mathematical structure—Gevrey-1 divergence, Borel summability, Stokes phenomena—is identical to QFT perturbation theory. The techniques of Chapter II apply without modification.

This universality is why we develop the resurgent framework in generality: the tools work for ODEs, PDEs, and QFT alike.

Three Canonical Examples

To ground the abstract discussion, we now examine three canonical examples that demonstrate the universality of perturbative structure across different physical domains. These examples form a ladder of increasing complexity.

The three examples form a ladder: oscillator $\to$ field theory $\to$ PDE. Each adds capabilities the previous lacked.

The Anharmonic Oscillator

The anharmonic oscillator is the simplest example and suffices to demonstrate secular terms and running parameters, the resolution via RG equations, Gevrey-1 divergence and the Borel plane, and the basic transseries structure.

It is too simple for non-trivial fixed points, operator mixing or anomalous dimensions, and statistical RG with coarse-graining.

Box 5.2: Complete Analysis of the Damped Anharmonic Oscillator

Scales and divergence. UV scale: oscillation period $\tau_{\text{fast}} \sim 1/\omega_0$. IR scale: amplitude-decay time $\tau_{\text{slow}} \sim 1/\gamma$. Small parameters: $\gamma \ll \omega_0$ (weak damping), $\epsilon \ll 1$ (weak nonlinearity). Breakdown: secular terms at $t \sim \tau_{\text{slow}}$. Non-perturbative: complex-time instantons.

Perturbation theory. The perturbative solution $x(t) = A\cos(\omega_0 t) + O(\epsilon)$ develops secular terms. The frequency series $\omega = \omega_0(1 + \frac{3\epsilon A^2}{8\omega_0^2} + c_2\epsilon^2 + \cdots)$ diverges with $|c_n| \sim n!$. The Borel transform $\hat{\omega}(\zeta)$ has singularities at $\zeta = \omega_0^3/(3\epsilon)$ (instanton action).

Running parameters. Perturbative: (A, ϕ). Extended: (A, ϕ, σ) with σ weighting instanton sector.

Beta functions.

$$\frac{dA}{dt} = -\gamma A \tag{320}$$

$$\frac{d\phi}{dt} = \frac{3\epsilon A^2}{8\omega_0} \tag{321}$$

Transseries corrections: $O(\sigma e^{-S/\epsilon})$. The Stokes constant S_1 relates perturbative and instanton sectors.

Fixed points and stability. Perturbative fixed point: $A = 0$ (trivial, stable due to damping). No non-perturbative fixed points. All $A > 0$ trajectories flow to $A = 0$.

Physical prediction. The effective frequency is:

$$\omega_{\text{eff}} = \omega_0 \left(1 + \frac{3\epsilon A^2}{8\omega_0^2}\right) + O(\epsilon^2) \tag{322}$$

For quantitative accuracy at larger ϵ, resum using median prescription.

The damped anharmonic oscillator example is developed fully in Chapter II, where we show how to extract non-perturbative physics from the factorial divergence.

The 1D ϕ^4 Theory

The 1D ϕ^4 theory adds non-trivial beta functions with multiple couplings, the Gaussian fixed point and its stability, renormalon singularities from RG running, and statistical mechanics interpretation.

It is still too simple for non-trivial interacting fixed points (which require $d < 4$) and anomalous dimensions.

Box 5.3: Complete Analysis of 1D ϕ^4 Theory

Scales and divergence. UV scale: cutoff Λ (lattice spacing). IR scale: correlation length $\xi \sim 1/\sqrt{r}$. Small parameter: $\lambda/\Lambda^2 \ll 1$. Breakdown: tadpole corrections grow with Λ. Non-perturbative: renormalons from RG running.

Perturbation theory. The beta functions $\beta_r = 2r + 3\lambda\Lambda/\pi(\Lambda^2 + r)$ and $\beta_\lambda = 2\lambda$ are perturbative leading terms. Higher-order coefficients grow factorially. The Borel transform has renormalon singularities at $\zeta_k = k/2$.

Running parameters. Perturbative: (r, λ). Extended: $(r, \lambda, \sigma_{\text{ren}})$.

Beta functions.

$$\beta_r = 2r + \frac{3\lambda\Lambda}{\pi(\Lambda^2 + r)} + O(\sigma_{\text{ren}} e^{-1/(2\lambda)}) \tag{323}$$

$$\beta_\lambda = 2\lambda + O(\sigma_{\text{ren}} e^{-1/(2\lambda)}) \tag{324}$$

The renormalon Stokes constant: $S_{\text{ren}} = 1/\beta_1 + O(1) = 1/2 + O(1)$.

Fixed points and stability. Perturbative: Gaussian fixed point $(0, 0)$. Stability matrix eigenvalues: both $= 2$ (relevant, unstable). No non-perturbative fixed points in 1D. In $d = 4 - \epsilon$, the Wilson-Fisher fixed point appears.

Physical prediction. Running couplings:

$$\lambda(\mu) = \lambda_0 \left(\frac{\mu}{\mu_0}\right)^2 \tag{325}$$

Physical correlation functions computed from resummed expressions.

The Porous Medium Equation

The porous medium equation adds anomalous dimensions (second-kind self-similarity), non-trivial scaling exponents from dynamics, Wasserstein gradient flow structure, and selection principles for physical solutions.

Together, the three examples demonstrate the complete framework. Any new problem will share features with one or more of these examples, and the techniques transfer accordingly.

Box 5.4: Complete Analysis of the Porous Medium Equation

Scales and divergence. UV scale: initial localization width. IR scale: late-time spread $L(t) \sim t^{\beta}$. Small parameter: $(m-1)$ (deviation from linear diffusion). Breakdown: anomalous exponent $\beta \neq 1/2$ for $m \neq 1$. Non-perturbative: sub-leading self-similar modes.

Perturbation theory. Expand $\beta(m)$ around $m = 1$:

$$\beta = \frac{1}{2} - \frac{d}{4}(m-1) + O((m-1)^2) \tag{326}$$

This is asymptotic with singularities corresponding to competing modes.

Running parameters. The exponent β is determined by the self-similar ansatz. Extended space includes mode weights selecting among solutions.

Selection principle. Mass conservation: $\alpha = d\beta$. Self-consistency: $\beta(md + 2 - d) = 1$. Result:

$$\beta = \frac{1}{d(m-1)+2} \tag{327}$$

The physical mode is selected by boundary conditions (finite mass, compact support).

Fixed points and stability. The Barenblatt profile is the unique stable self-similar attractor. Other self-similar modes exist but are unstable.

Physical prediction. The late-time density profile:

$$\rho(x,t) = \frac{1}{t^{\alpha}}\left[C - \frac{(m-1)}{4md}\frac{|x|^2}{(Dt)^{2\beta}}\right]_+^{1/(m-1)} \tag{328}$$

This is exact for the PME. More general nonlinear diffusion would require resummation.

When Is RG Needed? A Decision Tree

Not every problem requires the full RG machinery. Following Sethna's pedagogical approach, we provide a decision tree for determining when RG methods are essential versus when simpler approaches suffice.

This decision tree helps identify whether full RG analysis is needed or if simpler methods suffice.

The Diagnostic Questions

Ask the following questions in order:

1. Is there a scale hierarchy?

- If **NO**: Standard methods apply. Perturbation theory converges; no running parameters needed.
- If **YES**: Proceed to question 2.

2. Do naive methods exhibit pathologies?

Look for secular terms (growing corrections), UV/IR divergences, or boundary layer mismatches.

- If **NO**: Scale separation is benign. Use matched asymptotics or multiple scales without full RG.
- If **YES**: Running parameters are needed. Proceed to question 3.

3. Are you near a phase transition or bifurcation?

- If **NO**: Perturbative RG (few running parameters, truncated beta functions) may suffice.
- If **YES**: Non-perturbative effects matter. Proceed to question 4.

4. Are universal critical exponents or scaling functions needed?

- If **NO**: Mean-field or Landau theory may be adequate.
- If **YES**: Full RG analysis with fixed points, stability analysis, and possibly resummation is required.

Box 5.5: The Decision Tree Applied

Example 1: Simple harmonic oscillator

- Scale hierarchy? NO (single timescale $1/\omega_0$)
- $\Rightarrow$ No RG needed. Exact solution exists.

Example 2: Damped anharmonic oscillator with $\epsilon \ll 1$, $\gamma \ll \omega_0$

- Scale hierarchy? YES ($1/\omega_0$ vs $1/\gamma$ and $\omega_0/\epsilon A^2$)
- Pathologies? YES (secular terms at $O(\epsilon t)$)

- Near bifurcation? NO (far from any transition)
- $\Rightarrow$ Perturbative RG (Lindstedt-Poincaré/multiple scales) suffices.

Example 3: Ising model at $T \approx T_c$

- Scale hierarchy? YES (lattice spacing a vs correlation length $\xi \to \infty$)
- Pathologies? YES (fluctuations on all scales)
- Near bifurcation? YES (second-order phase transition)
- Universal exponents needed? YES (experimental predictions)
- $\Rightarrow$ Full RG with Wilson-Fisher fixed point analysis required.

Example 4: Porous medium equation with $m = 1.1$

- Scale hierarchy? YES (initial width vs late-time spread)
- Pathologies? YES (dimensional analysis fails)
- Near bifurcation? NO (smooth transition at $m = 1$)
- Universal exponents? YES (anomalous Barenblatt exponent)
- $\Rightarrow$ RG for anomalous dimensions; exact solution exists here.

The Sethna Problem-Solving Template

For problems where RG *is* needed, Sethna advocates a systematic approach. Before diving into calculations, answer three fundamental questions.

Sethna's template: identify order parameter, symmetry, and topology before computing.

What Is the Order Parameter?

The order parameter determines the *coordinates on theory space* $\mathcal{M}$:

System	Order Parameter	Theory Space Coords
Ferromagnet	Magnetization M	$(T - T_c, h, \dots)$
Superfluid	$\psi = \lvert\psi\rvert e^{i\theta}$	$(T - T_\lambda, \mu, \dots)$
Ising model	Spin density σ	$(K - K_c, H, \dots)$
Fluid turbulence	Velocity field $\mathbf{u}$	(Re, geometry)

What Symmetry Is Broken?

The broken symmetry determines the *group structure* of the RG:

Transition	**Broken Symmetry**	**Universality Class**
Ferromagnetic (uniaxial)	$\mathbb{Z}_2$	Ising
Ferromagnetic (isotropic)	$O(3)$	Heisenberg
Superfluid/superconductor	$U(1)$	XY
Crystallization	Translation	Solid

What Are the Topological Defects?

Topological defects correspond to *singular points or surfaces* in theory space:

System	**Order Space**	π_1	**Defects**
2D XY model	S^1	$\mathbb{Z}$	Vortices
3D Heisenberg	S^2	0	None (monopoles from π_2)
Nematic	$\mathbb{RP}^2$	$\mathbb{Z}_2$	Half-integer disclinations
Crystal	T^3	$\mathbb{Z}^3$	Dislocations

Only after answering these questions should you begin detailed calculations.

This discipline prevents common errors: computing without understanding what the order parameter is, missing symmetry-protected features, or overlooking topological contributions to the partition function.

UV Divergences and Regularization

Regularization makes divergent integrals finite. Renormalization then absorbs the divergences into redefined parameters. These are distinct operations.

Before perturbation theory can produce even a divergent series, we must first deal with a more immediate problem: individual Feynman diagrams often involve *divergent integrals*. These ultraviolet (UV) divergences arise from loop momenta that extend to infinity. **Regularization** is the process of introducing a parameter that renders these integrals finite, allowing us to manipulate them algebraically before ultimately removing the regulator.

The Need for Regularization

Consider the simplest divergent integral in four-dimensional quantum field theory: the one-loop correction to the scalar propagator in ϕ^4

theory. The self-energy diagram gives:

$$\Sigma(p^2) = \frac{\lambda}{2} \int \frac{d^4k}{(2\pi)^4} \frac{1}{k^2 + m^2} \tag{329}$$

This integral diverges quadratically: as $k \to \infty$, the integrand behaves as $1/k^2$, giving $\int^{\Lambda} k\,dk \sim \Lambda^2$.

The solution: Introduce a *regulator* that makes the integral finite, compute the result as a function of that parameter, and then carefully take the limit where the regulator is removed. The divergences that appear are absorbed into redefinitions of physical parameters—this is renormalization.

Dimensional Regularization

The most powerful regularization method is **dimensional regularization**, which analytically continues the number of spacetime dimensions from 4 to $d = 4 - \epsilon$.

Dimensional regularization was developed by 't Hooft and Veltman (1972) for gauge theories.

The key features are:

- **Preserves gauge invariance:** No explicit cutoff breaks symmetry.
- **Algebraically simple:** Divergences appear as $1/\epsilon$ poles.
- **No power-law divergences:** Scaleless integrals vanish by definition.

Other Regularization Methods

Pauli-Villars: Modifies propagators by introducing fictitious heavy particles. Preserves Lorentz and gauge invariance in QED.

Zeta function: Uses analytic continuation of sums. Elegant for Casimir-type calculations.

Lattice: Discretizes spacetime. Essential for non-perturbative calculations.

The key principle is that *physical predictions are regularization-independent*. Different schemes give different intermediate expressions, but after renormalization, all observables agree.

Renormalization Schemes

Once divergences are regulated, they must be absorbed into redefinitions of parameters. The precise way finite parts are treated defines a **renormalization scheme**.

Renormalization absorbs divergences into redefined parameters. The scheme specifies how finite parts are handled.

The On-Shell Scheme

The **on-shell scheme** defines renormalized parameters to equal directly measurable physical quantities. For QED, the renormalized mass and charge are exactly the physical electron mass and charge.

Advantages: Parameters have direct physical meaning.

Disadvantages: IR divergences for massless theories; complexity at higher orders.

Minimal Subtraction: MS and $\overline{MS}$

Minimal subtraction (MS) works with dimensional regularization, subtracting only the $1/\epsilon$ poles. The $\overline{\textbf{MS}}$ scheme also subtracts $\gamma_E - \ln 4\pi$.

$\overline{\text{MS}}$ is the standard scheme for QCD calculations.

Advantages: Computational simplicity; preserves symmetries; mass-independent.

Disadvantages: Parameters not directly physical.

Scheme Independence

A fundamental result is that *physical observables are scheme-independent*. Different schemes are different coordinate systems on theory space $\mathcal{M}$. Physical quantities are geometric invariants.

The first two coefficients of the beta function, β_0 and β_1, are universal across mass-independent schemes.

Summary and Road Ahead

This chapter has covered the foundations of perturbation theory:

1. Perturbation series generically diverge with factorial ($n!$) growth—Gevrey-1 structure.

2. The divergence encodes non-perturbative physics (developed in Chapter II).

3. The same mathematical structure appears in ODEs, PDEs, and QFT.

4. UV divergences in loop integrals require regularization and renormalization.

5. Physical predictions are independent of regularization and renormalization scheme.

The next two chapters complete the machinery:

- **Chapter II**: Resurgence—extracting non-perturbative physics from divergent series

- **Chapter II**: The deeper algebraic structure—Hopf algebras and Riemann-Hilbert

Exercises

1. **Identifying scales.** For each of the following systems, identify the scales and describe the scale hierarchy:
   (a) A pendulum with small amplitude oscillations and weak damping.
   (b) Heat conduction in a rod with both ends at different fixed temperatures.
   (c) The quantum double-well potential $V(x) = \lambda(x^2 - a^2)^2$.
2. **Applying the decision tree.** For each system below, work through the decision tree to determine whether RG methods are needed:
   (a) A damped driven pendulum far from resonance.
   (b) The Navier-Stokes equations at Reynolds number Re $= 10$.
   (c) The Navier-Stokes equations at Re $= 10^6$.
   (d) A polymer chain in good solvent.
3. **Factorial growth.** The solution to $\epsilon y' + y = 1$ with $y(0) = 0$ has the exact form $y(x) = 1 - e^{-x/\epsilon}$.
   (a) Expand $y(x)$ in powers of ϵ to find the formal series.
   (b) Show that the coefficients grow factorially.
   (c) Verify that the series is Gevrey-1.
   (d) Explain why truncating the series at any finite order fails to capture the exponentially small term $e^{-x/\epsilon}$.
4. **Boundary layer.** Consider the boundary layer equation $\epsilon y'' + y' + y = 0$ with $y(0) = 0$, $y(1) = 1$.
   (a) Identify the outer and inner solutions.
   (b) Show that the outer solution has secular behavior near $x = 0$.
   (c) Set up the matched asymptotic expansion and identify the running parameter.
5. **Sethna template.** Apply the Sethna problem-solving template to the following systems:
   (a) Liquid-gas critical point.
   (b) Antiferromagnetic Ising model.
   (c) Cholesteric liquid crystal.
6. **(Challenge) Van der Pol divergence.** For the Van der Pol oscillator $\ddot{x} + \epsilon(x^2 - 1)\dot{x} + x = 0$:

(a) Set up the multiple-scales expansion for the limit cycle amplitude.

(b) Compute the first three terms in the series $A = 2 + a_1\epsilon + a_2\epsilon^2 + \cdots$.

(c) Argue on physical grounds why the series must diverge for large ϵ (hint: relaxation oscillations).

7. **(Challenge) Instanton action.** For the double-well potential $V(x) = \frac{\lambda}{4}(x^2 - a^2)^2$:

(a) Find the classical instanton solution interpolating between the two minima.

(b) Compute the instanton action $S_{\text{inst}} = \int_{-\infty}^{\infty} \frac{1}{2}\dot{x}^2 + V(x)\, dt$.

(c) Explain why this action appears in the large-order behavior of the ground state energy expansion.

Algebraic Foundations of Renormalization

The preceding chapters developed the practical machinery for perturbation theory, and we have seen perturbative expansions fail in various ways. This chapter reveals the deeper algebraic structure that organizes these expansions and their renormalization. The remarkable fact is that the same algebraic structure appears in two seemingly unrelated contexts, namely ordinary differential equations and quantum field theory.

This chapter reveals the deep algebraic structure underlying renormalization, starting with its origins in the numerical analysis of ODEs before showing how the same structure appears in quantum field theory.

- **Section II**: The Butcher group and B-series for ODEs, where rooted trees organize perturbative solutions
- **Section II**: The Hopf algebra of Feynman graphs, showing the same structure in QFT
- **Section II**: The Riemann-Hilbert correspondence, connecting renormalization to complex analysis through the Birkhoff decomposition
- **Section II**: Connection to resurgent structure, showing how the algebraic picture complements the analytic one

The key insight is that renormalization is not an ad hoc procedure for canceling infinities. Rather, it is a mathematically natural operation with deep algebraic structure. This structure was first discovered by Butcher (1963) in the context of numerical methods for ODEs, and was later recognized by Connes and Kreimer (1998–2000) to be the same structure governing renormalization in quantum field theory.

Connes and Kreimer (1999) wrote of Butcher's work on numerical integration methods as "an impressive example that concrete problem-oriented work can lead to far-reaching conceptual results."

The Butcher Group: Hopf Algebras from ODEs

Before encountering Hopf algebras in quantum field theory, we develop the same structures in a simpler setting: ordinary differential equations. This is not merely pedagogy. Historically, the Hopf algebra of rooted trees arose first in numerical analysis, and Connes–Kreimer recognized that the Hopf algebra of Feynman graphs is essentially the same object.

John C. Butcher introduced the algebraic theory of Runge–Kutta methods in 1963. The infinite-dimensional Lie group of characters was identified by Hairer and Wanner (1974) and is now called the **Butcher group**.

Rooted Trees and Elementary Differentials

Consider the autonomous ODE

$$\frac{dx}{ds} = f(x), \qquad x(0) = x_0 \tag{330}$$

where $x \in \mathbb{R}^N$ and $f : \mathbb{R}^N \to \mathbb{R}^N$ is smooth. We seek a formal power series solution in time s. The key observation, going back to Cayley (1857), is that the higher derivatives of $x(s)$ are naturally indexed by **rooted trees**.

Definition 0.3 (Rooted Tree)**.** A **rooted tree** is a connected graph with no cycles and a distinguished node called the **root**. The number of nodes in a tree t is denoted $|t|$.

The first few rooted trees, organized by number of nodes, are shown below. We denote the single-node tree (just a root) by $\bullet$.

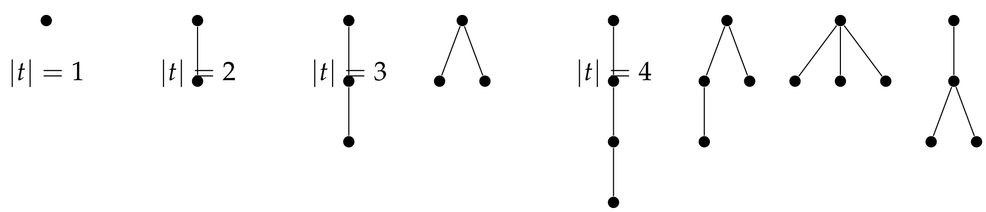

There are 1, 1, 2, 4, 9, 20, 48, 115, ... rooted trees with $n = 1, 2, 3, 4, 5, 6, 7, 8, \ldots$ nodes. This is OEIS sequence A000081.

Given a tree $t = [t_1, t_2, \ldots, t_k]$ formed by attaching the roots of subtrees $t_1, \ldots, t_k$ to a new common root, we define the **elementary differential** $\delta_t(x)$ recursively.

Definition 0.4 (Elementary Differential)**.** For a vector field $f : \mathbb{R}^N \to \mathbb{R}^N$, define the elementary differentials by

$$\delta^i_\bullet(x) = f^i(x) \tag{331}$$

$$\delta^i_{[t_1,\ldots,t_k]}(x) = \sum_{j_1,\ldots,j_k=1}^{N} \left(\delta^{j_1}_{t_1}(x) \cdots \delta^{j_k}_{t_k}(x)\right) \frac{\partial^k f^i}{\partial x^{j_1} \cdots \partial x^{j_k}}(x) \tag{332}$$

Physical interpretation: Each rooted tree encodes a specific pattern of nested differentiations. The root corresponds to the outermost function f, and each subtree corresponds to differentiation with respect to one argument, followed by substitution of another instance of f. This structure captures exactly the chain rule applied repeatedly.

Box 7.1: Elementary Differentials for Small Trees

Goal: Compute the elementary differentials for trees with up to 3 nodes.

The single-node tree $\bullet$:

$$\delta_\bullet = f \tag{333}$$

This is just the vector field itself.
The two-node tree $[\bullet]$**:**

$$\delta^i_{[\bullet]} = \sum_j f^j \frac{\partial f^i}{\partial x^j} = (f \cdot \nabla) f^i = (Df) \cdot f \tag{334}$$

This is the directional derivative of f along f, representing $\ddot{x} = \frac{d^2 x}{ds^2}$.
The three-node chain $[[\bullet]]$**:**

$$\delta^i_{[[\bullet]]} = \sum_{j,k} f^k \frac{\partial f^j}{\partial x^k} \frac{\partial f^i}{\partial x^j} + \sum_{j,k} f^j f^k \frac{\partial^2 f^i}{\partial x^j \partial x^k} \tag{335}$$

This corresponds to $\dddot{x}$ computed via repeated application of the chain rule.
The three-node "fork" $[\bullet, \bullet]$**:**

$$\delta^i_{[\bullet,\bullet]} = \sum_{j,k} f^j f^k \frac{\partial^2 f^i}{\partial x^j \partial x^k} \tag{336}$$

This is the second derivative of f contracted with two copies of f.
Key insight: Different trees at the same order correspond to different ways of differentiating f. The tree structure keeps track of the combinatorics automatically.

B-Series: Formal Solutions Indexed by Trees

The remarkable fact is that the Taylor series solution of (330) can be written as a sum over rooted trees.

Theorem 0.5 (B-Series Expansion)**.** *The formal solution of* $\dot{x} = f(x)$*,* $x(0) = x_0$ *is*

$$x(s) = x_0 + \sum_{\text{trees } t} \frac{s^{|t|}}{\sigma(t)} \delta_t(x_0) \tag{337}$$

where the sum runs over all rooted trees t*, and* $\sigma(t)$ *is the* ***symmetry factor*** *of the tree (the order of its automorphism group times the tree factorial).*

The symmetry factor $\sigma(t)$ accounts for equivalent ways of building the same tree. It is analogous to the symmetry factors of Feynman diagrams.

The B-series ("Butcher series") provides a universal framework for analyzing:

- The exact flow of a vector field (expanding the exponential map)
- Runge–Kutta and other numerical integration methods
- Composition of flows and near-identity transformations

Connection to the Prologue: The perturbative solution of the damped anharmonic oscillator from the Prologue can be written as a B-series.

Each tree corresponds to a specific pattern of interactions between the linear and nonlinear parts of the vector field. Secular terms arise when certain tree contributions grow unboundedly in time.

The Hopf Algebra of Rooted Trees

The set of rooted trees carries a natural **Hopf algebra** structure. This structure organizes the composition and decomposition of flows.

A Hopf algebra is an algebra with a compatible coalgebra structure (coproduct, counit) and an antipode. It generalizes the notion of a group algebra.

Definition 0.6 (Hopf Algebra $\mathcal{H}_R$ of Rooted Trees)**.** Let $\mathcal{H}_R$ be the polynomial algebra over $\mathbb{C}$ generated by rooted trees, with the following structures.

Product: The product is the disjoint union of trees (forming a forest):

$$t_1 \cdot t_2 = t_1 \sqcup t_2 \tag{338}$$

The unit is the empty forest $\mathbf{1}$.

Coproduct: The coproduct $\Delta : \mathcal{H}_R \to \mathcal{H}_R \otimes \mathcal{H}_R$ encodes how trees can be "cut":

$$\Delta(t) = t \otimes \mathbf{1} + \mathbf{1} \otimes t + \sum_{\text{admissible cuts } c} P^c(t) \otimes R^c(t) \tag{339}$$

where $P^c(t)$ is the "pruned" part (subtrees removed by the cut) and $R^c(t)$ is the "remainder" (what remains attached to the root).

Counit: $\varepsilon(t) = 0$ for any non-empty tree, $\varepsilon(\mathbf{1}) = 1$.

Antipode: Defined recursively by

$$S(t) = -t - \sum_{\text{cuts } c} S(P^c(t)) \cdot R^c(t) \tag{340}$$

Box 7.2: The Coproduct for Small Trees

Goal: Compute the coproduct for trees with 1, 2, and 3 nodes.
Single node $\bullet$: No non-trivial cuts are possible.

$$\Delta(\bullet) = \bullet \otimes \mathbf{1} + \mathbf{1} \otimes \bullet \tag{341}$$

This says $\bullet$ is **primitive** (no internal structure to decompose).
Two nodes $[\bullet]$: One cut is possible, separating the root from its child.

$$\Delta([\bullet]) = [\bullet] \otimes \mathbf{1} + \mathbf{1} \otimes [\bullet] + \bullet \otimes \bullet \tag{342}$$

The third term represents cutting the edge: the pruned part is $\bullet$ and the remainder is $\bullet$.
Three-node chain $[[\bullet]]$: Two cuts are possible.

$$\Delta([[\bullet]]) = [[\bullet]] \otimes \mathbf{1} + \mathbf{1} \otimes [[\bullet]] + \bullet \otimes [\bullet] + [\bullet] \otimes \bullet + \bullet \cdot \bullet \otimes \bullet \tag{343}$$

The terms correspond to: no cut, full cut, cutting the top edge, cutting the bottom edge, and cutting both edges.

Physical meaning: The coproduct encodes how a complicated operation (flow to time $s+t$) decomposes into simpler operations (flow to time s, then flow to time t). Each cut corresponds to a way of factoring the computation.

The Butcher Group

The **Butcher group** G is the group of characters of the Hopf algebra $\mathcal{H}_R$. A **character** is an algebra homomorphism $\phi : \mathcal{H}_R \to \mathbb{C}$ (or more generally into any commutative algebra A).

Group structure: Characters form a group under the **convolution product**:

$$(\phi_1 \star \phi_2)(t) = m \circ (\phi_1 \otimes \phi_2) \circ \Delta(t) \tag{344}$$

where m is multiplication in the target algebra.

The Butcher group is an infinite-dimensional Lie group. Its Lie algebra consists of infinitesimal characters, which are derivations of the Hopf algebra.

- **Identity:** The counit ε
- **Inverse:** $\phi^{-1} = \phi \circ S$ (composition with the antipode)

Physical interpretation:

- Each character ϕ assigns numerical values to trees, specifying a particular flow or numerical method.
- The convolution product corresponds to **composition of flows**.
- The inverse corresponds to **time reversal** or **undoing a transformation**.

Renormalization in the ODE Context

The B-series solution (337) may contain **secular terms** that grow without bound, invalidating the perturbative expansion. This is the ODE analog of UV divergences in QFT.

The renormalization procedure: Just as in QFT, we absorb the problematic terms into redefined parameters (initial conditions, frequencies, amplitudes). In Hopf-algebraic terms:

1. The "bare" solution is a character $\phi_{\text{bare}} : \mathcal{H}_R \to A$ where A contains the secular terms.
2. The "renormalized" solution is obtained by Birkhoff-type factorization: $\phi_{\text{bare}} = \phi_-^{-1} \star \phi_+$
3. The counterterms are encoded in ϕ_-^{-1}; the finite answer is ϕ_+.

This is exactly the Goldenfeld–Oono RG procedure from the Prologue, now understood as Birkhoff factorization in the Butcher group.

Box 7.3: The Anharmonic Oscillator in B-Series Language

Goal: Connect the Prologue's anharmonic oscillator to the Hopf algebra framework.
Setup: The damped anharmonic oscillator $\ddot{x} + 2\gamma\dot{x} + \omega_0^2 x + \epsilon x^3 = 0$ can be written as a first-order system:

$$\frac{d}{dt}\begin{pmatrix} x \\ v \end{pmatrix} = \begin{pmatrix} v \\ -2\gamma v - \omega_0^2 x - \epsilon x^3 \end{pmatrix} = f_0 + \epsilon f_1 \tag{345}$$

where f_0 is the linear part and f_1 contains the cubic nonlinearity.
B-series expansion: The perturbative solution has the form

$$\begin{pmatrix} x(t) \\ v(t) \end{pmatrix} = \sum_{\text{trees } t} \frac{t^{|t|}}{\sigma(t)} a(t,\epsilon)\delta_t(x_0, v_0) \tag{346}$$

where each tree is decorated to indicate whether vertices correspond to f_0 or f_1.
Secular terms: Trees containing certain patterns (repeated f_0 insertions at resonant frequencies) produce elementary differentials that grow as $t \cdot \cos(\omega_0 t)$ rather than staying bounded. These are the secular terms.
The coproduct and counterterms: The coproduct of a "secular tree" t_{sec} contains terms of the form $t_{\text{sub}} \otimes t_{\text{rem}}$ where t_{sub} is the problematic subtree. The RG procedure corresponds to:

1. Identifying secular subtrees (via the coproduct)
2. Computing counterterms (via the antipode)
3. Factoring into $\phi_-^{-1} \star \phi_+$ (Birkhoff decomposition)

Result: The renormalized solution is the running amplitude and phase derived in the Prologue, now understood as the "ϕ_+" part of a Birkhoff factorization in the Butcher group.

From ODEs to Quantum Field Theory

The Hopf algebra of rooted trees $\mathcal{H}_R$ and the Hopf algebra of Feynman graphs $\mathcal{H}_{\text{FG}}$ are structurally identical. This is not a coincidence. Both encode the combinatorics of nested operations that must be systematically organized.

Connes and Kreimer showed that the Hopf algebra of Feynman graphs is a quotient of the Hopf algebra of rooted trees by relations encoding the specific Feynman rules of the theory.

The Dictionary

The following table summarizes the correspondence between the ODE and QFT settings.

ODEs / Dynamical Systems	**Quantum Field Theory**
Rooted trees	Feynman graphs
Elementary differentials δ_t	Feynman integrals
B-series coefficients $a(t)$	Renormalized amplitudes
Symmetry factor $\sigma(t)$	Symmetry factor of diagram
Secular terms	UV divergences
Nested secular terms	Subdivergences
Near-identity transformation	Counterterm
Running initial conditions	Running couplings
Butcher group G	Character group of $\mathcal{H}_{\text{FG}}$
Convolution product $\star$	Convolution product $\star$
Antipode S	Antipode S (BPHZ formula)
Birkhoff factorization	Renormalization
RG flow on amplitudes	RG flow on couplings

Why the same structure? In both cases, we have:

1. A perturbative expansion indexed by combinatorial objects (trees or graphs)
2. Nested problematic contributions (secular terms or subdivergences)
3. A recursive procedure to remove them (counterterms)
4. Composition of transformations (flows or renormalization maps)

The Hopf algebra axioms precisely encode the compatibility conditions for these operations.

Historical Remark

The historical order of discovery is worth noting. Butcher introduced the algebraic theory of integration methods in 1963, and the group structure was identified by Hairer and Wanner in 1974. The Hopf algebra structure was implicit in this work but not formalized. Kreimer

(1998) discovered the Hopf algebra of Feynman graphs in the context of QFT renormalization. Connes and Kreimer (1999–2000) then recognized that this was essentially the same as the Butcher–Connes–Kreimer Hopf algebra of rooted trees. The QFT application thus came full circle back to ODEs.

Modern work by Hairer (regularity structures for SPDEs) and others continues to develop Hopf-algebraic methods for dynamical systems and PDEs.

The Hopf Algebra of Feynman Graphs

Having seen how the Hopf algebra of rooted trees organizes perturbative solutions of ODEs, we now turn to quantum field theory. The combinatorics of renormalization in QFT has the same algebraic structure, with Feynman graphs playing the role of rooted trees. This parallel was recognized by Kreimer (1998) and developed by Connes and Kreimer (1999–2000), who showed that renormalization is a special case of the **Riemann-Hilbert problem**.

The Hopf algebra of Feynman graphs is structurally identical to the Hopf algebra of rooted trees from Section II. The coproduct encodes subdivergences just as it encoded "subflows" for ODEs.

From Trees to Graphs

Consider all one-particle irreducible (1PI) Feynman graphs in a renormalizable theory. These graphs form the basis for a **Hopf algebra** $\mathcal{H}_{\text{FG}}$, directly analogous to the Hopf algebra $\mathcal{H}_R$ of rooted trees.

As an algebra: $\mathcal{H}$ is the polynomial algebra generated by 1PI graphs. The product is disjoint union:

$$\Gamma_1 \cdot \Gamma_2 = \Gamma_1 \sqcup \Gamma_2 \tag{347}$$

This algebra is commutative. The unit element is the empty graph.

The coproduct: The key structure is the coproduct $\Delta : \mathcal{H} \to \mathcal{H} \otimes \mathcal{H}$, which encodes how divergences nest inside each other:

$$\Delta(\Gamma) = \Gamma \otimes 1 + 1 \otimes \Gamma + \sum_{\gamma \subsetneq \Gamma} \gamma \otimes \Gamma/\gamma \tag{348}$$

where the sum runs over all divergent subgraphs γ of Γ, and Γ/γ is the contracted graph obtained by replacing each component of γ by the corresponding local vertex.

The coproduct encodes the recursive structure of subdivergences—exactly what BPHZ renormalization handles.

The antipode: The antipode $S : \mathcal{H} \to \mathcal{H}$ is the algebraic inverse under convolution:

$$S(\Gamma) = -\Gamma - \sum_{\gamma \subsetneq \Gamma} S(\gamma) \cdot (\Gamma/\gamma) \tag{349}$$

This is exactly the recursive structure of counterterms in the BPHZ renormalization procedure!

The antipode S generates the counterterms. Its recursive structure is precisely the BPHZ forest formula.

Box 7.4: The Coproduct for a Two-Loop Graph

Example: Consider a two-loop self-energy graph Γ with one nested subdivergence γ (a one-loop subgraph).
The coproduct:

$$\Delta(\Gamma) = \Gamma \otimes 1 + 1 \otimes \Gamma + \gamma \otimes (\Gamma/\gamma) \tag{350}$$

The three terms correspond to:

- $\Gamma \otimes 1$: The graph as a whole (no subdivergence extracted)
- $1 \otimes \Gamma$: All divergences internal
- $\gamma \otimes (\Gamma/\gamma)$: The subdivergence γ extracted, leaving the reduced graph

Comparison with trees: This is exactly analogous to Box 7.2 for rooted trees. The subdivergence γ plays the role of a "pruned subtree," and the contracted graph Γ/γ plays the role of the "remainder" attached to the root.
The antipode:

$$S(\Gamma) = -\Gamma - S(\gamma) \cdot (\Gamma/\gamma) = -\Gamma + \gamma \cdot (\Gamma/\gamma) \tag{351}$$

Physical meaning: The counterterm for Γ is the sum of:

1. $-\Gamma$: subtract the overall divergence
2. $+\gamma \cdot (\Gamma/\gamma)$: add back the subdivergence contribution

This is the BPHZ prescription in algebraic form, structurally identical to the ODE renormalization of Section II.

The Group of Characters

The physically meaningful structures are **characters** of the Hopf algebra—algebra homomorphisms $\phi : \mathcal{H} \to A$ into some target algebra A.

Characters of the Hopf algebra form a group under convolution. This is the "renormalization group" in an algebraic sense.

The convolution product: Two characters ϕ_1, ϕ_2 can be combined via:

$$(\phi_1 \star \phi_2)(\Gamma) = m_A \circ (\phi_1 \otimes \phi_2) \circ \Delta(\Gamma) \tag{352}$$

where m_A is the multiplication in A.

The characters form a group G under convolution:

- Identity: the counit ε
- Inverse of ϕ: $\phi^{-1} = \phi \circ S$

The Lie algebra: The group G has an associated Lie algebra $\mathfrak{g}$ consisting of infinitesimal characters. The beta function can be understood as an element of $\mathfrak{g}$—an infinitesimal generator of the flow on theory space.

Renormalization as the Riemann-Hilbert Problem

The deepest result of Connes and Kreimer is that renormalization in dimensional regularization is a special case of the **Riemann-Hilbert problem**—a classical problem in complex analysis concerning the decomposition of loops in Lie groups.

The Riemann-Hilbert problem asks: given a loop $\gamma(z)$ in a complex Lie group G, decompose it as $\gamma = \gamma_-^{-1}\gamma_+$ where $\gamma_\pm$ are holomorphic inside/outside the loop.

The Birkhoff Decomposition

Let C be a simple closed curve in the complex plane dividing the Riemann sphere into two regions: C_+ (inside, containing 0) and C_- (outside, containing ∞).

Definition 0.7 (Birkhoff Decomposition)**.** Given a loop $\gamma : C \to G$ with values in a complex Lie group G, the **Birkhoff decomposition** (when it exists) is:

$$\gamma(z) = \gamma_-(z)^{-1}\gamma_+(z) \tag{353}$$

where $\gamma_+(z)$ extends holomorphically to C_+ and $\gamma_-(z)$ extends holomorphically to C_- with $\gamma_-(\infty) = 1$.

The Birkhoff decomposition separates the "pole part" from the "holomorphic part"—exactly what renormalization does.

Dimensional Regularization as a Loop

In dimensional regularization, we work in $d = D - \epsilon$ dimensions. The bare theory defines values for each Feynman graph that are meromorphic functions of ϵ, with poles at $\epsilon = 0$.

The key observation: The collection of all bare values defines a *loop* in the group G of characters. As ϵ varies on a small circle C around 0, this defines a loop $\gamma : C \to G$.

Theorem 0.8 (Connes-Kreimer)**.** *The renormalized theory is obtained by the Birkhoff decomposition:*

$$\gamma(\epsilon) = \gamma_-(\epsilon)^{-1} \star \gamma_+(\epsilon) \tag{354}$$

The renormalized values are given by $\gamma_+(0)$—the evaluation of the holomorphic part at the physical dimension.

Physical interpretation:

- $\gamma_-(\epsilon)^{-1}$: Contains the poles in ϵ—these are the **counterterms**
- $\gamma_+(\epsilon)$: Holomorphic at $\epsilon = 0$—this is the **renormalized theory**
- $\gamma_+(0)$: The physical limit, free of divergences

The Connes-Kreimer theorem: renormalization = Birkhoff decomposition. The counterterms are γ_-^{-1} and the renormalized values are γ_+.

Box 7.5: Birkhoff Decomposition and Minimal Subtraction

Goal: Show that the Birkhoff decomposition reproduces the MS scheme.

Setup: Consider a one-loop integral with a single pole:

$$\gamma(\epsilon) = 1 + \frac{a}{\epsilon} + b + c\epsilon + \dots \tag{355}$$

Step 1: Identify γ_-.

The "negative part" is:

$$\gamma_-(\epsilon) = 1 + \frac{a}{\epsilon} \tag{356}$$

Step 2: Compute γ_+.

For the abelian case:

$$\gamma_+(\epsilon) = \gamma_-(\epsilon)^{-1} \cdot \gamma(\epsilon) \tag{357}$$

Step 3: The renormalized value.

$$\gamma_+(0) = 1 + b \tag{358}$$

This is exactly the MS-renormalized result: subtract the pole, keep the finite part.

Key insight: The Birkhoff decomposition *is* minimal subtraction, elevated to a group-theoretic principle.

The Twisted Antipode

The connection between the Birkhoff decomposition and the Hopf algebra antipode is made precise by the **twisted antipode**.

Let $R : A \to A$ be the projection onto the polar part. Define the twisted antipode S_R recursively:

$$S_R(\Gamma) = -R\left[\phi(\Gamma) + \sum_{\gamma \subsetneq \Gamma} S_R(\gamma) \cdot \phi(\Gamma/\gamma)\right] \tag{359}$$

The twisted antipode S_R directly computes counterterms. It combines the Hopf algebra structure with the choice of renormalization scheme.

Theorem 0.9. *The components of the Birkhoff decomposition are:*

$$\gamma_-^{-1} = S_R \star \phi \quad \textit{(counterterms)} \tag{360}$$

$$\gamma_+ = (S_R \star \phi) \star id \quad \textit{(renormalized values)} \tag{361}$$

Scheme dependence: Different choices of the projection R give different renormalization schemes. The algebraic structure is universal; only the choice of R changes.

Why This Matters

The Connes-Kreimer perspective has profound implications:

1. **Conceptual clarity:** Renormalization is not an ad hoc procedure for canceling infinities. It is a mathematically natural operation—the Birkhoff decomposition—applied to a loop arising from the bare theory.

2. **Scheme independence:** Different schemes correspond to different ways of splitting holomorphic and antiholomorphic parts. The ambiguity is parameterized by a finite-dimensional group.

3. **Connection to number theory:** The Hopf algebra $\mathcal{H}$ is related to the Hopf algebra of multiple zeta values. This explains why Feynman integrals often evaluate to special values.

4. **Non-perturbative extensions:** As we will see in Chapter II, this algebraic structure connects perturbation theory to non-perturbative physics through resurgence.

Connection to Resurgent Structure

The Hopf algebra framework developed above deals with UV divergences—the infinities in individual loop diagrams. Chapter II dealt with IR divergences in a different sense—the factorial growth of the perturbative series itself. These two perspectives are deeply connected.

The Hopf algebra and resurgent pictures complement each other: Hopf algebra handles the *combinatorics* of subdivergences; resurgence handles the *analyticity* of the summed series.

Complementary viewpoints:

- **Hopf algebra**: Organizes the *combinatorics* of nested divergences (BPHZ forest formula)

- **Resurgence**: Organizes the *analyticity* of the Borel-summed answer (alien calculus)

The bridge: The Stokes automorphism of Chapter II can be understood as a transformation on the character group G. The alien derivative Δ_ω probes singularities in the Borel plane; these singularities often correspond to renormalon poles whose structure is dictated by the Hopf algebra.

Key insight: The full structure of perturbative QFT combines:

1. The Hopf algebra for handling UV divergences (making the series well-defined term by term)

2. Resurgence for handling IR divergences (making the summed series well-defined)

3. Both structures are needed for a complete non-perturbative answer

This unified picture—Hopf algebra + resurgence—represents the state of the art in understanding the mathematical structure of perturbative quantum field theory.

Summary

This chapter revealed the deep algebraic structure underlying renormalization, showing that the same Hopf algebra appears in both dynamical systems and quantum field theory.

1. **The Butcher group and B-series** organize perturbative solutions of ODEs. Rooted trees index the terms in a formal power series solution, and the Hopf algebra structure encodes how these terms compose and decompose. Secular terms in ODEs are the analog of UV divergences in QFT.

2. **The Hopf algebra of Feynman graphs** has the same structure, with graphs playing the role of trees. The coproduct encodes subdivergences and the antipode generates counterterms. The BPHZ forest formula is the antipode in algebraic form.

3. **The Riemann-Hilbert correspondence** shows renormalization is the Birkhoff decomposition of a loop in the character group. This applies to both ODEs (removing secular terms) and QFT (removing UV divergences). Minimal subtraction is this decomposition in coordinates.

4. **Connection to resurgence**: The Hopf algebra handles the combinatorics of nested divergences; resurgence handles the analyticity of the summed series. Both are needed for a complete nonperturbative picture.

The unified viewpoint shows that renormalization is not specific to quantum field theory. The same algebraic structure governs any perturbative expansion with nested problematic contributions, whether they are secular terms in ODEs or UV divergences in QFT. This explains why RG methods are so broadly applicable across physics.

Exercises

1. **Elementary differentials.** For the ODE $\dot{x} = f(x)$ with $f(x) = ax + bx^2$:

   (a) Compute the elementary differentials $\delta_\bullet$, $\delta_{[\bullet]}$, and $\delta_{[[\bullet]]}$.

   (b) Write out the B-series solution up to order t^3.

(c) Identify which terms grow secularly when $a = i\omega_0$ (pure imaginary).

2. **Tree coproduct.** For the four-node "chain" tree [[[•]]]:

(a) List all admissible cuts (there should be 7 including the trivial ones).

(b) Write out the full coproduct $\Delta([[[\bullet]]])$.

(c) Verify that the coproduct is coassociative: $(\Delta \otimes \mathrm{id})\Delta = (\mathrm{id} \otimes \Delta)\Delta$.

3. **Hopf algebra coproduct for Feynman graphs.** For a three-loop graph Γ with two nested subdivergences $\gamma_1 \subset \gamma_2 \subset \Gamma$:

(a) Write out all terms in the coproduct $\Delta(\Gamma)$.

(b) Compute the antipode $S(\Gamma)$ recursively.

(c) Compare with the tree case and identify the correspondence.

4. **(Challenge) Birkhoff decomposition.** For the two-loop Laurent series:

$$\gamma(\epsilon) = 1 + \frac{a}{\epsilon^2} + \frac{b}{\epsilon} + c + d\epsilon + \dots \tag{362}$$

(a) Find the Birkhoff decomposition $\gamma = \gamma_-^{-1}\gamma_+$.

(b) Verify that $\gamma_+(0) = c +$ (terms involving a, b).

(c) Interpret the result in terms of BPHZ subtraction of nested divergences.

5. **Character group structure.** For the Hopf algebra of rooted trees:

(a) Show that the set of characters forms a group under convolution.

(b) Verify that the inverse of a character ϕ is $\phi \circ S$ where S is the antipode.

(c) Explain why this group is called the "renormalization group" in the algebraic sense.

6. **ODE-QFT dictionary.** Consider the damped anharmonic oscillator from the Prologue.

(a) Identify the analog of "bare coupling" and "renormalized coupling."

(b) What plays the role of the "UV cutoff" in the ODE context?

(c) Explain why the RG equation $\frac{dA}{dt} = -\gamma A$ corresponds to a flow in the Butcher group.

7. **(Challenge) Hopf-resurgence connection.** Consider a theory with both UV subdivergences and IR renormalons.

(a) Explain how the Hopf algebra handles the UV structure order by order.

(b) Explain how resurgence handles the summed series.

(c) Argue why both structures are needed for a complete answer.

Resurgence and Transseries

This chapter develops the machinery for extracting physics from divergent series: Borel resummation, transseries, and resurgence. These tools reveal that perturbation theory "knows" about non-perturbative physics.

Chapter II showed that perturbation series generically diverge with factorial growth. This chapter develops the analytical tools for extracting *physical predictions* from these divergent series.

The key insight is that factorial divergence is not a failure—it *encodes* non-perturbative physics. The pattern of divergence tells us about instantons, tunneling, and other effects invisible to any finite order of perturbation theory.

- **Section II**: The Borel transform converts factorial divergence to convergence
- **Section II**: Singularities (instantons, renormalons) encode non-perturbative physics
- **Section II**: Stokes phenomena—what happens when singularities obstruct resummation
- **Section II**: Transseries—the complete answer beyond perturbation theory
- **Section II**: The resurgence triangle—organizing the non-perturbative sectors
- **Section II**: Alien calculus—systematic extraction of non-perturbative information
- **Section II**: Renormalons from the RG equation
- **Section II**: Median resummation—obtaining physical predictions

Throughout this chapter, we illustrate the machinery with the **damped anharmonic oscillator** from the Prologue—the same system whose RG equations we derived in Chapter I.

The Borel Transform

The Borel transform converts factorial divergence into geometric growth, transforming a divergent series into a convergent one.

Definition and Basic Properties

Definition 0.10 (Borel Transform)**.** Given a formal series $\tilde{f}(\epsilon) = \sum_{n=0}^{\infty} a_n \epsilon^n$, its **Borel transform** is:

$$\hat{f}_B(\zeta) = \sum_{n=0}^{\infty} \frac{a_n}{n!} \zeta^n \tag{363}$$

For a Gevrey-1 series with $|a_n| \leq CK^n n!$:

$$\left| \frac{a_n}{n!} \right| \leq CK^n \tag{364}$$

Dividing by $n!$ converts factorial growth $a_n \sim n!$ into bounded growth $a_n/n! \sim 1$.

The Borel transform converges for $|\zeta| < 1/K$.

The Borel plane: The complex ζ-plane is called the **Borel plane**. It is a new geometric arena where the divergent series becomes a well-defined analytic function (at least near the origin).

Box 6.1: Borel Transform of a Simple Series

Problem: Compute the Borel transform of the divergent series $\tilde{f}(\epsilon) = \sum_{n=0}^{\infty} n!\, \epsilon^n$ and identify its singularity structure.

Solution: The series diverges for all $\epsilon \neq 0$ because $|n!\epsilon^n| \to \infty$.
Borel transform:

$$\hat{f}_B(\zeta) = \sum_{n=0}^{\infty} \frac{n!}{n!} \zeta^n = \sum_{n=0}^{\infty} \zeta^n = \frac{1}{1-\zeta}$$

This converges for $|\zeta| < 1$ and has analytic continuation to $\mathbb{C} \setminus \{1\}$ with a **simple pole at** $\zeta = 1$.
Key insight: The divergent series encodes a meromorphic function. The position of the singularity ($\zeta = 1$) carries physical information about the non-perturbative structure.

Borel-Laplace Resummation

The Borel transform alone doesn't give us a function of the original variable ϵ. We need to "undo" the Borel transform using the Laplace transform.

Definition 0.11 (Borel Sum)**.** The **Borel sum** of $\tilde{f}(\epsilon)$ is:

$$\mathcal{S}[\tilde{f}](\epsilon) = \mathcal{L}[\hat{f}_B](\epsilon) = \int_0^{\infty} e^{-\zeta/\epsilon} \hat{f}_B(\zeta)\, d\zeta \tag{365}$$

Borel resummation: transform to make convergent, analytically continue, transform back. This extracts a function from a divergent series.

Key identity: For $g(\zeta) = \zeta^n$:

$$\int_0^{\infty} e^{-\zeta/\epsilon} \zeta^n\, d\zeta = n!\, \epsilon^{n+1} \tag{366}$$

This shows that the Laplace transform "undoes" the $1/n!$ factor in the Borel transform.

Box 6.2: Borel Resummation in Action

Problem: Resum the divergent alternating factorial series $\tilde{f}(\epsilon) = \sum_{n=0}^{\infty}(-1)^n n!\,\epsilon^n$ using Borel-Laplace.

Step 1: Borel transform

$$\hat{f}_B(\zeta) = \sum_{n=0}^{\infty}(-1)^n \zeta^n = \frac{1}{1+\zeta}$$

Pole at $\zeta = -1$ (negative real axis, **not** on integration path).
Step 2: Laplace transform

$$\mathcal{S}[\tilde{f}](\epsilon) = \int_0^{\infty} e^{-\zeta/\epsilon}\frac{1}{1+\zeta}\,d\zeta$$

Step 3: Evaluate
Using the exponential integral $E_1(x) = \int_x^{\infty}(e^{-t}/t)\,dt$:

$$\boxed{\mathcal{S}[\tilde{f}](\epsilon) = e^{1/\epsilon}E_1(1/\epsilon)}$$

Verification: Expanding for small ϵ: $e^{1/\epsilon}E_1(1/\epsilon) \sim \epsilon - \epsilon^2 + 2\epsilon^3 - 6\epsilon^4 + \cdots$ ✓
The divergent series has been resummed to a well-defined function!

When Resummation Fails: Singularities on the Path

The Borel sum requires integrating along the positive real axis. If $\hat{f}_B(\zeta)$ has a singularity on $[0,\infty)$, the integral is ambiguous.

Singularities on the positive real axis obstruct naive resummation. This is where Stokes phenomena enter.

The problem: Consider $\hat{f}_B(\zeta) = 1/(1-\zeta)$ with a pole at $\zeta = 1$. The integral

$$\int_0^{\infty} e^{-\zeta/\epsilon}\frac{1}{1-\zeta}\,d\zeta \qquad (367)$$

diverges because the integrand blows up at $\zeta = 1$.

The resolution: We must specify how to navigate around the singularity. Different choices give different answers—this is the Stokes phenomenon.

Singularities in the Borel Plane

The singularities of $\hat{f}_B(\zeta)$ are not defects to be avoided. They are the primary carriers of non-perturbative information.

Instantons

In theories with tunneling or classical solutions of finite action, the Borel transform has singularities at:

Instantons are classical solutions with finite action. They contribute $\sim e^{-S_{\text{inst}}/\epsilon}$ to physical quantities.

$$\zeta_{\text{inst}} = S_{\text{inst}} \tag{368}$$

where S_{inst} is the classical action of the instanton.

Physical interpretation: The instanton contributes $\sim e^{-S_{\text{inst}}/\epsilon}$ to the path integral. This exponentially small effect is "invisible" to perturbation theory but encoded in the singularity structure.

For the anharmonic oscillator: The inverted potential $-V(x)$ has classical solutions (instantons) with action:

$$S_{\text{inst}} = \frac{\omega^3}{3\lambda} \tag{369}$$

The Borel transform has a singularity at $\zeta = S_{\text{inst}}$.

Renormalons

In quantum field theory, a distinct class of singularities arises from the factorial growth induced by RG running.

Renormalons are singularities at $\zeta = k/\beta_1$ from the factorial growth caused by integrating over all momentum scales.

Origin: Consider a loop integral with running coupling. This gives $a_n \sim \beta_1^n n!$ where β_1 is the one-loop beta function coefficient.

Position: Renormalon singularities occur at:

$$\zeta_k = \frac{k}{\beta_1}, \quad k = 1, 2, 3, \ldots \tag{370}$$

IR vs UV renormalons:

- **IR renormalons** ($\beta_1 > 0$, asymptotically free): Singularities on positive real axis, obstruct resummation
- **UV renormalons** ($\beta_1 < 0$): Singularities on negative real axis, do not obstruct resummation directly

Box 6.3: Renormalon Position in QCD

Problem: Find the position of the leading IR renormalon in QCD with $N_c = 3$ colors and $N_f = 3$ light flavors.

One-loop beta function:

$$\beta_1 = \frac{11N_c - 2N_f}{12\pi} = \frac{33 - 6}{12\pi} = \frac{9}{4\pi}$$

Renormalon positions:

$$\zeta_k = \frac{k}{\beta_1} = \frac{4\pi k}{9}, \quad k = 1, 2, 3, \ldots$$

Leading IR renormalon: $\boxed{\zeta_1 = \frac{4\pi}{9} \approx 1.4}$

Physical interpretation: This singularity reflects sensitivity to long-distance physics. The resummation ambiguity $\sim e^{-4\pi/(9\alpha_s)} \sim \Lambda^2_{\text{QCD}}/Q^2$ matches expected power corrections.

The Instanton-Renormalon Correspondence

A profound insight from compactified QFT is that IR renormalons have a *semiclassical interpretation*. In theories on $\mathbb{R}^3 \times S^1$:

Neutral bions—instanton–anti-instanton configurations at the same position—produce contributions at:

$$e^{-2S_{\text{monopole}}} = e^{-1/(\beta_0 g^2)} \tag{371}$$

This is *exactly* the form of the leading IR renormalon, demonstrating that resurgence and semiclassical analysis are two sides of the same coin.

Stokes Phenomena

When the integration contour for Borel resummation encounters a singularity, we must make a choice. The systematic study of these choices is the theory of Stokes phenomena.

Stokes Lines

Definition 0.12 (Stokes Line)**.** A **Stokes line** for a singularity at ζ_* is the ray in the ϵ-plane where:

$$\arg(\epsilon) = \arg(\zeta_*) \tag{372}$$

On a Stokes line, the Laplace integration path passes through the singularity. The resummation prescription must change as we cross this line.

On a Stokes line, the singularity lies directly on the integration path.

Lateral Resummations

When a singularity lies on $[0, \infty)$, we define **lateral resummations** by deforming the contour slightly above or below the real axis:

$$\mathcal{S}_+[\tilde{f}](\epsilon) = \int_0^{e^{i0^+}\infty} e^{-\zeta/\epsilon} \hat{f}_B(\zeta)\, d\zeta \tag{373}$$

$$\mathcal{S}_-[\tilde{f}](\epsilon) = \int_0^{e^{-i0^+}\infty} e^{-\zeta/\epsilon} \hat{f}_B(\zeta)\, d\zeta \tag{374}$$

These integrals are well-defined but generally different. The difference is exponentially small in $1/\epsilon$—a *non-perturbative* effect invisible to any finite order of the original series.

$\mathcal{S}_+$ and $\mathcal{S}_-$ go above and below the singularities, giving different results.

The Stokes Automorphism

The difference between lateral resummations defines the **Stokes automorphism**.

Definition 0.13 (Stokes Automorphism)**.** The **Stokes automorphism** $\mathfrak{S}$ is the transformation relating $\mathcal{S}_+$ to $\mathcal{S}_-$:

$$\mathcal{S}_+ = \mathfrak{S} \circ \mathcal{S}_- \tag{375}$$

For a simple pole at ζ_* with residue r:

$$\mathcal{S}_+[\tilde{f}] - \mathcal{S}_-[\tilde{f}] = 2\pi i \cdot r \cdot e^{-\zeta_*/\epsilon} \tag{376}$$

Box 6.4: Computing the Stokes Jump

Problem: Compute the Stokes jump for $\hat{f}_B(\zeta) = 1/(1-\zeta)$, which has a pole at $\zeta = 1$ on the positive real axis.

Lateral resummations (contours $\mathcal{C}_\pm$ pass above/below $\zeta = 1$):

$$\mathcal{S}_\pm[\tilde{f}] = \int_{\mathcal{C}_\pm} e^{-\zeta/\epsilon} \frac{1}{1-\zeta}\, d\zeta$$

The Stokes jump: By the residue theorem (residue at $\zeta = 1$ is -1):

$$\boxed{\mathcal{S}_+ - \mathcal{S}_- = 2\pi i \cdot e^{-1/\epsilon}}$$

Stokes constant: $S_1 = 2\pi i$
This exponentially small difference is invisible to perturbation theory but captured by the Stokes automorphism.

Stokes Constants as Monodromy

The Stokes phenomenon has a beautiful geometric interpretation: the jumps in transseries parameters are **monodromy** of parallel transport around singularities in coupling space.

The Stokes automorphism is precisely the monodromy of the connection on theory space around singularities.

Key property: Stokes constants are *scheme-independent*. They are intrinsic to the theory, not artifacts of how we parameterize it.

Transseries

To fully resolve the ambiguity from Stokes phenomena, we must go beyond perturbation theory. The complete answer is a **transseries**.

Definition

Definition 0.14 (Transseries)**.** A **transseries** is a formal expression combining perturbative and non-perturbative sectors:

$$\tilde{f}(\epsilon, \sigma) = \sum_{k=0}^{\infty} \sigma^k e^{-kS/\epsilon} \hat{f}^{(k)}(\epsilon) \tag{377}$$

where:

- $\hat{f}^{(0)}(\epsilon)$ is the perturbative sector (ordinary asymptotic series)
- $\hat{f}^{(k)}(\epsilon)$ for $k \geq 1$ are **instanton sectors**
- σ is the **transseries parameter**
- S is the instanton action

The transseries includes perturbative ($k = 0$) and non-perturbative ($k \geq 1$) sectors. The parameter σ weights the instanton contributions.

Physical Interpretation

The transseries structure reflects the physics of the path integral:

Sector $k = 0$: Perturbative fluctuations around the vacuum.

Sector $k = 1$: One-instanton contribution, weighted by $e^{-S/\epsilon}$ from the classical action and σ encoding boundary conditions.

Sector $k \geq 2$: Multi-instanton contributions.

The Role of σ

The transseries parameter σ is not fixed by the perturbative series. It encodes **boundary conditions** or other non-perturbative input.

Key insight: The perturbative series alone cannot determine σ. Non-perturbative input is required.

σ is the integration constant of the non-perturbative sector. It's determined by physics, not perturbation theory.

Worked Example: The Damped Anharmonic Oscillator

We now apply the machinery developed above to the **damped anharmonic oscillator—**the same system we analyzed in the Prologue and Chapter I:

We apply resurgent methods to the damped anharmonic oscillator from the Prologue, showing how the RG equations from Chapter I have transseries solutions.

$$\boxed{\ddot{x} + 2\gamma\dot{x} + \omega_0^2 x + \epsilon x^3 = 0, \quad \epsilon > 0} \tag{378}$$

As derived in Chapter I, the RG equations for amplitude A and phase ϕ are:

$$\frac{dA}{dt} = -\gamma A, \qquad \frac{d\phi}{dt} = \frac{3\epsilon A^2}{8\omega_0} \tag{379}$$

where the amplitude decays at rate γ (the damping coefficient) and the phase advances due to the nonlinearity. The key question: *what is the resurgent structure of these equations?*

Factorial Growth in the Beta Functions

As computed in Chapter I, the perturbative corrections to the phase equation grow factorially:

At higher orders, the beta function coefficients grow factorially—exactly the Gevrey-1 structure from Chapter II.

$$\phi_n(t) \sim (-1)^{n+1} \cdot \frac{n!}{S^n} \cdot f_n(t) \tag{380}$$

where $S = \omega_0/\gamma$ is the **instanton action** and $f_n(t)$ are bounded functions.

This factorial growth means the perturbative solution is a **divergent asymptotic series**—exactly the situation where resurgent methods are needed.

Applying the Resurgence Pipeline

The full resurgence analysis of the damped oscillator follows the pipeline developed in this chapter:

Resurgence Pipeline for the Damped Oscillator

Step 1: Borel Transform. The divergent phase expansion $\phi = \sum_n \phi_n \epsilon^n$ has Borel transform with singularities at:

$$\zeta_k = k \cdot \frac{\omega_0}{\gamma}, \quad k = 1, 2, 3, \ldots \tag{381}$$

The leading singularity at $\zeta_1 = \omega_0/\gamma$ is the **instanton action**.
Step 2: Physical Interpretation. The singularities encode the timescale $\tau_{\text{inst}} = \omega_0/\gamma$ at which the nonlinear correction becomes comparable to the linear behavior.
Step 3: Transseries. The complete solution is:

$$A(t) = \sum_{n=0}^{\infty} \sigma^n e^{-n\gamma t} A^{(n)}(t; \epsilon) \tag{382}$$

where σ is determined by initial conditions.
Step 4: Resurgent Relations. The large-order behavior of $A^{(0)}$ determines $A^{(1)}$:

$$A_n^{(0)} \sim \frac{S_1}{2\pi i} \frac{\Gamma(n)}{\zeta_1^n} A_0^{(1)} + \cdots \tag{383}$$

Key insight: The RG equations (379) are themselves **resurgent equations**—their solutions are transseries, not power series. The perturbative beta function is just the leading term of a larger resurgent structure.

For the negative ϵ case (double-well), the Borel singularities move to the positive real axis, corresponding to real tunneling instantons. This changes the Stokes structure qualitatively.

Connection to QFT Renormalons

The Borel singularity pattern $\zeta_n = n \cdot (\omega_0/\gamma)$ parallels the IR renormalon structure in QFT, where $\zeta_n = n/\beta_0$. Both arise from the **nonlinear structure of RG equations**—the oscillator provides a completely classical example of "renormalon-like" singularities.

The classical oscillator demonstrates that resurgence is a tool for *any* nonlinear system, not just quantum field theories.

The Resurgence Triangle

A remarkable discovery is that the relations between perturbative and non-perturbative sectors can be organized into a **graded resurgence triangle**. This structure reveals that *all* information about non-perturbative physics is encoded in the perturbative expansion.

The resurgence triangle organizes the intricate connections between all transseries sectors into a systematic structure.

The Triangle Structure

Consider a theory with instanton action S. The transseries sectors are arranged:

- $\hat{f}^{(0)}$ is the perturbative sector (apex)
- $\hat{f}^{(k)}$ are k-instanton sectors (left edge)
- $\hat{f}^{(\bar{k})}$ are k-anti-instanton sectors (right edge)
- $\hat{f}^{(k\bar{l})}$ are mixed instanton–anti-instanton sectors (interior)

The Key Insight: Perturbation Theory Knows Everything

The **graded resurgence** property states that the large-order behavior of any sector determines the neighboring sectors:

$$a_n^{(k)} \sim \sum_m \frac{S_{k\to m}}{(S_{k\to m})^{n+1}} \Gamma(n + \beta_{km}) \cdot a_0^{(m)} \tag{384}$$

Starting from the perturbative sector $\hat{f}^{(0)}$, we can *systematically reconstruct all non-perturbative sectors*:

Step 1: Large-order behavior of $a_n^{(0)}$ determines $\hat{f}^{(1)}$ and $\hat{f}^{(\bar{1})}$

Step 2: Large-order behavior of $a_n^{(1)}$ determines $\hat{f}^{(2)}$ and $\hat{f}^{(1\bar{1})}$

Step 3: Continue recursively through the triangle

Graded resurgence: the asymptotic behavior of sector k is controlled by sectors at distance 1 in the triangle.

Alien Calculus

Alien calculus is the mathematical framework for analyzing how different sectors of a transseries are related. It provides computational tools for extracting non-perturbative information from perturbative data.

The Alien Derivative

Definition 0.15 (Alien Derivative)**.** The **alien derivative** Δ_ω is an operator that "probes" the singularity at $\zeta = \omega$ in the Borel plane. It extracts the coefficient relating the perturbative sector to the instanton sector at that singularity.

The alien derivative extracts information about the singularity at ω. It's "alien" because it probes directions invisible to ordinary calculus.

The Bridge Equation

The fundamental result of alien calculus is the **bridge equation**:

Theorem 0.16 (Bridge Equation)**.**

$$\Delta_\omega \tilde{f} = S_\omega \cdot \frac{\partial \tilde{f}}{\partial \sigma} \tag{385}$$

where S_ω is the Stokes constant at ω.

The bridge equation connects Borel plane analysis (alien derivatives) to transseries parameter space (ordinary derivatives).

Physical interpretation: The alien derivative, which probes non-perturbative structure in the Borel plane, is equivalent to differentiating along the transseries direction.

Resurgent Relations

The alien derivatives satisfy algebraic relations:

$$\Delta_{\omega_1} \hat{f}^{(0)} = S_{\omega_1} \hat{f}^{(1)} \tag{386}$$

$$\Delta_{\omega_1} \hat{f}^{(1)} = S'_{\omega_1} \hat{f}^{(2)} + \cdots \tag{387}$$

These relations form a chain linking all sectors. Starting from the perturbative sector, alien derivatives generate the instanton sectors.

Resurgent relations link all sectors of the transseries. The perturbative sector "knows" about the instanton sectors.

This is resurgence: The perturbative series "resurges" into the non-perturbative sectors. All the information is encoded in the perturbative coefficients; alien calculus extracts it.

The Algebraic Structure

The alien derivatives $\{\Delta_\omega\}$ satisfy remarkable algebraic relations:

Commutation relations: For singularities at ω_1 and ω_2:

$$[\Delta_{\omega_1}, \Delta_{\omega_2}] = (\omega_1 - \omega_2)\Delta_{\omega_1+\omega_2} + \text{lower order terms} \tag{388}$$

This Virasoro-like structure encodes how non-perturbative effects "talk to each other."

Renormalons from the RG Equation

Renormalons emerge directly from the RG equation, without reference to Feynman diagrams.

A remarkable result connects resurgence directly to the renormalization group. Renormalons can be derived from the RG equation alone.

The RG Equation as a Resurgent Equation

Consider a physical observable $R(Q^2)$ depending on an energy scale Q. Using $\mu\, dg/d\mu = \beta(g)$:

$$\beta(g)\frac{dR}{dg} = \gamma(g)R \tag{389}$$

This equation has a *singular point* at $g = 0$, forcing the solution to be a transseries.

The RG equation in coupling space has the structure of a **resurgent equation**—its solutions are necessarily transseries.

IR Renormalons from the RG

When $\gamma(g)$ and $\beta(g)$ are both expanded perturbatively, the ratio γ/β has a $1/g$ singularity. This produces Borel singularities at:

$$\zeta_k = \frac{k}{\beta_0}, \quad k = 1, 2, 3, \ldots \tag{390}$$

These are **IR renormalons**—they arise from the running of the coupling at low momentum.

Box 6.5: Deriving Renormalons Without Feynman Diagrams

Problem: Show that IR renormalons emerge from the RG equation $\beta(g)\frac{dR}{dg} = \gamma(g)R$ without computing any Feynman diagrams. Assume $\beta(g) = -\beta_0 g^2(1 + O(g))$ and $\gamma(g) = \gamma_1 g + O(g^2)$.

Step 1: Series ansatz
Expand $R = \sum_{n=0}^{\infty} r_n g^n$ and substitute into the RG equation.
Step 2: Recursion relation
Matching powers of g: $r_{n+1} = \frac{(\text{polynomial in } \gamma_1, \beta_0, n)}{\beta_0} \cdot r_n$
Step 3: Large-order behavior
For $n \to \infty$: $r_n \sim n! \cdot \beta_0^n \cdot \text{const}$
Step 4: Borel singularity
The Borel transform $\hat{R}(\zeta) = \sum r_n \zeta^n / n!$ has a singularity at:

$$\boxed{\zeta_1 = \frac{1}{\beta_0}}$$

Conclusion: IR renormalons emerge from the **structure of the RG equation**, not from summing diagrams!

Implications for the RG Framework

1. Beta functions are resurgent objects: The perturbative beta function is part of a larger transseries.

2. Fixed points beyond perturbation theory: Non-perturbative fixed points from the transseries sector may exist.

The RG is fundamentally a resurgent framework: perturbative and non-perturbative physics are inseparably linked through the flow equations.

3. **Scheme dependence and resurgence:** Renormalons at $\zeta = k/\beta_0$ are scheme-independent since β_0 is universal.

Median Resummation and Physical Predictions

To extract physical predictions, we need a resummation prescription that gives real, unambiguous answers.

The Ambiguity Problem

For real $\epsilon > 0$, we want a real answer. But $\mathcal{S}_+$ and $\mathcal{S}_-$ are generally complex.

The difference is purely imaginary for real ϵ:

$$\mathcal{S}_+ - \mathcal{S}_- = (\text{purely imaginary}) \tag{391}$$

Lateral resummations are complex. Physical observables must be real. How do we reconcile this?

Median Resummation

The **median resummation** takes the average:

$$\mathcal{S}_{\text{med}}[\tilde{f}] = \frac{1}{2}\left(\mathcal{S}_+ + \mathcal{S}_-\right) \tag{392}$$

This is real when the series has real coefficients.

Physical interpretation: Median resummation corresponds to a specific value of the transseries parameter σ determined by requiring the physical answer to be real.

Median resummation: average above and below. This gives real answers for series with real coefficients.

Ambiguity Cancellation

In the full transseries, ambiguities cancel between sectors:

$$\text{Im}[\mathcal{S}[\hat{f}^{(0)}]] + \text{Im}[\sigma \cdot \mathcal{S}[\hat{f}^{(1)}]] + \cdots = 0 \tag{393}$$

This cancellation is automatic when we include all sectors with the correct Stokes constants.

Ambiguities cancel between sectors. The full transseries is unambiguous.

Connection to the Geometric Framework

Part I developed the geometric picture of RG: metrics, connections, and monodromy on parameter space. The resurgent framework fits naturally into this picture.

Extended Parameter Space

The transseries parameter σ extends the perturbative parameter space to the **extended parameter space**:

$$\mathcal{M}_{\text{ext}} = \{(g^1, \ldots, g^n, \sigma^1, \sigma^2, \ldots)\} \tag{394}$$

The full RG flow lives on this extended space. The beta functions have components for both perturbative couplings and transseries parameters.

The full theory space includes transseries parameters as additional coordinates.

Stokes as Monodromy

The Stokes automorphism is **monodromy** in the extended parameter space.

When the coupling g makes a loop around the origin in the complex plane, the transseries parameter σ transforms:

$$\sigma \mapsto \sigma + S_\omega \tag{395}$$

This is exactly the monodromy transformation from parallel transport around the Stokes line.

Alien Derivatives as Covariant Derivatives

The alien derivative Δ_ω extends the covariant derivative to include non-perturbative directions:

$$D_{\text{ext}} = \nabla_g + \sum_\omega e^{-\omega/g} \Delta_\omega \tag{396}$$

This completes the geometric picture: alien calculus is differential geometry on the extended parameter space.

The alien derivative is the covariant derivative in the direction of the ω-singularity.

When to Trust Perturbation Theory

The unified framework includes both perturbative and non-perturbative physics, but in many practical situations perturbation theory alone is sufficient.

Conditions for Perturbative Accuracy

Perturbation theory gives accurate answers when:

- The coupling is small ($\epsilon \ll 1$)
- No Stokes lines are crossed in the physical region
- We stay near a perturbative fixed point

Under these conditions, the exponentially suppressed transseries corrections $e^{-S/\epsilon}$ are genuinely negligible.

Perturbation theory works when you're far from Stokes lines and close to a perturbative fixed point with small coupling.

When Full Analysis Is Required

The full resurgent analysis becomes necessary when:

- The coupling is not small
- Stokes lines are crossed (e.g., analytic continuation in parameters)
- We approach non-perturbative fixed points
- Ambiguities must cancel for physical predictions

In these situations, truncating the perturbative series can give qualitatively wrong answers.

Common Pitfalls

Several common errors can derail an RG analysis:

Ignoring Divergence Structure: Treating perturbative series as convergent and simply truncating at some order ignores the information encoded in the divergence pattern.

Ignoring divergence structure throws away non-perturbative information encoded in the pattern of coefficients.

Missing Stokes Lines: When continuing analytically in parameters, Stokes lines may be crossed. Ignoring the resulting jumps in transseries parameters leads to wrong answers.

Confusing Scheme Dependence with Physics: Beta functions and anomalous dimensions are scheme-dependent. Only scheme-independent quantities (critical exponents, Stokes constants, physical observables) are meaningful.

Overlooking Non-Perturbative Fixed Points: If only perturbative fixed points are sought, non-perturbative ones are missed. For some problems, the physically relevant fixed point may be non-perturbative.

Summary

This chapter developed the mathematical framework for extracting physics from divergent series. The key tools are:

1. **Borel transform**: Converts factorial divergence to geometric growth
2. **Borel-Laplace resummation**: Recovers a function from a divergent series
3. **Transseries**: The complete answer combining perturbative and non-perturbative sectors
4. **Stokes phenomena**: The ambiguity in resummation when crossing singularities
5. **Alien calculus**: The machinery for relating different transseries sectors

6. **Median resummation**: A prescription giving real, physical answers

The key insight connecting to the geometric framework of Part I is that:

Resurgence is not an optional refinement. It is how we extract physics from the inherently divergent series that perturbation theory produces.

- Transseries parameters extend theory space to $\mathcal{M}_{\text{ext}}$
- Stokes phenomena are monodromy in this extended space
- Alien derivatives are covariant derivatives probing non-perturbative directions
- The RG equation itself is a resurgent equation with transseries solutions

Part III applies these tools to specific physical systems: chaotic dynamics, fluid turbulence, statistical mechanics, and quantum field theory.

Exercises

1. **Borel transform computation.** Compute the Borel transform for the following series:
   (a) $\tilde{f}_1(\epsilon) = \sum_{n=0}^{\infty} n!\,\epsilon^n$ (hint: result is $1/(1-\zeta)$)
   (b) $\tilde{f}_2(\epsilon) = \sum_{n=0}^{\infty}(2n)!\,\epsilon^n$ (hint: consider $1/\sqrt{1-4\zeta}$)
   (c) $\tilde{f}_3(\epsilon) = \sum_{n=0}^{\infty}(-1)^n(n+1)!\,\epsilon^n$
2. **Singularity structure.** A Borel transform has the form $\hat{f}_B(\zeta) = \frac{1}{(1-\zeta)(2-\zeta)}$.
   (a) Identify all singularities and their nature.
   (b) Expand in partial fractions and relate each term to large-order behavior.
   (c) Compute the Stokes discontinuity when integrating along the positive real axis.
3. **Transseries construction.** Consider the differential equation $\epsilon\, dy/dx = y - y^2$ with $y(0) = y_0$.
   (a) Find the perturbative solution by expanding $y = y_0 + \epsilon y_1 + \cdots$.
   (b) Identify the non-perturbative solution $y_{\text{np}} = e^{-x/\epsilon}/(1 + ce^{-x/\epsilon})$.
   (c) Write the general transseries solution $y(x;\epsilon,\sigma)$.
4. **Alien derivative.** For the simple transseries $\tilde{f}(\epsilon,\sigma) = \tilde{f}^{(0)}(\epsilon) + \sigma e^{-S/\epsilon}\tilde{f}^{(1)}(\epsilon)$:
   (a) Verify the bridge equation $\Delta_S\tilde{f} = S_1\partial_\sigma\tilde{f}$.

(b) Explain why $\Delta_S \tilde{f}^{(0)} = S_1 \tilde{f}^{(1)}$.

(c) If $\Delta_S \tilde{f}^{(1)} = S_2 \tilde{f}^{(2)}$, write the resurgent relation connecting all sectors.

5. **(Challenge) Median resummation.** For a series with Borel transform $\hat{f}_B(\zeta) = 1/(1-\zeta)$:

(a) Compute the lateral Borel sums $\mathcal{S}_+$ and $\mathcal{S}_-$.

(b) Verify that $\mathcal{S}_+ - \mathcal{S}_- = 2\pi i \, e^{-1/\epsilon}$.

(c) Show that the median resummation $\mathcal{S}_{\text{med}} = (\mathcal{S}_+ + \mathcal{S}_-)/2$ is real for real $\epsilon > 0$.

6. **Perturbation failure at phase boundaries.** The mean-field free energy for a ferromagnet is $F(M, T) = a(T - T_c)M^2 + bM^4 - hM$.

(a) For $h = 0$, find the equilibrium magnetization $M^*(T)$ for $T < T_c$ and $T > T_c$.

(b) Expand $M^*(T)$ around $T = T_c$ (from below). Show $M^* \sim (T_c - T)^{1/2}$.

(c) Explain how this non-analyticity signals the failure of perturbation theory at the phase boundary.

7. **(Challenge) RG and renormalons.** For a theory with beta function $\beta(g) = -\beta_0 g^2 - \beta_1 g^3 + \cdots$:

(a) Show that the ratio $\gamma(g)/\beta(g)$ has a $1/g$ singularity when $\gamma(g) = \gamma_1 g + \cdots$.

(b) Derive the large-order behavior of perturbative coefficients from the RG equation.

(c) Identify the position of the leading IR renormalon in the Borel plane.

Mathematical Toolkit

This appendix provides a compact reference for the mathematical tools used throughout the book. Each topic is treated in the main text and this serves as a quick-lookup resource rather than a standalone introduction.

This appendix collects definitions, formulas, and key results for quick reference. The material has been developed throughout Part I and is gathered here for convenience.

Asymptotic Series and Gevrey Classes

Asymptotic Expansions

A formal series $\tilde{f}(z) = \sum_{n=0}^{\infty} a_n z^n$ is **asymptotic** to a function $f(z)$ as $z \to 0$ if:

$$\left| f(z) - \sum_{n=0}^{N-1} a_n z^n \right| \leq C_N |z|^N \tag{397}$$

for each N and $|z|$ sufficiently small. We write $f(z) \sim \tilde{f}(z)$.

Gevrey Classes

A series is **Gevrey of order** s (written Gevrey-s) if its coefficients satisfy:

$$|a_n| \leq C \cdot K^n \cdot (n!)^s \tag{398}$$

for some constants $C, K > 0$.

Gevrey-0: Convergent series with $|a_n| \leq CK^n$.

Gevrey-1: Factorially divergent with $|a_n| \leq CK^n \cdot n!$. This is the generic case in physics.

Gevrey-s for $s > 1$: Faster than factorial growth, less common.

Borel Transform and Laplace Transform

The Borel Transform

Given a formal series $\tilde{f}(z) = \sum_{n=0}^{\infty} a_n z^n$, its **Borel transform** is:

$$\hat{f}_B(\zeta) = \sum_{n=0}^{\infty} \frac{a_n}{n!} \zeta^n \tag{399}$$

For Gevrey-1 series, the Borel transform has finite radius of convergence and can be analytically continued.

The Laplace Transform

The **Laplace transform** of $g(\zeta)$ along direction θ is:

$$\mathcal{L}_\theta[g](z) = \int_0^{e^{i\theta}\infty} e^{-\zeta/z} g(\zeta)\, d\zeta \tag{400}$$

Borel-Laplace Resummation

The **Borel sum** of $\tilde{f}$ along direction θ is:

$$\mathcal{S}_\theta[\tilde{f}](z) = \mathcal{L}_\theta[\hat{f}_B](z) = \int_0^{e^{i\theta}\infty} e^{-\zeta/z} \hat{f}_B(\zeta)\, d\zeta \tag{401}$$

This recovers a function from a divergent series when no singularities obstruct the integration path.

Singularities in the Borel Plane

Types of Singularities

Common singularities in the Borel plane of physical theories include the following.

Instantons: Singularities at $\zeta = S_{\text{inst}}$ (classical instanton action). These encode tunneling effects and typically have the form:

$$\hat{f}_B(\zeta) \sim \frac{c}{(\zeta - S)^\alpha} \log(\zeta - S) + \text{regular} \tag{402}$$

Renormalons: Singularities at $\zeta = k/\beta_1$ (multiples of inverse one-loop beta function). These arise from factorial growth induced by RG running:

$$\hat{f}_B(\zeta) \sim \frac{1}{(1 - \beta_1 \zeta)^p} \tag{403}$$

IR renormalons: Singularities on the positive real axis, obstructing naive Borel resummation.

UV renormalons: Singularities on the negative real axis, not obstructing resummation but encoding UV sensitivity.

Stokes Phenomena

Stokes Lines

A **Stokes line** is a direction in the z-plane where the integration contour for Borel-Laplace resummation crosses a singularity in the Borel plane. For a singularity at ζ_*, the Stokes line occurs at:

$$\arg(z) = \arg(\zeta_*) \tag{404}$$

The Stokes Automorphism

When crossing a Stokes line, the resummation changes discontinuously. The **Stokes automorphism** $\mathfrak{S}$ acts on the transseries parameter:

$$\mathfrak{S} : \sigma \mapsto \sigma + S_\omega \tag{405}$$

where S_ω is the **Stokes constant** associated with the singularity at ω.

Stokes Constants

The Stokes constant encodes the "residue" of the ambiguity in crossing a singularity. It relates different sectors of the transseries and is computed from:

$$S_\omega = 2\pi i \cdot \mathrm{Res}_\omega[\hat{f}_B] \tag{406}$$

for simple poles, with generalizations for branch points.

Transseries

Definition

A **transseries** combines perturbative and non-perturbative sectors:

$$\tilde{f}(z,\sigma) = \sum_{k=0}^{\infty} \sigma^k e^{-kS/z} \hat{f}^{(k)}(z) \tag{407}$$

where $\hat{f}^{(0)}$ is the perturbative series, $\hat{f}^{(k)}$ for $k \geq 1$ are instanton sectors, σ is the transseries parameter, and S is the instanton action.

More General Form

Multi-instanton transseries with multiple types of non-perturbative effects:

$$\tilde{f}(z,\{\sigma_i\}) = \sum_{n_1,n_2,\ldots} \prod_i \sigma_i^{n_i} e^{-(\sum_i n_i S_i)/z} \hat{f}^{(n_1,n_2,\ldots)}(z) \tag{408}$$

Reality Conditions

For real z, physical observables must be real. This constrains transseries parameters:

$$\text{If } \bar{\sigma} = \sigma^*, \text{ then } \overline{\tilde{f}(z,\sigma)} = \tilde{f}(\bar{z},\bar{\sigma}) \tag{409}$$

Alien Calculus

The Alien Derivative

The **alien derivative** Δ_ω probes the singularity at $\zeta = \omega$ in the Borel plane. It extracts the coefficient relating the perturbative sector to the instanton sector:

$$\Delta_\omega \hat{f}^{(0)} = S_\omega \hat{f}^{(1)} \tag{410}$$

where S_ω is the Stokes constant.

The Bridge Equation

The alien derivative is related to ordinary differentiation along transseries directions:

$$\Delta_\omega \tilde{f} = S_\omega \cdot \frac{\partial \tilde{f}}{\partial \sigma} \tag{411}$$

This is the **bridge equation**. It connects the Borel plane structure to the transseries parameter space.

Properties

The alien derivative satisfies a Leibniz rule:

$$\Delta_\omega(fg) = (\Delta_\omega f)g + f(\Delta_\omega g) \tag{412}$$

Multiple alien derivatives compose:

$$\Delta_{\omega_1}\Delta_{\omega_2} = \Delta_{\omega_2}\Delta_{\omega_1} \tag{413}$$

Median Resummation

Lateral Resummations

When a singularity lies on the positive real axis, define:

$$\mathcal{S}_\pm[\tilde{f}](z) = \mathcal{L}_{0^\pm}[\hat{f}_B](z) \tag{414}$$

by integrating just above or below the real axis.

The Median Resummation

The **median resummation** is the average:

$$\mathcal{S}_{\text{med}}[\tilde{f}](z) = \frac{1}{2}\left(\mathcal{S}_+[\tilde{f}] + \mathcal{S}_-[\tilde{f}]\right) \tag{415}$$

This gives a real result when the singularities come in conjugate pairs.

Ambiguity Cancellation

The difference between lateral resummations is:

$$\mathcal{S}_+[\tilde{f}] - \mathcal{S}_-[\tilde{f}] = 2\pi i \cdot \text{Disc}[\hat{f}_B] \tag{416}$$

For physical observables, this ambiguity must cancel against contributions from other sectors of the transseries.

Beta Functions and RG Flow

Definition

The **beta function** for coupling g^i is:

$$\beta^i(g) = \mu \frac{dg^i}{d\mu} = \frac{dg^i}{d\ell} \tag{417}$$

where μ is the RG scale and $\ell = \log(\mu/\mu_0)$.

Fixed Points

A **fixed point** satisfies $\beta^i(g^*) = 0$ for all i.

Perturbative fixed points: $\beta_{\text{pert}}(g^*) = 0$.

Non-perturbative fixed points: $\beta_{\text{pert}}(g^*) \neq 0$ but $\beta_{\text{full}}(g^*) = 0$.

Stability

Near a fixed point, linearize: $\delta\dot{g}^i = B^i{}_j \delta g^j$ where $B^i{}_j = \partial\beta^i/\partial g^j|_{g^*}$.

The eigenvalues Δ_α of B classify directions. When $\Delta_\alpha > 0$ the direction is relevant, when $\Delta_\alpha < 0$ the direction is irrelevant, and when $\Delta_\alpha = 0$ the direction is marginal.

Connections and Monodromy

Connections

A **connection** $\Gamma^a{}_{bc}$ on parameter space specifies parallel transport:

$$\nabla_b V^a = \partial_b V^a + \Gamma^a{}_{bc} V^c \tag{418}$$

The **curvature** measures path dependence:

$$R^a{}_{bcd} = \partial_c \Gamma^a{}_{bd} - \partial_d \Gamma^a{}_{bc} + \Gamma^a{}_{ec}\Gamma^e{}_{bd} - \Gamma^a{}_{ed}\Gamma^e{}_{bc} \tag{419}$$

Monodromy

Monodromy is the transformation acquired by parallel transport around a closed loop:

$$M(\mathcal{C}) = \mathcal{P}\exp\left(\oint_{\mathcal{C}} \Gamma^a{}_{bc}\, dg^b\right) \tag{420}$$

Stokes as monodromy: The Stokes automorphism is monodromy around the Stokes line in extended parameter space.

Key Formulas Summary

Name	**Formula**
Gevrey-1 bound	$\lvert a_n \rvert \le C K^n n!$
Borel transform	$\hat{f}_B(\zeta) = \sum_n \frac{a_n}{n!} \zeta^n$
Laplace transform	$\mathcal{L}[g](z) = \int_0^\infty e^{-\zeta/z} g(\zeta)\, d\zeta$
Borel sum	$\mathcal{S}[\tilde{f}] = \mathcal{L}[\hat{f}_B]$
Transseries	$\tilde{f} = \sum_k \sigma^k e^{-kS/z} \hat{f}^{(k)}$
Bridge equation	$\Delta_\omega \tilde{f} = S_\omega \partial_\sigma \tilde{f}$
Beta function	$\beta^i = \mu\, dg^i / d\mu$
Fixed point	$\beta^i(g^*) = 0$
Callan-Symanzik	$(\mu \partial_\mu + \beta^i \partial_i + n\gamma) G_n = 0$
Operator mixing	$\mu\, d\mathcal{O}_a / d\mu = \gamma_a{}^b \mathcal{O}_b$

References for Further Reading

Asymptotic Analysis and Resurgence

The foundational work on resurgence is Écalle's treatise on analysable functions. Accessible introductions include Costin's monograph on exponential asymptotics and the lecture notes by Mariño on resurgence in quantum field theory. The paper by Aniceto, Başar, and Schiappa provides a modern physics perspective.

Renormalization Group

Wilson's original papers remain essential reading. The textbooks by Goldenfeld, by Cardy, and by Amit and Martín-Mayor provide comprehensive treatments. For the geometric perspective, see the papers by Zamolodchikov on the c-theorem and the reviews by Komargodski.

Differential Geometry

For connections and fiber bundles in physics contexts, see the books by Nakahara and by Frankel. The information geometry perspective is developed in the book by Amari.

Bibliography